UNIVERSITY OF ALBERTA

A Study of the Rheology, Stability and Pore Blocking Ability of Non-Aqueous Colloidal Gas Aphron Drilling Fluids

by

Shishir Shivhare

A thesis submitted to the Faculty of Graduate Studies and Research
in partial fulfillment of the requirements for the degree of

Master of Science

in

Petroleum Engineering

Department of Civil and Environmental Engineering

Fall 2011

Edmonton, Alberta

Examining Committee

Dr. Ergun Kuru, Civil and Environmental Engineering

Dr. Japan Trivedi, Civil and Environmental Engineering

Dr. Phillip Y. K. Choi, Chemical and Materials Engineering

ABSTRACT

Colloidal gas aphrons (CGAs) recently used as part of water-based drilling fluids have been found effective in controlling the filtration rate by bridging the pores of the reservoir rock and therefore, reducing the formation damage. This research aims to generate colloidal gas aphrons (CGA) in oil based drilling fluids; to study stability, rheology and the filtration loss characteristics of CGAs and to investigate formation damage properties of CGAs as a drilling fluid.

Aphrons were generated in mineral oil using a polymer-surfactant mix. Based on how changing the polymer and surfactant concentration affects the physico-chemical characteristics of the fluid, an optimum formulation for the aphron drilling fluid was suggested.

The stability of microbubbles was investigated by looking at the effects of time, temperature and pressure on the aphron yield and bubble size distribution. Effects of temperature and pressure on the density of the oil-based aphron fluids have been investigated. Based on the PVT analysis results, an equation of state was proposed.

Finally, the performance of the oil-based aphron fluid in porous media was investigated. The effects of changing the CGA fluid injection rate, the type of saturating fluid and the wettability of the porous media on the pressure drop were examined. An assessment of the formation damage following the oil-based CGA fluid injection was also made.

ACKNOWLEDGMENTS

It is a great pleasure to express my deepest gratitude and appreciation to my supervisor Dr. Ergun Kuru who's highly professional and immensely valuable advice, mentorship, guidance and unconditional support throughout the research study made this thesis possible.

I am heartily thankful to my family back home, my father and mother, my sister Parul and my brother Dev for their support and encouragement. A warmly expressed gratitude is also for all my friends here in Edmonton – Akila, Jignesh, Neha, Amit, Mudit, Rajpreet, Jasjeet, Harmeet, Pedro, Santhosh and Shivana. My stay and time here at the University was possible because of them.

I would also like to make a special reference to Nancy Ann Bjorndalen whose work was immensely helpful as a guidance for my research project.

This work has been supported by the Natural Sciences and Engineering Research Council of Canada (NSERC). Financial support from NSERC is greatly acknowledged. I would also like to thank BASF and Kraton Polymers for donating samples used in this research study.

TABLE OF CONTENTS

LIST OF TABLES

LIST OF FIGURES

1. INTRODUCTION

1.1 Overview

The increasingly limited availability of easy to access crude oil has shifted the focus in the oil and gas industry towards exploitation of heavy oil and partially depleted reserves. Stricter regulations and an increased demand on recovery and efficiency have put a lot of focus on improved technologies. A very important way to reduce costs and meet standards is to improve drilling technologies. For an improvement in drilling technologies, it is imperative to have an improvement in drilling fluids to be used. Particularly for drilling in partially depleted reserves, i.e., reserves with low reservoir pressures, specialized drilling fluids are required. Besides low pressure reservoirs, exploitation of horizontal and multilateral wells will be made feasible with improved drilling fluids.

The drilling fluid performs multiple tasks when the well is being drilled. The primary function of the drilling fluid is to carry the rock cuttings away from the drill bit face and transport them from the bottom of the well to the surface where they are separated from the fluid. For this, drilling fluid is pumped down through the drill bit and then back to the surface through the annulus. In this way it helps clean the surface of the rock being drilled and in keeping the cuttings suspended when the drilling process is paused.

The drilling fluid has some other functions like lubricating and cooling the system and eliminating differential sticking. Another major function of the drilling fluid is to balance the pressure exerted by the formation fluids (fluids present in the

rock) by the virtue of its own pressure. If there is nothing in the well to offset the pressure exerted by the formation fluids, they will flow into the well. Also, the formation walls around the wellbore may cave in. So the drilling fluid has to provide a pressure to offset the fluid pressure in the reservoir.

This is the common method of drilling, maintaining the wellbore pressure above the formation pressure. Drilling in this manner is termed as drilling overbalanced. However drilling overbalanced is fraught with many problems. If the drilling fluid pressure in the wellbore is maintained considerably higher than the formation pore pressure, the drilling fluid may invade the formation. This can result in blocking of pores and an eventual occurrence of formation damage. Other problems like differential pipe stuck can also occur.

Much is said about underbalanced drilling as an alternative to eliminate the aforesaid problems of overbalanced drilling. In underbalanced drilling, the drilling fluid pressure in the wellbore is maintained at a pressure that is lower than the pore pressure in the formation. Thus, it allows the formation fluids to be produced while drilling. A natural consequence of drilling underbalanced is that it rules out the possibility of fluid invasion and the ensuing formation damage. However, drilling underbalanced is always an expensive proposition, with specialized equipment required for mixing of air into the drilling mud. Meeting the safety standards (because of danger of blowouts) and the associated costs can be a drain on the drilling rig operator. Another problem is borehole instability because of the wellbore pressure being lesser than the pore pressure.

1.2 Statement of the problem

In most of the situations drilling underbalanced is not feasible. The reasons are normally the high costs and the technical problems. Drilling overbalanced has its own complications of formation damage; these problems are even more pronounced in low pressure reserves.

At balance drilling is drilling with the pressure of the drilling fluid in the wellbore closely matching the formation fluid pressure. If the drilling mud density (equivalent circulating density, ECD) is monitored carefully to maintain an at-balance drilling situation the problems associated with drilling overbalanced and underbalanced can be overcome. More precisely, possibilities of formation invasion (drilling overbalanced) and borehole instability (drilling underbalanced) are ruled out.

Normally, suspended solid particles are added to the drilling mud. The purpose is to form a filter cake at the borehole walls so as to limit further leak-off of the drilling mud. These solids are referred to as bridging solids. The namesake is because of the bridging action of the solid particles whereby they bridge and seal the pores of the formation rock. However, the filter cake formed by the bridging solids is usually hard to remove later on. This alters (i.e. lowers) the permeability of the nearby rock. The consequence is hampered flow of formation fluids while production.

While drilling at-balanced, specialized drilling fluids have been used often. It is in an at-balance situation that colloidal gas aphron (CGA) based drilling fluids have

been developed for application. Aphrons are tiny microbubbles (10-100μm in size) that have unique properties of non-coalescence and longevity. Aphrons can be generated with the help of surfactants; they can be stabilized for extended periods by a polymer-surfactant mix. Understandably, the use of aphrons as bridging agents (like the bridging solids) has been tried, with notable success in several field applications.

CGAs have a unique bridging ability to bridge pores. It is expected that when drilling begins, the microbubbles will move to the fluid front, collect at the rock walls and form aggregates that will block the pores. These CGAs can be removed later when the well is opened for production. So this is the real advantage of using aphrons as bridging agents, there is no skin effect caused.

Colloidal gas aphrons were developed initially for a variety of applications like water decontamination and particle floatation. Use of aphrons in drilling has been tried extensively too. Formulations of drilling fluids have been suggested and their application in case studies has been discussed. Studies have been done on the development, characterization and testing of aphronized drilling fluids.

However, almost all of the work done on CGA drilling fluids is with aqueous based drilling fluids, i.e. aphrons have been generated with water as a base fluid. If aphrons could be generated in oil, an oil based aphron drilling fluid can be developed. Such a fluid is expected to enhance the ability of aphron fluids to drill in low pressure reservoirs even more. It will also be particularly useful in certain

formations, e.g. shale where aqueous drilling fluids are fraught with instability problems.

Hence, the motivation behind this project has been to generate aphrons using mineral oil as a base fluid. Following creation of aphrons in mineral oil, a formulation for an aphron drilling fluid has been developed. Characterization, investigation of the stability of the microbubbles and the performance of the fluid in a sand packed core has been studied.

1.3 Objectives and scope of the study

The first step in the project is to generate colloidal gas aphrons in mineral oil. Broadly, the objectives of this study can be classified as; development, characterization and testing of the stability and performance of the aphron drilling fluid. This project is essentially an experimental study.

Overall, the major objectives can be grouped as below:

1. Literature Review and theoretical study
    - A review of early work on aphrons and applications of aphrons
    - Theoretical study and review of surfactants and polymers suitable for mineral oil
2. Generation of CGAs in mineral oil
    - Testing of the surfactants to see whether aphrons are formed
    - Identifying the mixing devices and techniques
3. Characterization of the CGA fluid

- Investigate the effect of surfactant concentration on the density, yield of aphrons, average CGA bubble size, rheology and API fluid loss
- Investigate the effect of polymer concentration on the density, average bubble size, rheology and API fluid loss
- Identify an optimal formulation with respect to surfactant and polymer concentration for the use of the CGA fluid as an aphron drilling fluid
- Enhance suspension ability of CGA fluid using organophilic clays
- Analyse the effect of time on the yield of aphrons and the average CGA bubble diameter
- Study the change in average CGA bubble diameter, rheology and API fluid loss with increase in temperature
- Study the change in rheology and API fluid loss with an increase in pressure
- Analyse the PVT characteristics of the CGA fluid and develop an equation of state for the CGA fluid

4. Performance of the fluid in a core flow experiments
    - The pressure drop profile of the CGA fluid across a radial core holder packed with glass beads is observed
    - The formation damage characteristics of the fluid are analysed
    - Effect of changing flowrate, saturation fluid and wettability on the pressure drop across the porous media and the formation damage are examined

During the course of this study, two conference proceedings have been published:

1. Shivhare, S. And Kuru, E. (2010) Physico-Chemical Characterization of Non-Aqueous Colloidal Gas Aphron Based Drilling Fluids. SPE 133274, presented at the Canadian Unconventional Resources & International Petroleum Conference held in Calgary, Alberta, Canada, October 19–21 and
2. Shivhare, S. and Kuru, E. (2011) Rheology and Stability of Non-Aqueous Microbubble Based Drilling Fluids. SPE 141166, presented at the SPE International Symposium on Oilfield Chemistry held in The Woodlands, Texas, USA, April 11–13

The first paper titled Physico-Chemical Characterization of Non-Aqueous Colloidal Gas Aphron Based Drilling Fluids is under review for publication with the Journal of Canadian Petroleum technology (Shivhare and Kuru, JCPT-0211-0014). A third abstract for a paper covering the final part of the project has been submitted.

1.4 Structure of the thesis

Chapter 1 gives a general background of drilling, an introduction to aphrons and the relevance of drilling with aphrons in an at-balance scenario. The objectives of the study are presented in detail.

Chapter 2 gives a literature review about the subject of this study. Chiefly the literature review covers two areas of work done by previous authors- the generation of aphrons and their use in several applications and the development of aphrons as a drilling fluid.

Chapter 3 covers the materials and equipment used in this project. Details about all the reagents and the equipment used in the experimental program are provided.

Chapter 4 is about the Physico-Chemical characterization of the CGA drilling fluid. The experimental procedure followed by the results and analysis is given.

Chapter 5 discusses the stability of the aphron drilling fluid by describing how time, temperature and pressure affect the characteristics of the fluid.

Chapter 6 contains details about the core flooding experiments. A step by step detailing of the methods and procedures employed is given, followed by the results.

Chapter 7 concludes the thesis with conclusions and recommendations for further research.

Chapter 8 contains the references.

2 LITERATURE REVIEW

When a well is drilled, the pressure in the wellbore is usually kept above the pressure in the formation to prevent the formation fluids from entering the well. This is called overbalanced drilling. Drilling overbalanced has several limitations- it can cause formation damage where the drilling mud is forced into the formation (fluid invasion). Large amounts of the drilling mud can be lost into the formation uncontrollably (lost circulation). Differential sticking is also a problem associated with overbalanced drilling.

A lot has been written about underbalanced drilling as an alternative to overbalanced drilling so as to overcome these issues. While drilling underbalanced, the wellbore pressure is maintained lower than the formation pressure. The primary advantage of drilling underbalanced is in preventing fluid invasion and the resultant formation damage. It also helps in reducing differential sticking and in increasing the rate of penetration. However drilling underbalanced is an expensive task and meeting the safety requirements is not easy. A lot of problems like borehole instability, well control and using downhole equipment come up (Ivan et al., 2001).

At-balance drilling means drilling with the wellbore fluid pressure closely matching the formation fluid pressure, so that there is minimal fluid invasion and the formation fluids also do not come into the wellbore. In an at-balance situation, use of colloidal gas aphron (CGA) based drilling fluids helps to produce lower drilling fluid densities and to seal the pores by bridging (Brookey, 1998). The use

of such a system will be particularly useful in drilling depleted and low pressure reservoirs.

2.1 CGA as a drilling fluid

Colloidal gas aphrons are dispersions of microbubbles and differ from regular foams not only regarding their geometric structure, but also in terms of their rheological properties, longevity and drainage characteristics (Spinelli et al., 2009). Normal foams are essentially gas–liquid–gas systems where fine liquid lamellae encircle polyhedral structures that in turn encapsulate the gas phase. Microfoams (aphrons) have much higher liquid phase content around the gas phase and are characterized by tiny and practically spherical bubbles. Foams are thermodynamically unstable and also produce a significant pressure gradient as they pass through porous media (Oliveira et al., 2004).

Aphrons were first discussed by Sebba (1987), who coined the term Colloidal Gas Aphron (CGA). Aphron comes from the Greek word αφρός, which means foam. So Sebba named the foam-like microbubbles with colloid-like properties as aphrons. Aphrons are small bubbles; they have a size range of 10-100 microns in diameter. Sebba noted that the most remarkable property of these microbubbles is their non-coalescing nature.

Subsequently, the usefulness of aphrons for different types of applications was suggested. Longe (1989) wrote his PhD dissertation about the applicability of Colloidal gas aphrons to decontaminate soil and groundwater. Usefulness of CGA suspensions for in situ flushing of soil to remove non aqueous hydrocarbon

contaminants has been demonstrated (Roy et al., 1994). Oliveira et al. (2004) also looked at the use of CGAs for soil remediation. Paula Jauregi (1996) looked at the application of colloidal gas aphrons for lysozome separation and protein recovery. CGAs can be used for the floatation and subsequent recovery of palm oil (Hashim et al., 1999). Hashim et al. also studied the floatation characteristics of CGA fluids for the purpose of yeast floatation (2000).

Efforts were made to characterize CGA fluids. Amiri and Woodburn (1990) were the first to characterize aphron fluids. They studied the average CGA size and drainage rate of CGA solutions. Further size analysis and stability with time of CGA bubbles was studied by Parthasarathy et al. (1991). Use of a particle size analyzer for studying size distribution and stability was done by Chaphalkar et al. (1993). They also wrote about yield of aphrons from a batch of fluid and drainage with time. Save and Pangarkar (1993) wrote in detail about stability of CGA solutions and effect of pH, time of stirring, choice of surfactant and viscosity on the stability. Analysis on stability was done mostly by using a parameter called half life of the CGA (τ_s). The half life (τ_s) of CGA was defined as the time taken for draining half the liquid used for generation of CGA.

Colloidal gas aphrons incorporated into drilling mud to form a CGA drilling fluid have been studied extensively too. Brookey (1998) suggested use of CGA drill-in fluid while drilling at balance. Ivan et al. (2001) proposed a reduction in fluid losses when drilling with aphron fluid systems. This was demonstrated in the case of field experience in California. Growcock (2005) made a detailed study on increasing wellbore stabilization and reservoir productivity by making use of

aphron drilling fluid technology. CGAs are stable in drilling fluids at ambient pressures. Ivan et al. (2002) conducted visualization tests to show that CGAs can be maintained upto pressures of 1500 psi. Above a critical pressure, the CGAs will collapse (Growcock, 2005). Aphron based drilling fluids are non-coalescing and can be recirculated (Brookey, 1998) without being affected by downhole equipment. Because of the altered wellbore pressure drop as compared to overbalanced drilling, aphron drilling systems eliminate the problem of differential sticking (Rea et al., 2003). Downhole tools, such as MWD, turbines and motors do not suffer interference by aphrons (Oyatomari et al., 2002). As a replacement of Under Balanced Drilling techniques, use of aphron fluids does away with the need of costly downhole tools, leading to more than 50% reduction in drilling costs (Oyatomari et al., 2002). CGAs can be produced easily at the surface and no separate equipment like compressors are required to inject gases at high pressure. In Underbalanced drilling, the presence of high concentrations of air creates a condition of extreme corrosion where air and water are in constant contact with the drillstring (Brookey, 1998). Corrosion problems are reduced with aphronized fluids, since most of the air in the system is encapsulated in the aphron shell. Also, it's a common practice to add an oxygen scavenger to the drilling fluid formulation (Growcock, 2005). So very soon after they are created, the oxygen is scavenged by one of the components in the fluid, leaving the aphrons with a core of nitrogen (Growcock, 2005). This gives aphrons their non corrosive nature.

All of the above work on aphrons has been done using water as a base fluid, i.e. the colloidal gas aphrons have been generated in water. Sebba (1987) had discussed the existence and use of polyaphrons; aphrons in which the core was oil and the surrounding film was aqueous. Sebba also wrote about the existence of invert aphrons; aphrons in which the core is water and the film is oil, oil being the continuous phase too. Generation of true CGAs in oil (in which the core is air and the continuous phase is oil) was first discussed by Growcock, Khan and Simon in 2003. Growcock proposed a structure for oil based aphrons and suggested a composition for an oil based aphronized drilling fluid. Međimurec (2009) also wrote about a similar structure and formulation table. Spinelli et al. (2009) worked on the generation of aphrons with an ester and an ester-water mixture as base fluids.

2.2 CGA Structure

For the first time, a structure for aphrons was proposed by Sebba in his book Foams and Biliquid Foams- Aphrons (1987). Sebba stated that the structure and encapsulating layers of an aphron will be fundamentally different than that of conventional foam. A figure for a conventional foam bubble is shown in Figure 2-1. Physically, the bubble in Figure 2-1 is a sphere of gas separated from its surroundings by a thin soapy film.

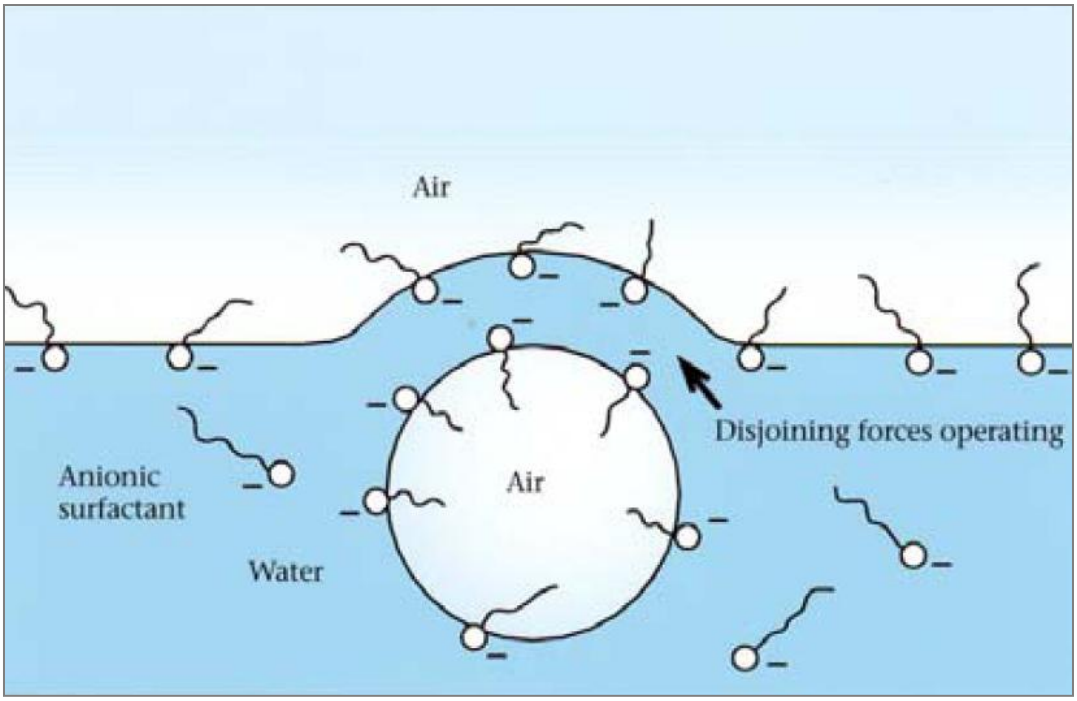

Figure 2-1: A conventional foam bubble (Sebba, 1987)

A foam can be thus be defined as an aggregate of gas bubbles held in a continuous aqueous matrix (Sebba, 1987). Like foams, aphrons have a spherical core too which is filled with air. However, unlike a conventional air bubble, which is stabilized by a surfactant monolayer (like shown in Figure 2-1), the outer shell of the aphron consists of an inner shell as well as an outer shell. This is shown in Figure 2-2. The inner surfactant film is enveloped by a viscous water layer, outside of which is an outer bilayer of surfactants. The inner layer contains surfactants whose hydrophobic ends point into the core and whose hydrophilic ends reside within the shell. The outer layer has surfactants whose hydrophilic ends point into the shell and whose hydrophobic ends lie in the bulk of the liquid. Since this bubble is in contact with the bulk water, it is believed that there is another layer in which the surfactant molecules are hydrophobic inwards and

hydrophilic outwards. The resultant tri-layer of surfactants is what we have in Figure 2-2

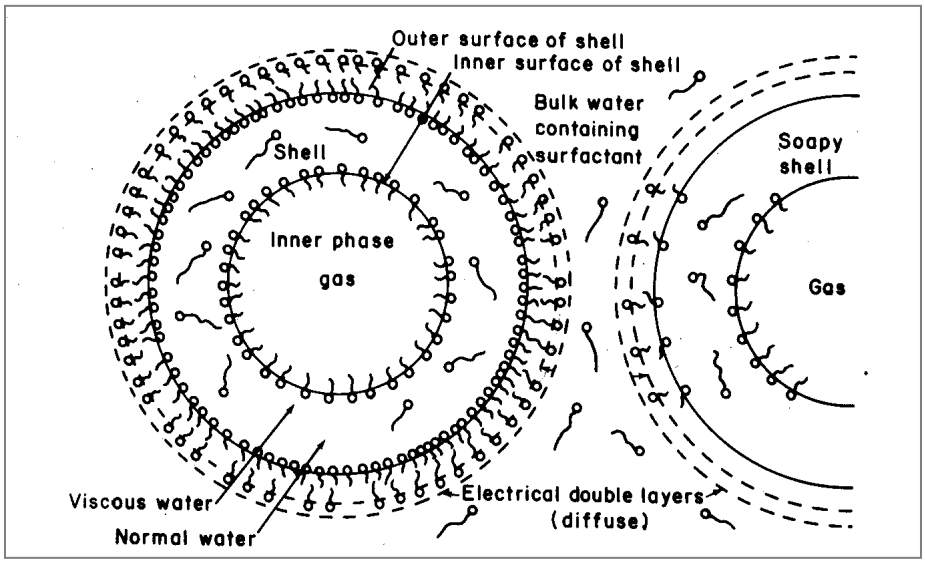

Figure 2-2: Structure of a CGA (Sebba, 1987)

For oil-based aphrons, the structure will be somewhat different. Growcock et al. (2003) suggested that a viscosified aqueous or polar layer will surround the inner surfactant film, and this is kept in place by an outer monolayer of surfactants. Another interpretation of oil-based aphron structure incorporates no aqueous layer at all, so that the inner and outer surfactant films come together to form a bilayer. This is predicted to depend a lot on the additives (especially polar additives) added, if any, to the base fluid. The structure postulated by Growcock et al. (2004) is shown in Figure 2-3. As can be seen, a viscosified polar layer surrounds the air core, stabilized by the surfactant double layer. This surfactant double layer also helps in stabilizing the aphron, preventing it from coalescing with other aphrons.

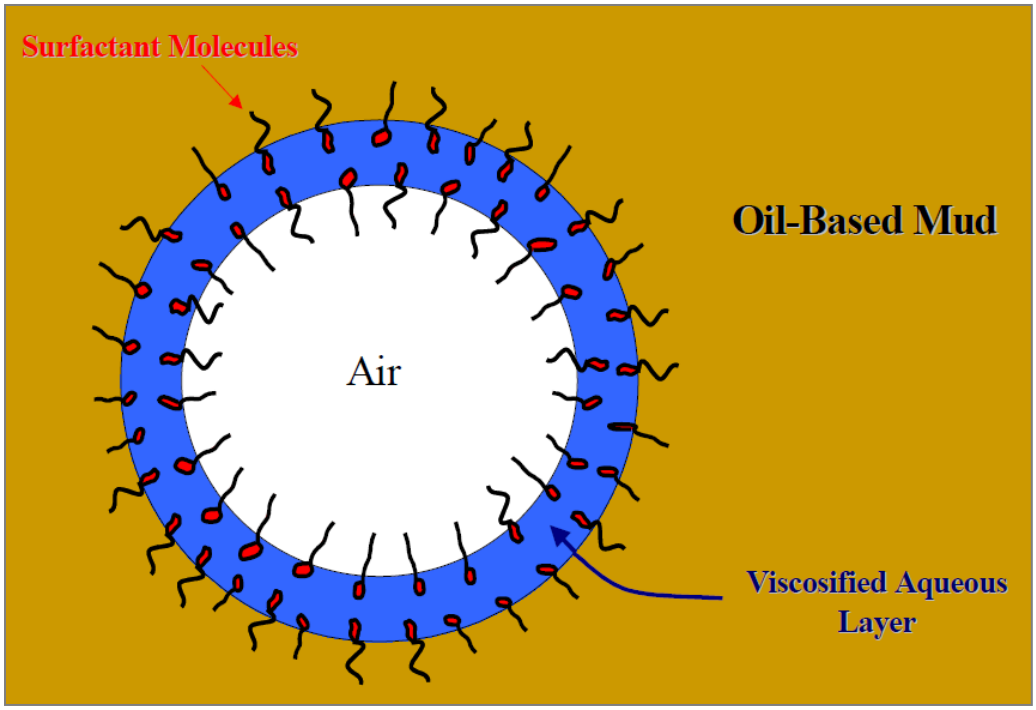

Figure 2-3: Structure of an oil-based aphron (Growcock et al., 2003)

2.3 CGA bridging mechanism

The blocking/bridging mechanism of CGAs is yet to be understood completely. A lot of studies have been done in the blocking mechanisms of foams, so it is appropriate to look at how foam blocking works.

Foam bridging mechanism is defined by the Jamin effect. The Jamin action is the resistance caused by the boundary condition of detached gas and liquid bubbles confined to capillary spaces (Gardescu, 1930). The Jamin effect was first described by the French physicist Jamin in 1860. It describes a non-wetting fluid's resistance to proceed into a pore of water-wet capillary. Although the description suits foams better, but in the case of CGAs the CGA itself acts as the

non-wetting phase whereas the fluid which surrounds it acts as the wetting phase. The Jamin effect can be described by

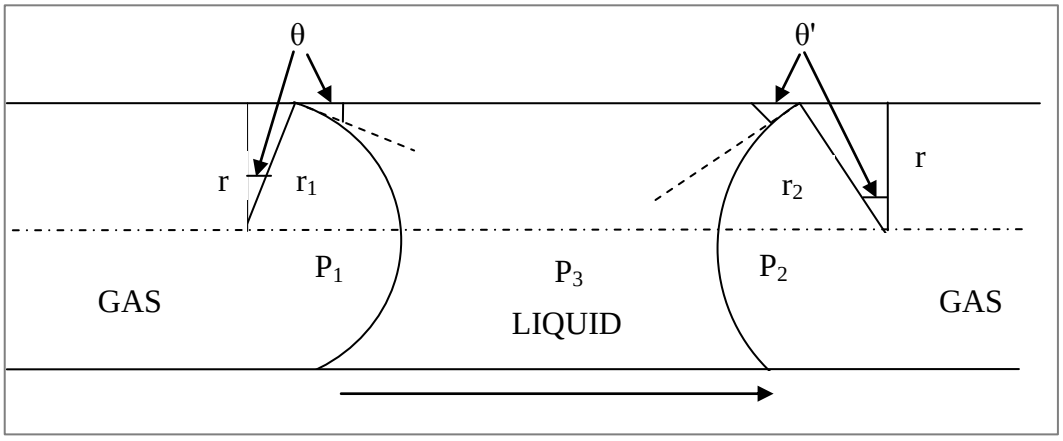

Figure 2-4 below:

In the Jamin tube (the tube in

Figure 2-4) it is assumed that the liquid does not wet the surface of the glass. The surface of the glass tube is dry initially, with the gas bubble moving along the tube. So in the case of the first bubble (the one moving ahead), the liquid film comes in contact with a dry surface, while for the second bubble (the one behind)

Figure 2-4: Contact angles in a Jamin tube (Gardescu, 1930)

the liquid film comes in contact with a wet surface. So the contact angles for the two bubble will not be the same, with θ' being greater than θ. The law of minimum free energy tends to bring the meniscus of the liquid to a spherical surface. Therefore, the two radii for the two bubbles can be calculated:

$$r_1 = \frac{r}{\cos\theta} \qquad \text{(Equation 2-1)}$$

$$r_2 = \frac{r}{\cos\theta'} \qquad \text{(Equation 2-2)}$$

where r is the radius of the tube, and θ and θ' are the contact angles of gas bubbles 1 and 2 respectively.

Now, the Laplace pressure exerted on the interface will be given by:

$$P_1 = P_3 + \frac{2S}{r_1} \qquad \text{(Equation 2-3)}$$

$$P_2 = P_3 + \frac{2S}{r_2} \qquad \text{(Equation 2-4)}$$

where P_1 and P_2 are the pressures exerted by the gas bubbles 1 and 2 respectively, P_3 is the pressure exerted by the liquid and S is the interfacial tension between the gas and liquid. So the amount of pressure that the first bubble should have more than the second is given by the difference between the pressure P_1 of bubble 1 and the pressure P_2 of bubble 2:

$$P_1 - P_2 = 2S(1/r_1 - 1/r_2) \qquad \text{(Equation 2-5)}$$

This pressure difference is what will be required to push the aphron into a capillary like pore throat.

In his paper "Behavior of Gas Bubbles in Capillary Spaces", Gardescu (1930) discussed in a separate section, the distortion of gas bubbles when forced through

capillary openings. A gas bubble is forced through a reduced opening, the diagram is shown in Figure 2-5:

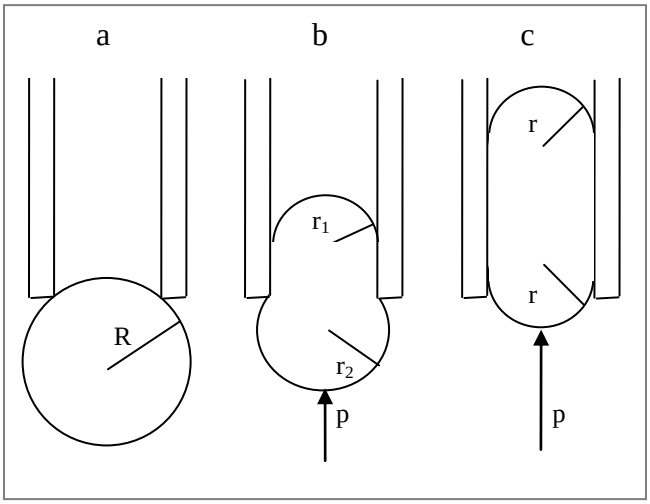

Figure 2-5: Change in form of gas bubble forced through reduced opening (Gardescu, 1930)

Before any pressure is applied at the gas bubble surface, the bubble is spherical (Figure 2-5a). As pressure is applied against the surface, the bubble gets distorted and enters the capillary. It takes a pear shape as shown in Figure 2-5b. This creates two different radii r_1 and r_2, akin to the flow of two bubbles discussed before. The neck of the pear shaped bubble will be gradually lengthened as the pressure applied against the bubble is increased. Consider equation 2-5; p is initially zero when the bubble is spherical with $r_1 = r_2$. A small decrease of r_1 corresponds to a small decrease of r_2, but r_1 decreases more rapidly than r_2. This is because the radius of the opening is small, so for the same volume change r_1 decreases more rapidly. Therefore p must be increased rapidly as the difference

between $1/r_1$ and $1/r_2$ becomes greater. The maximum pressure to be applied is reached when r_1 is equal to r, which is the minimum value that r_1 can assume. Thereafter r_1 will remain constant, while r_2 will continue to decrease, and consequently the required pressure to push in the bubble will also decrease. This continues until the pressure required becomes zero when r_2 becomes equal to r_1 and both equal to r. (Gardescu, 1930).

If the narrow opening can be compared to pore openings, then the situation described above is analogous to pushing the CGA bubbles through a narrow pore throat. The pressure required to push the bubble into the pore throat in this case will be provided by the overbalance pressure in the wellbore. Since majority of formations are water wet (Ivan et al, 2001) the aphron acting as a non wetting phase can be pushed through the pores with the same mechanism.

However, the bridging is also expected to be done by an aggregate of aphrons instead of single bubbles (Brookey, 1998). The CGA drilling fluid will invade the formation fractures and openings because of the pressure in the wellbore; on a micro level the CGAs will expand due to pressure drop. The aphrons aggregate at the openings of low pressure zones to form an "energized environment" in the form of a larger bubble (Ivan et al, 2001). This aggregate will build a solids free bridge which can later be removed by a change in hydrostatic pressure. However, Growcock (2005) found that CGAs have very little affinity for each other and therefore do not aggregate. As such, it can be argued that the aphrons are working only at the capillary dimensions (Ivan et al, 2003). For larger fractures and openings, the mechanism is still open to questions, but it brings into picture the

more important issue of proper sizing of microbubbles in accordance with pore size distribution.

When discussing the usefulness of aphron fluids in an at-balance drilling situation, Brookey (1998) wrote about the ability of the aphrons to create downhole bridging. Brookey wrote about the purposefulness of the surfactant being twofold; to reduce the surface tension for the film formation to contain the aphron as it is formed, and to create interfacial tension to bind the aphrons into a network capable of creating bridging.

Sebba (1987) said that aphrons with the encapsulating shell can attract one another to build up complex aggregates. These aggregated aphrons can be considered constituting a macrocluster system.

Brookey (1998) believed that aphrons can act as bridging solids in the filtrate mechanism. Like conventional solids, aphrons pack off at the formation openings of a permeable zone. Further, aphrons are also capable of adjusting to bridge a fractured or vugular opening by forming aggregates at the openings, something conventional bridging solids are inadequate in doing. These aphron bridging agents can be then readily removed when hydrostatic pressure is released without the need for any cake lift-off techniques.

The issue of sizing of bridging agents (microbubbles in our case) has been studied in a lot of detail if we talk about bridging solids. Abrams (1977) did a study on minimizing rock impairment due to particle invasion. He postulated the famous $1/3^{rd}$ rule: that the median particle size of the bridging additive should be equal to

or slightly greater than one-third the median pore size of the formation. Another rule applied to bridging solids is that particle sizes lesser than one-seventh of the median pore size will not cause any formation damage (Wang et al., 1992). White et al. (2003) stated that rather than Abram's rule, the bridging material should be sized according to the ideal packing theory (IPT). The IPT advocates using the largest particle sizes equal to the size of the fractures to be plugged. In effect, the rule is to have the D_{90} equal to the fractures openings size. White et al. said that the ideal packing defines the full range of particle size distribution required to effectively seal all voids.

With solids bridging, wherever invasion occurs, backflushing will not remove the impairment caused to the formation (Abrams, 1977). This is the advantage with CGAs, where lifting of wellbore pressure will ease out the CGAs from the pores. For CGA bridging, both the microbubble size distribution and the pore size distribution must be known. Proper sizing of the CGAs in accordance and their mechanism in sealing porous media can be studied by visualization studies.

2.4 CGA drilling fluid composition

To generate CGAs in water, the primary component needed is a surfactant. A polymer is generally needed to act as a viscosifier or stabilizer. Brookey (1998) gave a basic composition outline shown in Table 2-1

Table 2-1: Composition of Aphron Drilling Fluid (Brookey, 1998)

Component	**Formulation**
Fresh Water	1.0 bbl
LSRV Viscosifier	2.0 lb/bbl
Thermal Stabilizer	10.0 lb/bbl
Aphron Generator	1.0 lb/bbl

Following extensive work by Growcock in the development and applicability of Aphron based drilling fluid systems, a composition table was suggested by Growcock, Khan and Simon (2003). This table is reproduced here:

Table 2-2: Formulation of typical water based aphron drilling fluid. (*) denotes optional components (Growcock et al 2003)

Component	Function	Concentration
Base Fluid (fresh water or brine)	Provides continuous phase for system	0.97 bbl/final bbl
Soda Ash	Hardness buffer	0.25 lb/bbl
Biopolymer Blend	Viscosifier	5.0 lb/bbl
Polymer Blend	Fluid-loss control and thermal stabilization	5.0 lb/bbl
pH Buffer	pH control	0.5 lb/bbl
Surfactant	Aphronizer	1.0 lb/bbl
Biocide	Biocide	0.05 gal/bbl
Polymer/Surfactant Blend*	CGA Stabilizer	1 lb/bbl
Polymer*	Shale Inhibitor	1 lb/bbl
Oligomer*	Defoamer	1 lb/bbl

In the same paper, Growcock (2003) also discussed the possibility of development of oil based aphron drilling fluids. This is the first time that a discussion on oil

based aphron drilling fluids has been done. Growcock suggested a similar formulation table for oil based aphron drilling fluids:

Table 2-3: Typical compostion of oil based aphron drilling fluid. (*) denotes optional components (Growcock et al 2003)

Component	Function	Formulation
Oil or synthetic fluid	Continuous phase	0.97 bbl/final bbl
Clay or Polymer blend	Viscosifier	15 lb/bbl
Surfactant	Aphron Generator	1.0 lb/bbl
Water	Polar Activator	10.0 lb/bbl
Polymer*	Filtration Control Agent	1.0 lb/bbl
Polymer/ Surfactant blend*	Aphron Stabilizer	1.0 lb/bbl

Making use of colloidal gas aphrons in drilling fluids definitely entails several additional components for specific purposes. Earlier formulations of CGA fluids

made use of basic components – surfactants for CGA generation and polymers/ salts for stabilization.

The purpose of a surfactant is to adsorb itself at the interface, thereby reducing surface tension. Most of the work done in water based microbubbles use cationic or anionic surfactants.

Sebba (1987) talked about the use of Tergitol and Lauryl alcohol as surfactants for CGA generation. Amiri and Woodburn (1990) used a cationic Tetradecyltrimethyl ammonium bromide (TTAB) surfactant for aphron generation. Roy et al (1992) tested an anionic surfactant Sodium dodecyl benzene sulfonate and a cationic surfactant Hexadecyltrimethyl ammonium bromide.

Save and Pangarkar (1993) used four cationic surfactants: Dodecyl trimethyl ammonium chloride (DTAC), Cetyltrimethyl ammonium chloride (CTAC), Cetyl pyridinium chloride (CPC) and Dimethyl distearyl ammonium chloride (DMDSAC). CTAC surfactant gave a higher foam height (representative of yield) and half-life (representative of stability). DMSDAC resulted in highest foam height but a lower foam half life. Save and Pangarkar also tested anionic surfactants- Sodium dodecyl benzene sulphonate (SDBS) and Sodium lauryl sulphate (SLS). The half life was higher for SDBS. They also tested two non-ionic surfactants: Triton X 100 and a lauryl alcohol-ethylene oxide condensate. These non ionic surfactants were added to a solution containing the cationic surfactant CTAC. The result was no significant effect on foam height, but an improved half-life time was observed.

Chaphalkar et al. (1994) used Tergitol 15-S-12 as a non ionic surfactant, Sodium dodecyl benzene sulphonate (SDBS) as the anionic surfactant and Hexdecyltrimethyl ammonium bromide (HTAB) as the cationic surfactant. Jauregi et al (1996) used Sodium bis-(2-ethyl hexyl) sulfosuccinate (AOT) as the surfactant. Hashim et al. (1999) used dilute sodium dodecyl sulphate (SDS) for aphron generation. Hashim et al. (2000) have also uaed benzyl-dimethyl-hexadecyl-ammonium chloride (BDHA), a cationic surfactant for aphron generation. Zhao et al. (2008) used Tween 20 as a surfactant aside from CTAB and SDS.

Bjorndalen and Kuru (2005) used Sodium dodecyl benzene sulfonate (SDBS) and Hexdecyltrimethyl ammonium bromide (HTAB) as surfactants for their study on Colloidal Gas Aphrons. Dai and Deng (2003) tried hexadecyltrimethyl ammonium chloride (HTAC) for the surfactant.

Published work on oil based aphrons is little, and there is virtually no mention of types of surfactants suitable for aphron generation in oil or synthetic fluids. Growcock et al. (2003) talked about the generation of aphrons in oil and they gave a detailed formulation table. However, they do not give any specific information as to what type/class of surfactant is used.

Sebba (1987) used a surfactant called Tergitol 15-S-3, a polyglycol ether that dissolves in kerosene. However, it was used for the preparation of biliquid foams, not CGA's.

Spinelli et al. (2009) created synthetic fluid based aphrons by using ester as a base fluid. For this, they tried three separate surfactants: a nonionic polymeric fluorochemical surfactant, a poly(ethylene oxide)—poly(propylene oxide) (PEO-PPO) block copolymer with different number of units of ethylene oxide (EO) and propylene oxide (PO), and thirdly surfactants produced in the laboratory by saponification reactions using ester as a reagent.

Pan (2008) worked on the creation of aphrons in oil as a medium. He worked on two base fluids- mineral oil and canola oil. Pan tested several surfactants for their ability to generate aphrons with mineral oil; a sodium salt of bis (2-ethylhexyl) sulfosuccinate; two overbased calcium sulfonates with base numbers 300 and 500, and two types of polydimethylsiloxane (PDMS). He had limited success with the sodium salt of bis (2-ethylhexyl) sulfosuccinate and the overbased calcium sulfonate with a base number 500.

Labour (2009) also tried generating microbubbles in canola oil and mixtures of canola oil and mineral oil. For his work, he chose three types of surfactants: an anionic surfactant which was a derivative of phosphoric Acid, a polyoxyethylene-polyoxypropylene block copolymeric surfactant and a polyethylene glycol ester. The phosphoric acid derivative surfactant produced a few microbubbles.

Earlier literature on aphrons does not expound much on polymer additives for the aphron fluid. A reason could be the different applications where the aphron fluids were required. However, in aphronized drilling fluids, the rheology of the drilling

fluids is very critical, with a high LSRV being an important criterion for the microbubbles to be effective in bridging.

For aphron drilling fluids, a high yield stress shear thinning (HYSST) (Brookey 1998, Rea et al., 2003) fluid is best to use. A HYSST polymer serves the purpose of stabilizing the microbubbles in the drilling fluid. Brookey (1998) found a Xanthan biopolymer to be most effective in stabilizing the aphrons in drilling fluids. The Xanthan biopolymer was very good at producing high low shear rate viscosities (LSRV). Ivan et al. (2001) used a biodegradable organic polymer. Save and Pangarkar (1993) used polyethylene glycol (PEG) and polyacrylamide as polymer additives to the aphron fluids. Bjorndalen and Kuru (2005) prepared aphron fluids with a water-Xanthan gum mixture as a base fluid.

Growcock et al. (2003) while talking about oil based aphron drilling fluids say that a polymer or clay blend can be used as a viscosifier. They have also mentioned about separate polymers to be added as filtration control agents and aphron stabilizers. However, again no mention of what types of polymers have been used is there. Pan (2008) used a short chain polyisobutylene (PIB) polymer and Styrene Ethylene/ Propylene Linear copolymer (SEP Linear) for creating aphrons in mineral oil and canola oil separately. Labour (2009) tested a Styrene-Butadiene block copolymer. It dissolved in the mixture of canola oil and mineral oil, but not in mineral oil alone. Spinelli et al. (2009) added two viscosifiers to the ester for making aphrons; Versa, which is commonly used in drilling fluid formulations and Linovac, an ester based viscosifier.

Apart from polymer, other additives such as clays or solids can be added to the fluid. They can serve a more than one purpose- to act as a viscosifier and stabilizer, and as bridging solids. Growcock et al. (2005) tried both polymer viscosified and clay viscosified aphron drilling fluid systems, with both having similar filtration and formation damage characteristics. Spinelli et al. (2009) added to the fluid organophilic clay which had a particle size of less than 10μm.

Electrolytes have also been added in the formulation of CGA solutions. The primary objective has been to investigate the effect of electrolyte concentration on the bubble size distribution and stability of the bubbles. Xu et al. (2008) analysed the effect of salt (NaCl) concentration on the stability and initial size distribution of the aphrons they produced with SDS as a surfactant.

2.5 CGA Generation

CGAs are bubbles in fluid which are so small that they show colloidal properties. Expectedly, they can be produced by shearing reduced surface tension solutions (surfactant solutions) at high speed, or by bubbling fine bubbles into the fluid. Widely, the first method is used for producing aphrons, with variations in the equipment used and the power provided.

When Sebba (1985) first worked on the possibility of producing aphrons, he used a Venturi method for aphron generation. The device for generating aphrons was based upon rapid flow of the surfactant solution through a venture throat, at which point air was admitted through a fine orifice. The Venturi method was a good procedure to form small bubbles- in the range of 25 to 50μm. But the production

was very slow as it required recycling of the dispersion to build up the concentration of the bubbles. Also, the water had to be at a high flow rate so that the bubbles could be entrained in the liquid instead of forming a separate two phase flow. For this, a powerful pump was required. Without a minimum flowrate, the microbubbles could not be produced.

A newer method for CGA generation was subsequently described by Sebba (1985). It consists of a horizontal disc that rotates very rapidly- above 4000 rpm. The disc is mounted between two vertical baffles. The experimental set up is shown in Figure 2-6

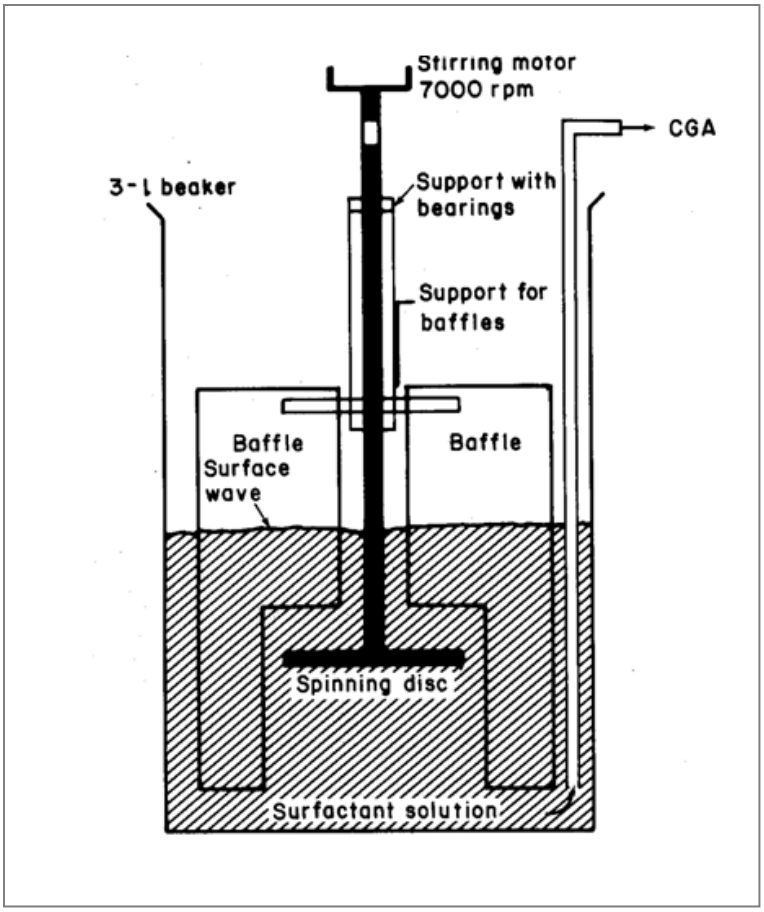

Figure 2-6: Spinning disc CGA generator (Sebba, 1987)

Sebba observed that if the disc rotates at a speed less than 4000 rpm, no CGA are formed, but once a critical speed is reached waves are produced on the surface. These beat up against the baffles/ side walls, and once they re-enter the liquid carries with it a thin film of gas which then becomes minute gas bubbles.

Importance of baffles to achieve the required turbulent mixing regime has been demonstrated. Longe (1989) in his PhD thesis studied the design of CGA generation equipment and suggested the importance of baffles and proper positioning of baffles. Roy et al (1993) used similar CGA spinning disc generators fabricated in laboratory for CGA generation. Chaphalkar et al. (1994)

used a spinning disc generator with baffles, the aphrons were created at a speed of 8000 rpm.

Dai and Deng produced CGAs using a four-blade agitator; they observed CGAs were formed when the agitator speed exceeded 4000 rpm. They surrounded the agitator with a bolt sleeve which had perforations on it. This served the purpose of passing air and water through the perforations which led to entrainment of air. It had two baffles for prevention of vortex formation.

Jauregi et al. (1997) produced aphrons in a fully baffled beaker which was stirred at very high speeds between 5000 to 10000 rpm. Feng et al. (2008) formed aphrons following the methods of Sebba. The stirring speed they used was 8000 rpm and 1 litre of fluid was sheared for 3 minutes to produce aphrons. Xu et al. (2008) recommended a speed of 4000 rpm and said that keeping to a lower speed helped in preventing foam generation. Hashim et al. (1999) produced aphrons with a four blade impeller at a speed of 8000 rpm. The CGA dispersion produced was continuously pumped out to another vessel, where a stirring speed of 1000 rpm is kept to minimize any possible foaming. Zhao et al. (2008) produced microbubbles by stirring at a speed of 7000 rpm. Bjorndalen and Kuru (2005) produced aphrons using a four baffle system at a speed of 5000 rpm.

Save and Pangarkar (1993) used a propeller instead of a spinning disc in order to make use of the propeller's excellent surface aeration properties which are conducive for CGA generation. The propeller rotational speed was 8000 rpm.

Spinelli et al. (2006) described a different procedure for CGA generation, in which the aphrons were formed by the action of a pressure difference in a high pressure high temperature (HPHT) filter press. The surfactant and base fluid mixture was passed through a HPHT filter press without a filter element, under a pressure differential of 1380 kPa to produce aphrons.

2.6 Creaming of Aphrons

Aphrons when produced tend to form a layer and cream to the top of the mixture if not continuously stirred. Sebba (1987) wrote in his book about the tendency of CGAs to rise to the top and form a creamed layer. Because of their lower density, the microbubbles will rise from the bulk of the liquid and collect at the top. On standing, a CGA will separate into conventional foam, which would be floating on clear water, in 10-15 minutes (Sebba, 1987).

Sebba suggested that creaming of the bubbles can be delayed if the solution is stirred at such a rate that the lateral movement conveyed to the bubbles is greater than the upward buoyancy due to gravity. Hashim et al. (1999) created aphrons and the CGA dispersion produced was continuously pumped out to another vessel, where a stirring speed of 1000 rpm is kept to minimize any possible foaming.

Creaming of aphrons, referred to as yield (of the aphrons produced) gives us an indication of the amount of aphrons produced. Save and Pangarkar (1993) evaluated the volume of aphrons formed as a part of characterization of the aphron fluid they generated. They introduced a parameter called dispersion height

(H_d). So the height of the foam that creamed at the top was measured. Jauregi et al. (1996) used a parameter called gas holdup as a part of characterizing the fluids. Gas holdup is the gas volumetric ratio, i.e. the ratio between the gas volume and the dispersion final volume. Feng et al. (2008) referred to the bubble volume fraction of the microbubble dispersion for looking at the amount of aphrons produced. Oliveira et al. (2004) looked at the gas volume fraction and its effect on rheology. Amiri and Woodburn (1990) used a modified Kynch analysis to predict the volume fraction of aphron bubbles immediately above the rising interface between the CGA dispersion and the clear water beneath.

2.7 Bubble Size Distribution

The sizes of the microbubbles and the size distribution of the microbubbles have been studied extensively. Average size of the bubbles is related to the pore blocking ability of the fluid, as such it is important to know the size characteristics of the colloidal gas aphrons produced.

Amiri and Woodburn (1990) found the average size of the microbubbles to be 35μm by analyzing optical microscopic photographs. Sebba (1987) found that when newly formed gas aphrons are examined under the microscope, they were seen to be strikingly uniform in size. However, eventually a size distribution emerged, with most of the bubbles 25μm or bigger.

Feng et al. (2008) took microscopic photographs of the bubbles. These pictures were then analyzed using an image analysis tool pack to obtain the bubble size distribution. About 100-300 bubbles were counted for each sample. Zhao et al.

(2008) measured 130 to 240 individual bubbles using image analysis software and a microscope. Spinelli et al. (2009) used a similar microscope and image analysis software combination to work on the size distribution. Dai and Deng (2002) also analysed slides containing aphrons with a microscope and analysed the pictures later. Save and Pangarkar (1993) used a projection microscope for their work on the size of CGAs created. Growcock (2005) obtained an optical system, which consisted of a viewing cell, microscope, camera and image analysis tools. The setup that Growcock used is shown in Figure 2-7.

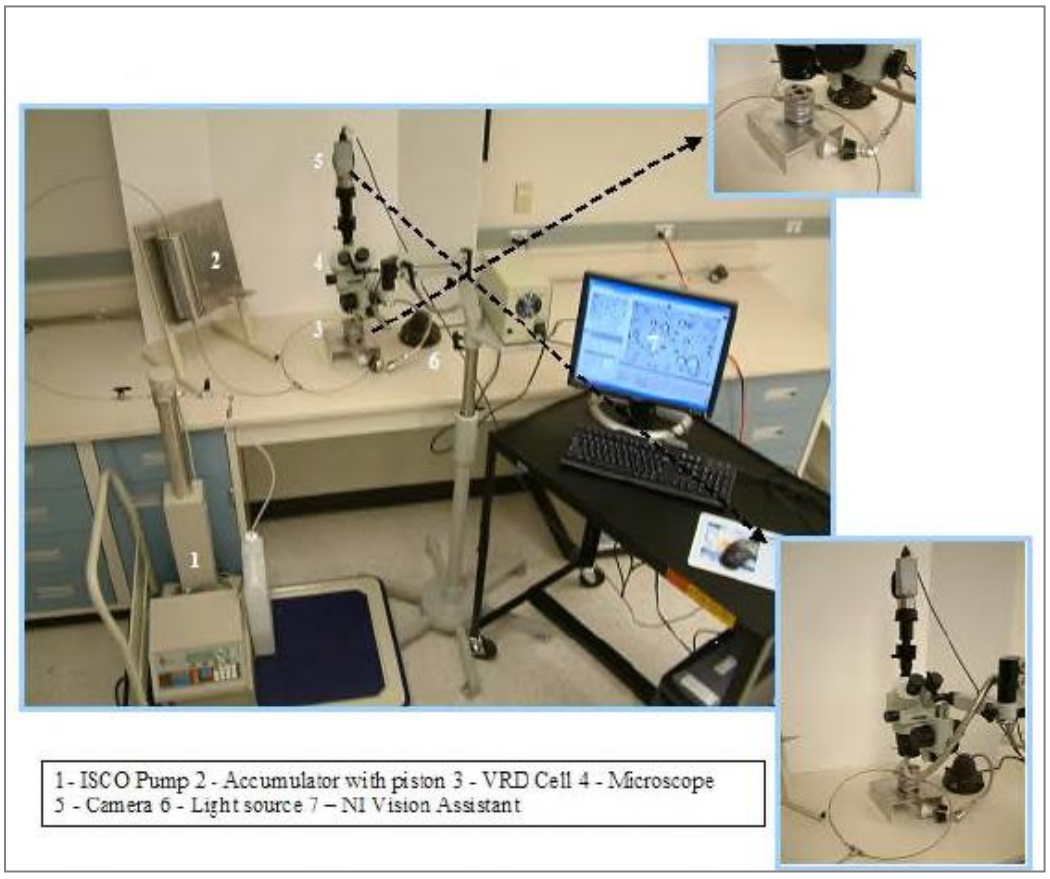

Figure 2-7: Setup for Viewing cell (Growcock, 2005)

A laser diffraction particle size analyzer with a measurement range between 0.03 to 1000 μm was used by Xu et al. (2008) to measure the average size and size distribution of bubbles. Quintero and Jones (2003) did droplet size determination of the internal phase using a light scattering technique. Parthasarty et al. (1991) developed mathematical bubble breakup equations for CGA diameter prediction. Growcock et al. (2004) used another method besides optical microscope photography to get bubble size distribution. They proposed acoustic bubble spectrometry as a way of determining bubble size distribution. It was suggested that acoustic spectrometry will be a good way for analysis of opaque fluids. Under ambient conditions, aphron size varies between 15 to 100 μm (Growcock et al. 2003).

Growcock also used laser light scattering to determine size distribution for the bubbles. A Laser granulometer was the equipment used for the same.

Hayatdavoudi (2006) generated microbubbles with different gases. He observed that the nature of the gas affects the gas bubble sizes, with methane gas producing smaller size bubbles than acetylene. Reid and Santos (2003) stated that the advantage of incorporating aphrons in drilling fluids is that they have a broader size distribution and are deformable.

Xu et al. (2008) looked at the effect of surfactant (SDS) and electrolyte concentration (NaCl) on the bubble size distribution. Zhao et al. (2008) studied the impact of changing the surfactant (SDS and CTAB) on the size distribution of the microbubbles. Dai and Deng (2002) added silica solution (based on hydrogen

silicate H_2SiO_3) to stabilize the bubbles; the effect of silica solution on average size was recorded. Spinelli et al. (2009) performed an important task of investigating the repeatability of bubble size distribution by taking three images for each sample and analyzing them separately, as well as their mean.

2.8 Filtrate Control

Solids in the drill mud serve the key role of providing filtrate control, which in turn is necessary to check formation damage. In the usual scenario the job of filtrate control is done by solids, which form a filter cake to prevent formation damage. Colloidal gas aphron based drilling fluids replicate the scenario except that aphrons act as bridging agents instead of the bridging solids, thus sealing the voids and pores of the formation.

Brookey (1998) advocated the use of high yield stress, shear thinning (HYSST) polymer to viscosify the aphron base fluid. In a HYSST system, because of the very high low shear rate viscosity (LSRV) the aphrons are capable of acting as bridging solids in the filtrate mechanism. The aphrons bridge and pack off at the formation openings of a permeable zone, but unlike conventional solids, they are also capable of adjusting to bridge a fractured or vugular opening (Brookey, 1998). An additional filtrate control additive material used by Brookey (1998) in the HYSST system was an oligosaccharide thermal stabilizer (TS) which was able to effectively control filtrate volume. It worked by enhancing the LSRV properties. Consequently, the control of spurt loss was excellent. Brookey also suggested increasing the intermediate shear rate viscosity (ISRV) so that when

large fractures or vugs are encountered where higher shear may be present, filtrate control still exists.

Growcock et al. (2003) conducted Leak off (spurt + filtration loss through the filter cake) tests in different porous media. In high permeability Ketton limestone cores, the main effect of aphrons was a reduction in spurt loss. In low-permeability cores, filtration rate was reduced more. Further tests were also done with an Aloxite (Aluminium oxide) core to determine whether aphrons could seal porous media with very high permeabilities. The setup is shown in Figure 2-8. Again it was found that aphrons can reduce losses even with cores of highest permeability. Finally, they compared the sealing performance of the water based aphron fluid and a typical drill-in fluid; the results show similar ability of aphron fluids to prevent formation invasion.

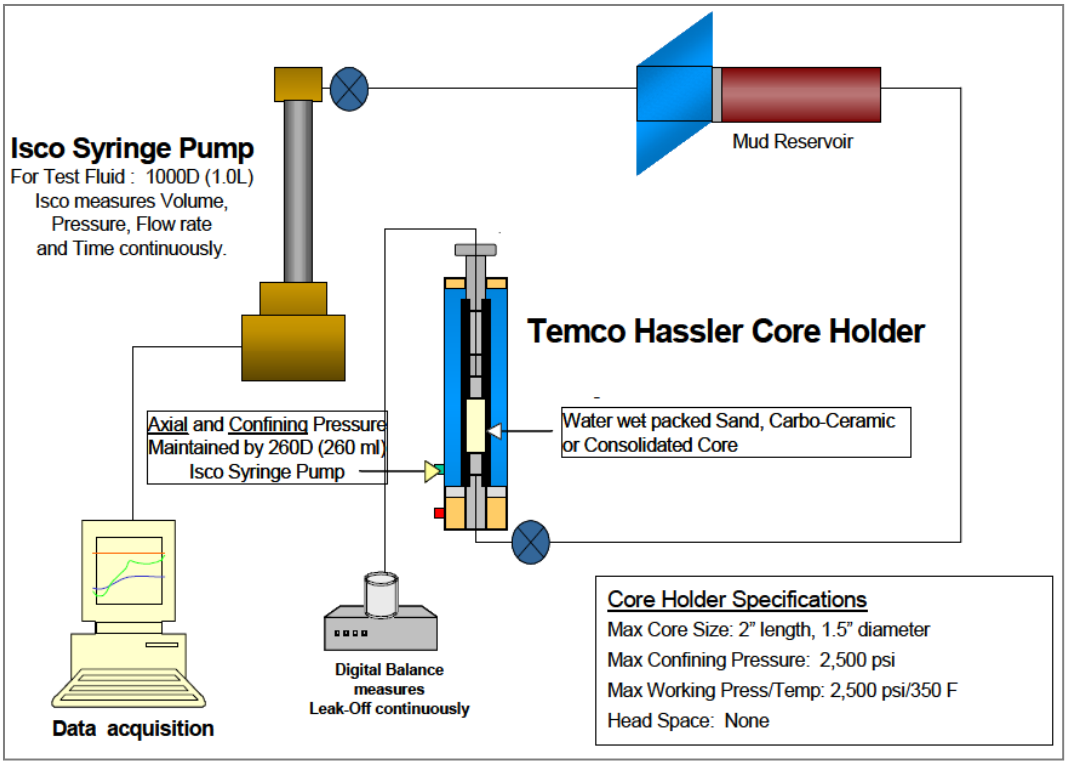

Figure 2-8: Setup for triaxial core holder to perform leak-off tests (Growcock, 2003)

Quintero et al. (2003) conducted dynamic and static filtration using a dynamic filtration device (DFD) and particle plugging apparatus (PPA). The fluid tested was not aphron based fluid, but a similar surfactant-polymer mud that had mixed micelles that produced elevated gel structures in the aqueous phase. The dynamic filtration test suggested that a good filter cake was formed; the spurt loss was further reduced by addition of solids. Static filtration suggested that the filtrate control was good at higher pressures, but bridging agents were strongly recommended.

Spinelli et al. (2009) evaluated the filtrate reduction abilities of aphron fluids. The aphrons were generated in ester. The filtration test was a static standard API test

conducted at 100 psi. They found that increasing the surfactant concentration lessened the rate of API filtrate loss.

2.9 Rheology

When we talk about the rheology of drilling fluids, we are interested primarily in two characteristics: viscosity variation over a broad range of shear rates and viscosity at a low shear rate. The second quantity, termed as LSRV is a very important characteristic of aphronized drilling fluids as LSRV is related to the pore blocking ability of aphrons.

The standard Fann 35 viscometer gives a shear rate range of 5 to 1000 sec^{-1} for a Fann speed of 3 to 6000 rpm. The standard Brookfield viscometer makes a measurement of LSRV at 0.06 sec^{-1}.

Brookey first advocated the use of high yield stress shear thinning (HYSST) fluids to ensure that the low shear rate viscosities of the fluid were sufficiently high. Growcock (2005) in his report "Enhanced Wellbore Stabilization and Reservoir Productivity with Aphron Drilling Fluid Technology" used a Grace M3500 viscometer which could measure for a shear rate range of 0.01 to 1000 sec^{-1} for ambient temperature and pressure. Feng et al (2008) measured the microbubble solution viscosity using a rheometer Physica UDS 200. The solution viscosity increased with surfactant concentration, while pH did not have any effect on the solution viscosity. Oliveira et al. (2004) fabricated a capillary viscometer to measure the viscosity of CGAs in an aqueous solution. They found that CGAs display a strong shear thinning behaviour. The viscosity and yield

stress increased significantly when the surfactant concentration and the gas volume fraction were increased. Zhao et al. (2008) conducted rheological measurements using a flow pipe viscometer and concluded that for all surfactant concentrations, CGA solutions can be treated as shear thinning in nature.

Spinelli et al. (2009) characterized the base fluid for their aphron fluids in a standard Fann 35A viscosimeter. Fann readings at 600 rpm and 3 rpm were recorded. Quintero and Jones (2003) studied the rheology of fluids using a Fann 35A viscometer, a Brookfield viscometer and a SR 5000 rheometer (for viscosity measurement at high temperatures). They found that addition of a thermal stabilizer (Magnesium Oxide) ensured that the viscosity difference between ambient temperature and at 138°C was very small. Growcock et al. (2005) showed that higher air concentrations affected viscosities only at higher shear rates, with LSRV not being affected by air content. Save and Pangarkar (1993) found out that higher viscosity of the liquid phase retarded the hydrodynamic drainage of the aphrons, dampened film deformation and gave stability to the aphron lamella. Bjorndalen and Kuru (2005) measured the viscosity of the aqueous aphron fluid by using a Brookfield DV II Digital Cone & Plate Viscometer and a Fann viscometer.

2.10 Stability

Stability of aphron fluids has been a subject of many studies. The CGAs are expected to change in size and foam volume with time. The size, yield (foam

volume), rheological and filtration characteristics may change when the temperature and pressure conditions are different from ambient conditions.

Sebba (1987) observed that when gas aphrons are newly formed and examined under the microscope, the microbubbles appear to be strikingly similar in size. However, after a few minutes a size distribution begins to emerge. Sebba investigated how higher temperatures influence the behavior of colloidal gas aphrons. He found out that when the CGA solution was heated to 60°C, the bubbles grew so large that even stirring could not keep them in suspension. So he concluded that if CGAs are to be used, it is essential to keep the temperature below 60°C.

Amiri and Woodburn (1990) examined stability by looking at the creaming rate and took microscopic photographs to record the images with time. They found that CGAs changed in size and shape from spheres to irregular polyhedral structures.

Save and Pangarkar (1993) provided a good detailed and extensive analysis on stability. Stability was evaluated in terms of half-life of the foam. The half life (τ_s) of CGAs was defined as the time taken for draining half the liquid used for generation of CGA. They evaluated the effect of type of surfactant and its concentration, time of stirring, viscosity, surface tension and pH of liquid, impeller position and enzyme concentration on the CGA drainage. Variation of pH had no effect on τ_s. With surfactants, the conclusion was that a surfactant with longer alkyl group chain length (CTAC) provides greater stability (τ_s) than a

surfactant with a shorter alkyl group chain (DTAC). Use of branched chain surfactant (DMSDAC) resulted in lesser stability. Addition of non-ionic surfactant increased stability, by increasing inter cohesive forces and imparting higher elasticity to the lamella. Higher viscosity was found to stabilize the microbubbles by increasing the half-life. This is because higher viscosity reduces the drainage rate and inparts strength to the lamellar walls. Addition of enzyme (β-Galactosidase) substantially increased τ_s. This is attributed to decrease in diffusivity of gas through the film due to the presence of long chain compounds. Similarly, half-life also increased with polymer addition. Mixing electrolytes, namely salt (NaCl) to the CGA fluid brought down the stability.

Save and Pangarkar also postulated a mathematical model for drainage:

$$\frac{\partial \varepsilon_L}{\partial t} = \frac{\rho g}{32\mu} \frac{8\varepsilon_L}{\pi n k^2} \frac{\partial \varepsilon_L}{\partial z} \qquad \text{(Equation 2-6)}$$

where ε_L is the liquid holdup, ρ is the bulk density in kg/m^3, μ is the liquid viscosity in kg/m-s, g is acceleration due to gravity in m/s^2, n is number of plateau borders per unit cross section area for dry foams, k is a proportionality constant between gas and liquid holdup and z is height of foam. Comparison of a simulated drainage curve and an experimental curve was made, both were found to be in agreement.

Jauregi (1996) studied the effect of surfactant concentration, salt concentration, pH, time of stirring and temperature on the stability and gas hold up of CGAs. Stability was again defined in terms of τ, the time required for half the amount of

the original liquid to drain. Stability was higher for higher stirring speeds, subsequently 8000 rpm was chosen for further experiments. Stability increased with surfactant concentration but decreased with salt concentration. Time and temperature had lesser effects.

Feng et al. (2008) proposed a drainage equation for a measure of how drainage changes with time:

$$\frac{dV_t}{dt} = V_{max}\frac{t^{n-1}\,K^n[(a-n)(t^a/K^a)+n]}{2(K^n+t^n\text{-}t^a/K^{a-n})^2} \qquad \text{(Equation 2-7)}$$

where V_t and V_{max} are the volume of drained liquid at time t and the final drained volume respectively, K is the half-life for liquid drainage and n and a are parameters.

Xu et al. (2008) found that surfactant provided maximum stability above the critical micelle concentration (CMC), and the presence of electrolyte (NaCl) may improve the stability of bubbles by decreasing the average bubble size.

Spinelli et al. (2009) examined stability by analyzing the change in bubble diameter with time for 0 hours, 2 hours and 24 hours. Stability was examined for aphrons in two separate base fluids: ester and an ester-water emulsion (95% ester + 5% water).The ester-water emulsion was constituted of bubbles that increased their size extremely fast, indicating low stability. On the other hand aphrons made with pure ester presented a slow bubble size increasing, and bubble breaking was only observed after 24 hours.

Dai and Deng (2003) imparted stability to their CGA solution by adding silicic solution and controlling the pH. Silicic solution was from sodium silicate (Na_2SiO_3) neutralized with hydrochloric acid.

Quintero and Jones (2003) added a thermal stabilizer so that the fluid rheological properties did not change with temperature. The thermal stabilizer was Magnesium oxide.

Brookey (1998) found a Xanthan Gum biopolymer to be the best for stabilizing the aphrons. An oligosaccharide did the job of acting as a thermal stabilizer.

Growcock (2005) probed the ability of aphrons to undergo pressurization and depressurization. He also looked at the longevity of aphrons under elevated pressures. It was found out that aphrons can survive pressures as high as 4000 psi. Aphrons compress under pressure, and over time they shrink further due to diffusion of air.

Bjorndalen and Kuru (2006) checked the stability of aphron fluids with respect to time, temperature and pressure. They looked at the change in bubble size as well as change in the creamed layer thickness (yield). It was found that with an increase in polymer (Xanthan gum) content, the bubble size growth was retarded, and the yield was more constant. The CGAs shrunk to about 60-70% of their original size when the pressure was increased from 0 to 50 psig. With increase in temperature, the bubbles grew in size, with the growth being more pronounced between 25 and 50°C than between 50 and 75°C.

2.11 PVT Analysis

The pressure-volume-temperature relationship of a colloidal gas aphron fluid is of particular interest, for the reason that we have gas in the form of aphrons in the bulk of the fluid. Bjorndalen (2010) in her PhD thesis has described a procedure of determining the PVT relation of the fluid using a PVT cell. Based on the PVT data, Bjorndalen developed an equation of state for the aqueous CGA fluid.

2.12 Core flooding tests

Core flooding tests consist of pumping the fluid through a porous medium/ packed core. The objective is twofold; to investigate the ability of the drilling fluid to build up a pressure difference (by bridging) across the core sample and to compare the permeability of the packing before and after the injection of the fluid.

Quintero et al. (2003) performed formation damage evaluation using a permeameter for their surfactant-polymer complex fluid. A measure of the return permeabilities at a high overbalance pressure indicated that formation invasion with the fluids was minimal.

Growcock et al. (2007) studied the flow of aphron fluids through porous media. When the drilling fluid enters the formation, the aphrons move forward rapidly (called bubbly flow) to concentrate at the fluid front and create a microenvironment that separates the bulk fluid from the formation. This inhibits movement of the fluid behind them and limits fluid invasion.

Growcock et al. (2005) examined the formation damage nature of the aphron drilling fluid by carrying out return permeability tests. The tests were carried out

in Berea sandstone at 65°C using inlet and outlet pressures of 2500psi and 200 psi respectively. It was inferred that the formation damage potential of the fluid was quite low (return permeabilities of 80% were recorded) and was comparable to the formation damage caused by a well constructed reservoir drilling fluid. It was also demonstrated that aphrons have a lack of affinity towards silica or limestone surfaces. Thus, they are expected to be pushed back out of a permeable formation easily by reversing the pressure differential, minimizing formation damage and cleanup.

Bjorndalen et al. (2007) conducted experiments using a micromodel to investigate the blocking mechanism. It was observed that foam from the micromodel can be successfully removed by water after injection indicating that the effect of foam is reversible. Bjorndalen et al. (2010) also used a radial core holder to simulate the flow of aphron fluids in a reservoir like scenario. A schematic of Bjorndalen's experimental setup for the formation damage tests is shown in Figure 2-9.

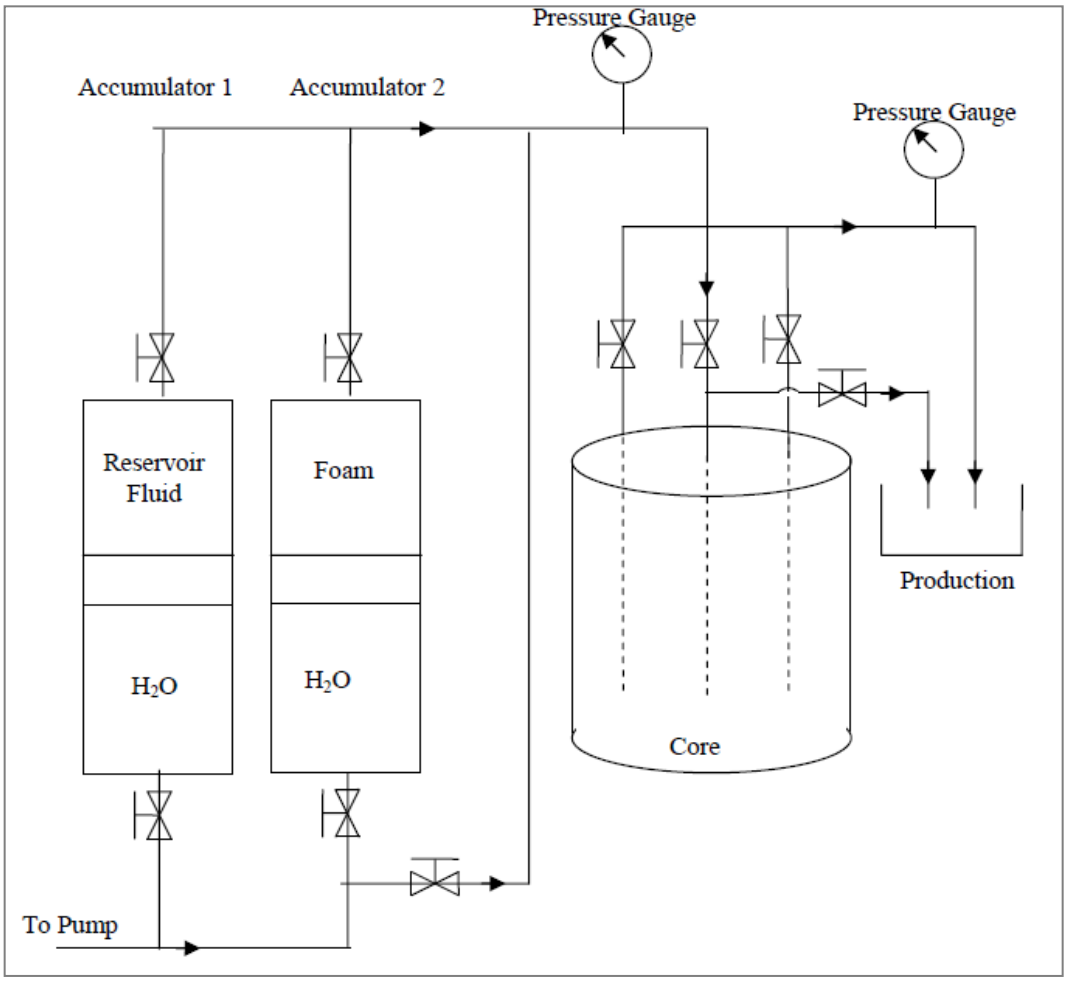

Figure 2-9: Schematic of the Experimental Setup for Core flooding tests (Bjorndalen et al. 2010)

The core was packed with sand which was saturated with a saturating fluid. The CGA fluid was then injected. An increasing pressure drop was observed between the injection and production wells, indicating a buildup of aphrons. After CGA injection, the saturating fluid was re-injected to get an idea about the return permeability.

2.13 Case histories of aphron drilling fluids

Aphron drilling fluids have been successfully used in many field applications. Drilling depleted reservoirs and mature fields is often associated with uncontrollable fluid losses (Growcock 2002). It is in these kind of formations that aphron fluids are suited for application.

Brookey (1998) presented four case studies where aphron fluids have been applied successfully. The first application was in West Texas where a horizontal re-entry well drilled. In the second application, in a dolomitic zone in North Texas where severe lost circulation due to large openings existed, the use of aphron fluids made it possible to drill with no losses. Thirdly, in a shale formation, the high yield stress shear thinning (HYSST) nature of the aphron fluids made it possible to control invasion while providing borehole stability. Fourthly, in a Sisquoc sand well (unconsolidated permeable sand) aphron HYSST drilling fluid provided invasion control and more importantly avoided instability that can be encountered in sand wells.

Ivan et al. (2001) gave a thorough case study of field experience in California while drilling in highly fractured sand in Elk Hills. To control the heavy mud losses, different fluids were tried: a solids free reservoir drilling fluid, a low solids non-dispersed bentonite system and a mineral oil-base system. All of them had limited success, with the losses in each case being in the range of 3500 bbl/well. However, when the aphron fluid system was used, the mud losses were reduced substantially to an average of 1500 bbl per well, with a typical 10% reduction in

drilling time. More importantly, the operator was able to reach the total depth intended without any problems of maintaining circulation.

Mac Phail et al. (2008) described several case studies of wells in Alberta and Mississippi. Aphron fluid technology was successfully applied in several completion and workover applications leading to reduced fluid loss. Rea et al. (2003) wrote about the utility of aphron fluids as a workover fluid in the Tajin field in Eastern Mexico. The bridging provided by aphrons created effective sealing. The aphron technology also provided to be a very economically viable solution.

3 EQUIPMENT AND MATERIALS

The materials and equipment used in this project are discussed in the following sections.

3.1 Materials used for CGA fluid formulation

3.1.1 Base Fluid

In this project, we wanted to produce aphrons in a non-aqueous medium. Mineral oil was chosen as the base fluid. It is a light paraffin oil composed mainly of paraffins and cyclic paraffins. Physical properties of mineral oil are presented in Table 3-1.

Table 3-1: Physical properties of Mineral oil (Fisher Scientific Technical sheets)

Property	Description
Physical State	Liquid
Appearance	Water-White
Odor	None
Vapor Pressure	<0.1 mm Hg
Viscosity	< 33.5 centistokes at 40°C
Boiling Point	260-426°C
Solubility	Insoluble in Water
Specific Gravity/ Density	0.83 @ 15.6°C
Molecular Composition	Paraffin mixture
API Gravity	39°API

3.1.2 **Surfactant**

The purpose of surfactant addition is to reduce surface tension. This aids in the generation of microbubbles, besides imparting a stability and non-coalescing nature to them. Earlier, cationic and anionic surfactants have been used to create colloidal gas aphrons. Because of the difference in nature of oil and water,

surfactants different from what have been commonly used for water-based aphron fluids will have to be employed for non-aqueous CGA generation.

As compared to water, which has a surface tension of 70 mN/m, mineral oil has a very low surface tension, in the range of 25-30 mN/m. So, addition of surfactant reduces the surface activity of mineral oil by a very small amount, therefore, measurement of this reduction of surface tension caused by surfactant becomes difficult. So surface tension measurement tests to check the activity of surfactants in oil may not be feasible. As such, a number of surfactants have been tested in mineral oil to make a check for each whether microbubble generation is possible.

A number of surfactants were tried by Pan (2008) and Labour (2009) in the laboratory, with limited success. Following this, a comprehensive screening study was conducted into the activity and suitability of various classes of surfactants in mineral oil. Unlike water, mineral oil is not a polar fluid, and so it was thought that only non-ionic surfactants will be used. A non-ionic surfactant will be better soluble in oil, and won't interact with any electrolytes present in the system.

Out of the non-ionic surfactants commercially available, the groups thought to be favourable to aphron generation in mineral oil were Sulphosuccinates (esters of sulphosuccinic acid), Sorbitan Esters (fatty acid esters of sorbitans and their ethoxylated derivatives), Fluoro Carbons and Silicone surfactants.

For surface activity in oil mediums a surfactant with a low HLB number should be chosen. HLB is the hydrophile-lipophile balance of a surfactant. HLB numbers

are in a range from 0-20, a higher HLB number indicating water solubility and a lower HLB number indicating oil solubility.

Out of these groups, a commercially available Sorbitan Fatty Acid Ester was selected for testing. The surfactant name is S-MAZ 20 M1. It is a BASF chemical product, the surfactant was supplied by L.V. Lomas Limited. Being a Sorbitan Monolaurate (Sorbitan Monododecanoate), this surfactant is a mixture of partial esters of sorbitol and its anhydrides, and is made from fatty acids, primarily lauric. It has a low HLB value of 8 and has a good solubility in mineral oil and other organic solvents. Physical properties of the surfactant used for the tests are summarized in Table 3-2.

Table 3-2: Physical properties of Smaz 20M1 (BASF technical bulletin)

Property	**Description**
Acid Value, mg KOH/g	6.0 max
Saponification Value, mg KOH/g	158.0 – 170.0
Hydroxyl Value, mg KOH/g	330.0 – 358.0
Water, %	1.5 max
Appearance @ 25°C	Amber Liquid
Form @ 25°C	Liquid
Boiling Point, °F	>300
Color, Gardner	7
HLB Value	8
Specific Gravity @ 25 °C	1.05
Flashpoint, °F	>200
Viscosity @ 25°C, cp	5000 max

3.1.3 **Polymer**

The use of polymer will help control the rheological characteristics (i.e., shear viscosity and low shear rate viscosity, LSRV). The polymer will also help in stabilization of the aphron bubbles by limiting the growth of bubble size with time.

In this study, a commercially available SEP (Styrene-Ethylene-Propylene) linear polymer was used as a viscosifier and stabilizer when formulating the non-aqueous aphron base fluids. The commercial name of the polymer is Kraton G 1702 H. It was supplied by the Kraton Polymer Company. Kraton G1702 H is a clear, linear di-block copolymer based on styrene and ethylene/propylene with a polystyrene content of 28%. The specifications of the polymer used in this study are presented in Table 3-3.

Table 3-3: Physical properties of Kraton G17302H (Kraton Polymers)

Property	**Description**
Polystyrene Content, %	26.2 to 29.0
Volatile Matter, %	< 0.4
Antioxidant, %	0.03 to 0.20
Elongation at break, %	< 100
Tensile Strength, psi	300
Melt Index 230°C, gms/10 min	< 1
Styrene/ Rubber ratio	28/72
Specific Gravity	0.91
Hardness, Shore A	41
Diblock content	100

3.1.4 **Clay**

Clays are often added to drilling fluids to enhance the rheological properties of the fluid. Addition of clay that will behave as suspended particle matter is expected to increase the LSRV and suspension properties of the fluid.

An organophilic clay called Suspentone was used to improve the fluid's ability to suspend weighting agents and drilled solids. So it helps reduce sagging or settling tendencies in deviated or high-angle wellbores. It is particularly suitable for invert emulsion fluids. Suspentone was supplied by the Baroid division of Halliburton. The physical properties of Suspentone are tabulated in Table 3-4

Table 3-4: Suspentone properties (Haliburton product data sheet)

Property	**Description**
Appearance	Tan powder
Specific Gravity	1.6
Bulk Density, kg/m^3	561
Solubility	Not soluble in water or oil
Dispersibility	Readily dispersible
Temperature stability	Upto 205°C

In this project, Suspentone was added only to study its effect on the rheological properties of the aphron drilling mud.

3.1.5 **Wettability Alteration Fluid**

Wettability alteration was done by using a wettability altering fluid. For this purpose, we used Surfasil Siliconizing fluid supplied by Fisher Scientific. SurfaSil

Siliconizing Fluid is a polymeric silicone fluid consisting primarily of dichlorooctamethyltetrasiloxane. The fluid is flammable, corrosive and moisture-sensitive. It has a specific gravity of 1.00-1.03 and a flash point of 87°C. SurfaSil fluid directly reacts with polar groups on the object's surface and results in a hydrophobic surface.

3.1.6 **Glass Beads**

SPHERIGLASS® A-GLASS 3000 solid glass spheres supplied by Potters Industries Inc. were used as porous media material. The glass beads had a particle size distribution of 30-50 microns. The specific gravity of the glass beads as specified by the manufacturer was equal to 2.5.

3.2 Equipment

3.2.1 **Magnetic Stirring Plate**

The magnetic stirring plate is a digital stirring hotplate bought from Fisher Scientific. It comes with magnetic stirring bars that can be placed inside the beaker in which the fluid has to be mixed. The magnetic bar can be rotated by the digital stirring hotplate at a speed range of 60 – 1200 rpm. The hot plate can heat the fluid up to 540˚C. A picture of the stirrer with a beaker on top is shown in Figure 3-1. The magnetic stirrer was used to dissolve the polymer in the fluid for preparation of the base fluid.

. 

Figure 3-1: Magnetic hot plate stirrer for preparation of base fluid

3.2.2 **Homogenizer**

CGAs have been generated using a Polytron PT 6100 digital homogenizer. The homogenizer was purchased from Kinematica Inc. A picture of the Polytron PT 6100 generator is shown in Figure 3-2

Figure 3-2: Polytron PT 6100 high speed homogenizer used for aphronization

It has a shaft which can rotate at speeds of up to 26,000 rpm.

3.2.3 **Digital Scale**

A precision balance called Ohaus EP2102 Explorer did the job of a digital scale. An image of the weight balance is shown in Figure 3-3.

Figure 3-3: Digital weight balance

3.2.4 **Microscope System**

For size analysis of the colloidal gas aphrons, a Leica DM 6000M microscope was used. A picture of the microscope is shown in Figure 3-4. The microscope has a camera attached to the top for taking images.

Figure 3-4: Leica DM 6000M microscope used for imaging

3.2.5 **Rheometer**

The rheometer is BOHLIN CVOR supplied by Malvern Instruments. Figure 3-5 is a photograph of the rheometer in the laboratory. The rheometer has a shear rate range of 0.0001 to 10,000s^{-1}, obviating the need of using Brookfield or Fann viscometers.

Figure 3-5: Bohlin CVOR cone and plate rheometer

The rheometer can be fitted with two types of cells for measuring rheology. The CVOR150 Peltier cell attached to the Bohlin rheometer (shown in Figure 3-5) is a cone and plate measuring system. This system was used to rheologically characterize the fluids. Samples were placed in a 0.15mm gap between a rotating upper cone with a 4° angle and a diameter of 40mm, and a fixed lower plate with a diameter of 60mm.

The rheometer also has a high pressure cell provided. This high pressure cell (HPC) can be attached instead of the cone and plate arrangement. The high pressure cell attached to the rheometer is shown in Figure 3-6.

Figure 3-6: High pressure cell fitted to the Bohlin CVO rheometer

3.2.6 **API Filter Press**

Standard API filtration tests (100psi, ambient temperature) were done using a standard API filter press. The equipment was supplied by Ofite testing equipments Inc. Figure 3-7 is a picture of the filter press.

Figure 3-7: Standard API filter press

3.2.7 **HTHP Filter Press**

High temperature and high pressure filtration (HTHP) tests were performed with HTHP API filtration equipment. The equipment was from Ofite testing equipments Inc. Figure 3-8 is an image of the HTHP filter press.

Figure 3-8: HTHP API filter press

3.2.8 **PVT Cell**

The pressure-volume-temperature (PVT) relationship of the fluid was measured with a Schlumberger DBR PVT cell. It is a 100cc, 15ksi cell specifically designed for the measurement of fluid properties and study of fluid phase behaviour. An image of the cell is depicted in Figure 3-9. The cell is placed inside a larger enclosement. There is a camera placed in the front so that it can focus on the cell. The live view from the camera is transmitted to a screen.

Figure 3-9: Schlumberger DBR PVT Cell used for PVT analysis

3.2.9 **Syringe Pump**

For the objective of core flooding, an ISCO LC-5000 syringe pump was used. A laboratory picture of the syringe pump is depicted in Figure 3-10. The ISCO LC-5000 syringe pump was used for pumping the aphron drilling fluid into the core. It is a constant rate pump with a flow rate range up to 400 ml/hour. The pump has a 500 ml capacity.

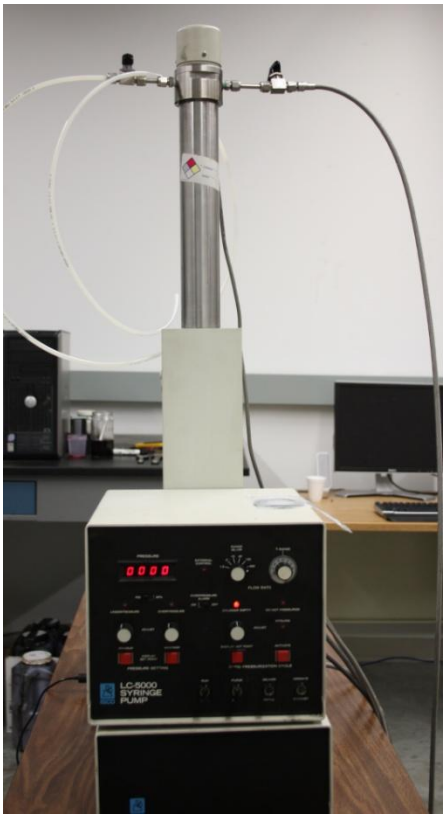

Figure 3-10: Syringe Pump for injecting fluid into the packed core

3.2.10 **Data Logging**

The data acquisition system consisted of transducers as pressure sensors and a data logging system. Two transducers from Omegadyne were available in the lab, with a pressure range from 0-100 psi and 0-500 psi respectively. Data logging was done with a National Instruments data acquisition system NI USB-9219. The data acquisition system transferred the pressure readings to the computer, where they were recorded in the Labview Signal Express software provided by National instruments.

3.2.11 **Radial Core Holder**

A radial core holder (a pressure vessel) was employed in the core flooding experiments for packing the glass beads. The core flooding experiments were conducted using a special core holder designed to simulate radial flow, which allowed to conduct flooding experiments in more realistic wellbore conditions.

A picture of the radial core holder is shown in Figure 3-11. One injection well and two production wells can be seen. Injection was done through the injector located at the center of the cell and fluid was produced through the producers located at the periphery.

The core holder has an internal diameter of 98 mm and a height of 191 mm. The perforated height is 145 mm. It had one injection line and two production lines. The radius of the injection line was 7 mm and the radius of both production lines was 3.6 mm. Injection was done through the injector located at the center of the cell and fluid was produced through the producers located at the periphery. The injector and the two producers were encased with a slotted screen with an opening size of approximately 10 microns. The cell was designed to roughly simulate radial flow by equipping the inner diameter of the aluminum pressure vessel with a screen. The screen encouraged flow around the outer edge of the pressure vessel to the producer tubes. Both ends have ports, with the bottom end utilized as a sand packing port to pack the vessel with glass beads.

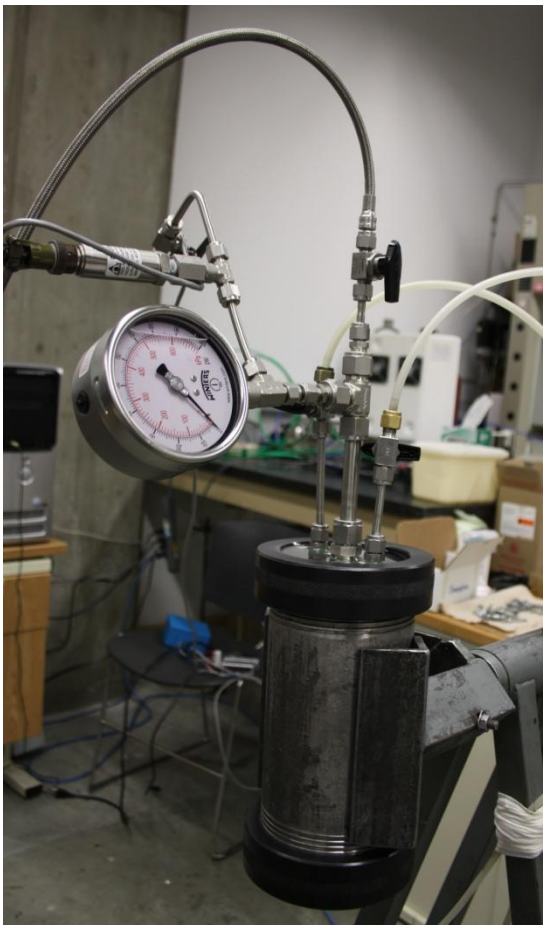

Figure 3-11: Radial core holder, fitted with pressure gauge and pressure transducer

4 PHYSICO-CHEMICAL CHARACTERIZATION OF CGA FLUID

In this chapter, the experimental procedure and the results for the CGA fluid characterization have been described. The procedure of generating the CGAs in the base fluid is presented first. Subsequently, the physico-chemical characteristics of the fluid i.e. the yield, average bubble size, density, rheology and API fluid loss were measured. The surfactant and polymer concentration were varied to look at their effect on the physico-chemical parameters that define the fluid. Based on the results of the change in properties of the fluid because of change in surfactant and polymer amount, an optimum formulation for the fluid has been proposed.

4.1 Experimental Procedure for Characterization of the CGA Fluid

4.1.1 Preparation of Aphronized fluids

Preparation of Base Fluid

The first step in creation of aphronized fluid is to formulate the base fluid. Normally, 100 ml of mineral oil is taken. The polymer is added in the desired concentration to mineral oil. This mixture is mixed in the digital stirring hotplate. The polymer-mineral oil mixture is then cooled and surfactant in the desired amount is added to the fluid.

Preparation of CGA fluid

The mixture is then mixed with the high speed homogenizer, Polytron® DT6100. This homogenizer has a dispersing aggregate attached to it which assists in air entrainment. Mixing was carried out at a shear speed of 7000 rpm for 45 seconds.

The shearing speed and shearing time were kept constant for the purpose of uniformity of microbubbles created throughout the experiments. Following aphronization, the fluid was taken for characterization without any rest time.

4.1.2 **Yield**

Evaluating yield

Yield is a measure of the quantity of aphrons generated. Upon aphronization of the solution, a sample of 50 ml is poured into a graduated flask. The aphrons will cream to the top and form a layer. An interface is formed between the layer of the risen bubbles and the bulk oil. This is depicted in Figure 4-1.

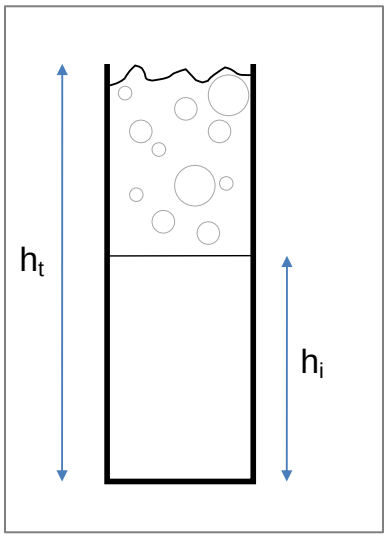

Figure 4-1: A sketch depicting how creaming is measured

Here h_t is the total height of the fluid in the measuring cylinder and h_i is the height of the interface between the creamed layer of bubbles and bulk oil. The difference

between total height h_t and the height of the interface h_i gives us the creamed volume. This creamed volume is a measurement of the aphron yield of the fluid and is calculated by using the following equation:

$$\text{Yield} = \left(\frac{h_t - h_i}{h_t}\right) * 100 \qquad \text{(Equation 4-1)}$$

Measurement of yield with formulation

Yield was measured for a range of surfactant concentrations. Several aphron fluids were prepared by using surfactant concentration varying from 0.1% w/w to 1% w/w.

With the addition of polymer, the aphrons tended to be more evenly distributed throughout the volume of the aphronized fluid. As a result, the interface between the creamed layer and the bulk volume of the base fluid became hazy and unclear. The variation of the yield as a function of polymer concentration could, therefore, not be depicted accurately.

4.1.3 Measurement of Aphron Bubble Diameter

Measurement of CGA bubble diameter

The size of aphrons has been determined by using a visual imaging system, which consists of a camera attached to an optical microscope. The microscope is connected to a computer for viewing and recording the images. A picture of the setup is shown in Figure 4-2.

Figure 4-2: Setup of Microscope and Camera with the picture viewed on the Computer

Immediately after aphronization the CGA sample was poured into a microscopic slide and the microscope was used for viewing the microbubbles. By doing so, any rest time/ gap between aphronization and image analyses was avoided. The pictures of the microbubbles were taken by using a camera attached to the microscope. The images of the microbubbles were taken through the camera using the microscope workstation software (Leica Materials workstation). The images were recorded for processing and bubble size analyses.

These pictures were then printed and the bubbles were manually measured for bubble diameters using a ruler. A scale of the image versus actual size is given by the Leica Materials workstation. This scale can be varied by changing the

magnification of the microscope lens. For example, when a 2.5x lens of the microscope was used, 50mm on the printed picture corresponded to a 1000μm. The scaling factor was used to convert the aphron diameter (measured on the printed picture) to the actual length in microns.

CGA diameter analysis

Care was taken to make a large number of measurements, so as to maintain uniformity of data and produce a representative size distribution. These size measurements were then recorded in Microsoft Excel. Typically, 300 bubble size measurements were made per picture. All these were entered into the spreadsheet program. The measurements were then sorted according to their size. Subsequently, a cumulative bubble size distribution curve (analogous to a particle size distribution curve) was drawn. A typical bubble size distribution curve is shown in Figure 4-3.

From this curve the median diameter D_{50} was determined. D_{50} is the diameter below which 50% of the bubbles have a smaller size and the rest 50% have a larger size.

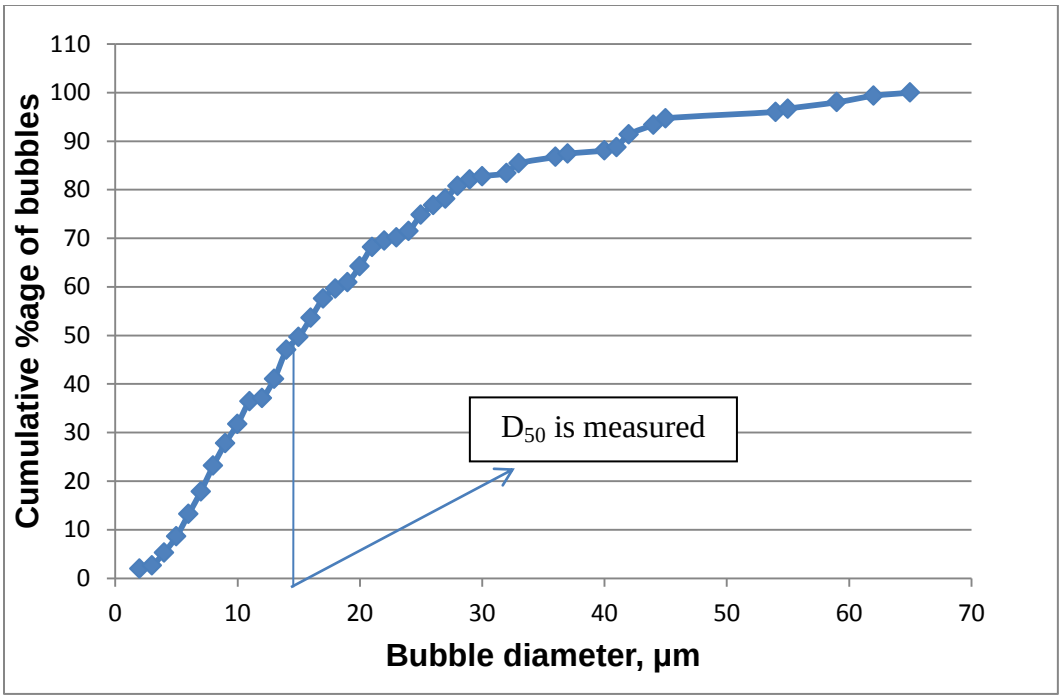

Figure 4-3: Typical cumulative bubble size distribution curve showing how D_{50} is measured

Measurement of CGA diameter with different formulations

The polymer and surfactant concentration were varied in the fluid formulation. Polymer was added to the mineral oil in increments of 0.5% w/w beginning with pure oil (0%), 0.5%, 1%, 1.5% and up to 2% w/w polymer. The surfactant was added in steps of 0.1% w/w, beginning with pure oil up to 1% w/w surfactant. These different formulations were studied for average bubble size, the aim being to find the effect of polymer and surfactant concentration on the average bubble size.

4.1.4 **Filtration Tests**

API Filtration

To have an idea about the effectiveness of the aphron drilling fluid in preventing invasion of the reservoir rock by the drilling fluid, and consequently minimizing formation damage, filtration loss tests were conducted.

Standard API filtration tests were conducted using a standard filter press at 100 psi pressure and room temperature. A schematic of a standard API filtration test is shown in Figure 4-4.

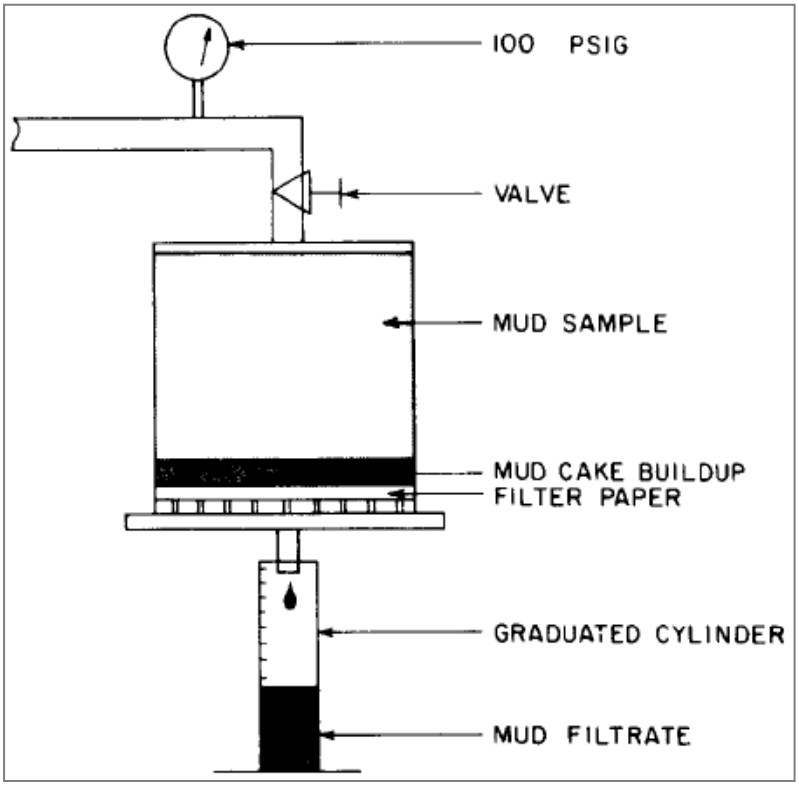

Figure 4-4: A schematic of a standard API filter press

The mud filtrate volume (in ml) collected over a 30 minute period is reported as the API filtration loss. The filtrate volume was continuously recorded as a function of time to see how the rate of filtration actually changed over time.

It has to be mentioned here that dynamic filtration tests were not conducted for the fluid. We do not have the equipment needed for performing dynamic filtration tests. As such, the static filtration test results reported here are only indicative results, and are not entirely representative for the fluid.

Filtration for different formulations

API filtration was measured for different formulations. The surfactant content was varied keeping the polymer content the same. Three aphronized fluids were prepared by using 1.5% polymer concentration and 0.2%, 0.4% and 0.6% surfactant concentrations.

Next, the polymer concentration was varied keeping the surfactant concentration the same. Four aphronized fluids were prepared by using 0.4% surfactant concentration and 0.5%, 1.0%, 1.5% and 2.0% w/w polymer concentrations.

4.1.5 Rheological Characterization

Measurement of rheological characteristics

Rheological characterization of the non-aqueous aphron fluids was conducted by using a cone and plate type rheometer (Bohlin CVOR). The flow characteristics of the sample were presented by plotting variation of shear stress versus shear rates. From the viscometry results, the shear viscosity versus shear rate was determined. These were measured for a shear rate ranging from 0.1 to 100 s^{-1}.

Viscosity for different formulations

The shear viscosity was measured over a range of shear rates for surfactant concentration varying from 0.1% to 1% wt/wt.

The shear viscosity was measured similarly with polymer concentrations varying between 0% and 2% wt/wt.

Investigation of hysteresis in rheology

As a part of the rheological characterization, it was investigated whether there is any hysteresis in the shear viscosity vs. shear rate analysis. For this purpose, the shear rate was raised to a point and lowered thereafter, continuously recording the shear viscosity. The two curves were then compared.

Low Shear Rate Viscosity (LSRV)

The low shear rate viscosity (LSRV) is an important characteristic for drilling fluids. The LSRV of the aphronized fluid were determined as part of the rheological characterization study.

The LSRV was measured at a shear rate of $0.1s^{-1}$. It was recorded for changing polymer concentrations. The effect of Suspentone on the LSRV was recorded too.

4.1.6 Density Measurement

The density of the fluid was measured by using the digital scale. An empty beaker was weighed with a digital scale. The beaker was then filled with a known volume of the CGA fluid. It was then weighed with a digital scale. The difference between the weight of the empty beaker and the weight of the beaker filled with the fluid was used to determine the weight of the CGA fluid. Since the

volume of the fluid in the cylinder was also known, the density of the fluid could be obtained from dividing the weight by the volume of the CGA fluid. The measurement of density was done to look at the variation of density with polymer concentration and surfactant concentration.

4.2 Results and Discussion (Physico-Chemical Characteristics)

Colloidal gas aphrons were created in mineral oil with the polymer and surfactant discussed in the Materials chapter of Materials and Equipment. A picture of the aphrons generated in oil is given. A structure is suggested for the oil based aphrons next.

After this, a characterization of the fluid has been attempted for the microbubbles developed. This has been done by measuring the physico-chemical characteristics relevant to the fluid. The characteristics measured are the yield of aphronized fluid, the size distribution of the micro bubbles, the API fluid loss, density and rheology. For each of the mentioned parameters, the surfactant and polymer concentration were changed and consequent effect on the physical parameters was analysed. So, the effects of polymer and surfactant concentration on the yield, aphron bubble diameter and the API fluid loss were investigated. Effects of surfactant and polymer concentration on the rheological behavior of the aphronized fluid were also investigated.

4.2.1 **Non-Aqueous CGA structure**

A picture of aphrons typically created is shown in Figure 4-5. A gas core is visible in the center surrounded by a viscosified oil-surfactant layer. Mineral oil is present in the bulk phase.

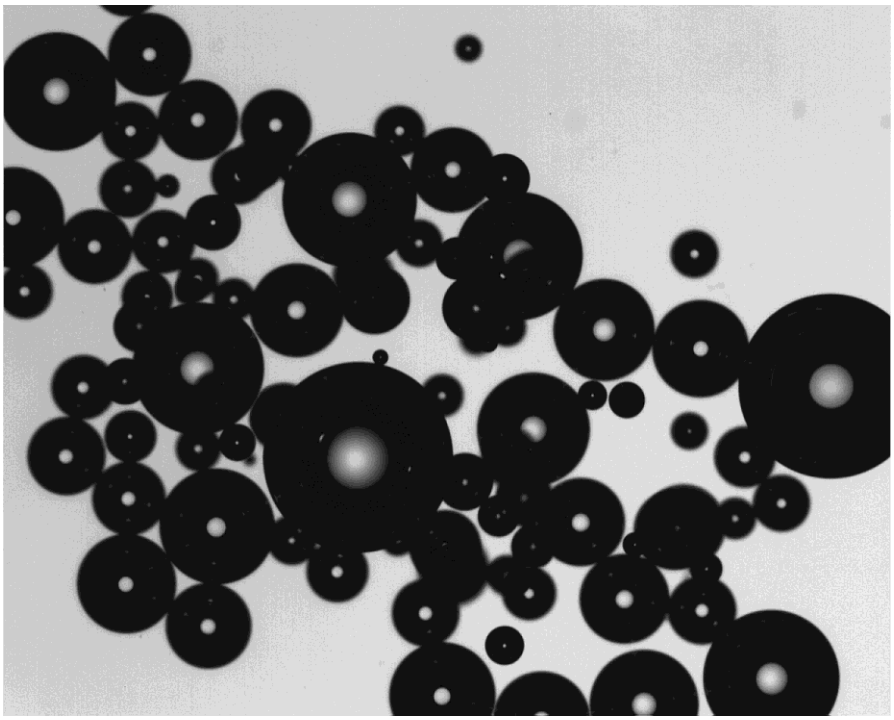

Figure 4-5: Picture of aphrons typically created in this study

Development of colloidal gas aphrons in a non aqueous medium was a relatively new thing to do; consequently there was not a lot of idea about how the structure and nature of the fluid will be. Sebba (1987) proposed a structure for CGAs in water. A film of viscosified water lies over the inner surfactant layer, and above that is a bilayer of surfactants (Figure 2-2).

Growcock et al. (2004) suggested a structure for oil based colloidal gas aphrons. In this structure, a viscosified aqueous or polar layer will surround the inner

surfactant film, and this is kept in place by an outer monolayer of surfactants (Figure 2-3).

One version of oil-based aphron technology incorporates no aqueous layer at all, so that the inner and outer surfactant films come together to form a bilayer. Since no water has been added to the fluid for aphron generation, this is the structure of the oil based aphrons expected in our study too. A proposed diagram is shown in Figure 4-6. A viscosified oil layer surrounds the air core, stabilized by the surfactant double layer. This surfactant double layer also helps in stabilizing the aphron, preventing it from coalescing with other aphrons. This structure corroborates with the microscopic picture of aphrons in oil given in Figure 4.6.

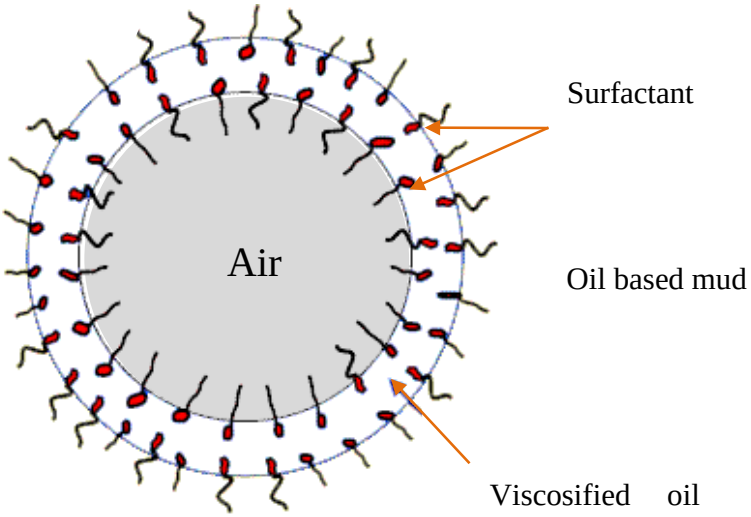

Figure 4-6: Proposed structure for aphrons in oil-based mud

4.2.2 **Yield**

Determination of yield is very important as it is a measure of the amount of aphrons generated in a sample. The measurement of yield has been done for a range of surfactant concentrations.

Surfactant effect on yield

The variation of yield with surfactant concentration is shown in the Figure 4-7. Several aphron fluids were prepared by using surfactant concentrations varying from 0.1 % w/w to 1% w/w. As the surfactant concentration increases from 0.1% to 0.4 %, the yield also increases. Increasing the surfactant concentration from 0.4 % to 1%, however, does show reverse trend by decreasing the yield. Maximum yield was obtained when the surfactant concentration was at 0.4% w/w.

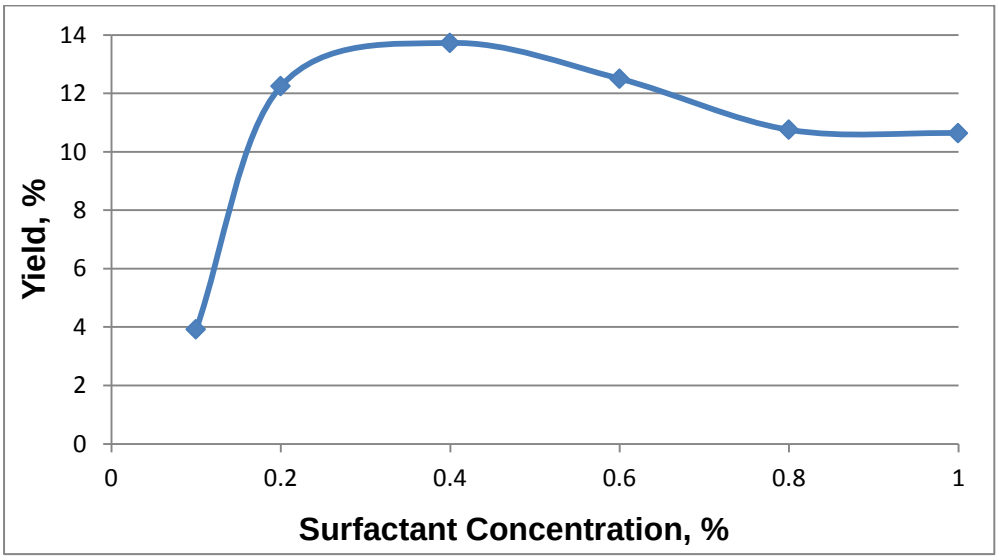

Figure 4-7: Effect of surfactant concentration on the yield of the aphronized fluid

With the addition of polymer, the aphrons tended to be more evenly distributed throughout the volume of the aphronized fluid. As a result, the interface between the creamed layer and the bulk volume of the base fluid became hazy and unclear. The variation of the yield as a function of polymer concentration could, therefore, not be depicted accurately.

4.2.3 **Aphron Bubble Size**

Aphron bubble size was measured using the photomicrographic technique discussed. The measurements were then analysed and presented graphically. The bubble size distribution of a typical aphron fluid is shown in Figure 4-8. In this graph, the frequency (number of bubbles expressed in percentage terms) has been plotted against the sizes of the bubbles.

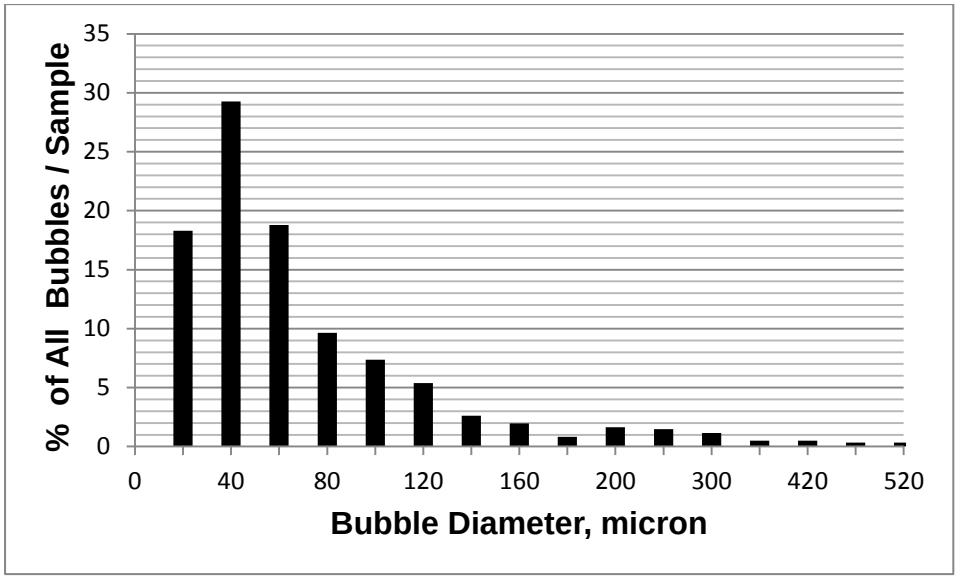

Figure 4-8: Typical size distribution of the microbubbles

Repeatability of Bubble Size Distribution

For statistical analyses purpose, we measured the bubble size distribution of four samples taken from the same batch of aphron fluid. Each of the four samples were analysed separately for size distribution data. This was done to know how repeatable the bubble size distribution measurements were. Figure 4-9 summarizes the results of repeatability of bubble size measurements.

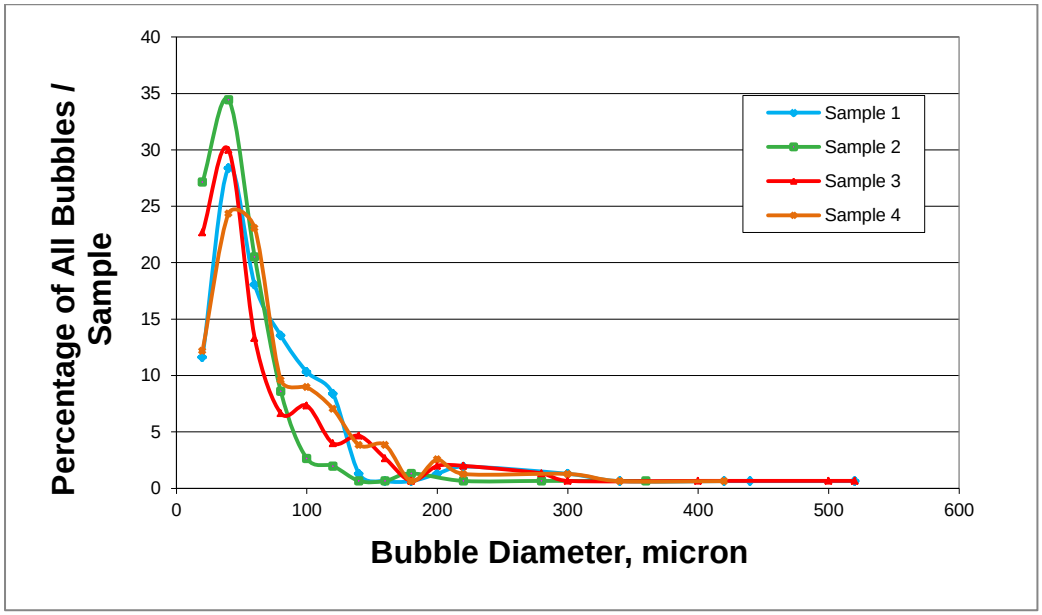

Figure 4-9: Repeatability of the bubble size distribution

It can be seen that the peaks of the curves representing the percentage of bubbles coincide at a near same bubble diameter. The frequency (percentage of bubbles) varies though.

Effect of Surfactant Concentration

The effect of surfactant concentration on average bubble size (D_{50}) is shown in Figure 4-10. Although there is no clear trend, on an average there is about 10 to 15% variation in bubble size with changing surfactant concentration.

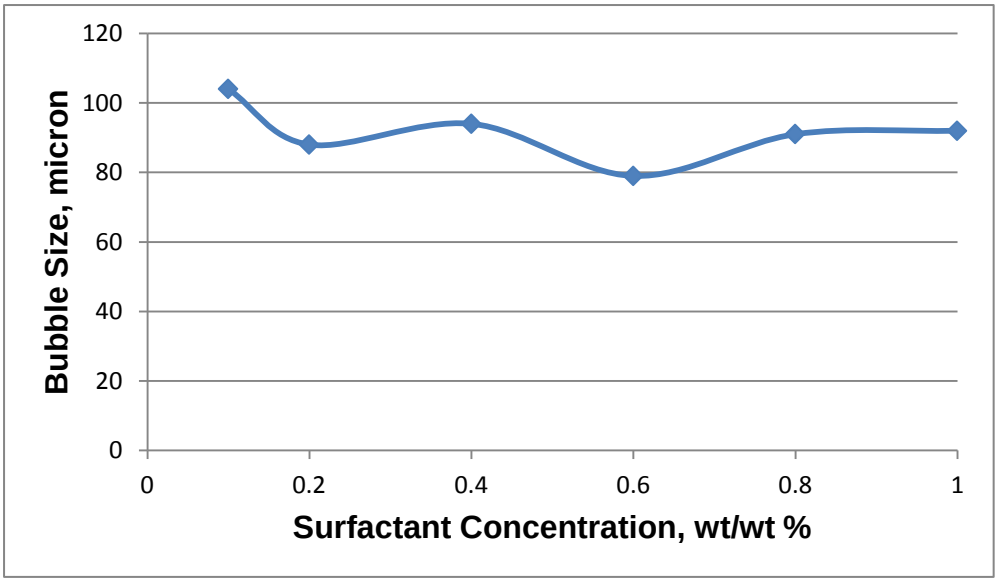

Figure 4-10: Effect of surfactant concentration on the average aphron bubble size (D_{50})

Effect of Polymer Concentration

The effect of polymer concentration on the average aphron bubble size (D_{50}) is presented in Figure 4-11. It confirms that an increase in viscosity of the base fluid increases the stability of the system by bringing down the average bubble size. Average bubble size (D_{50}) of the freshly prepared aphron fluid decreased by about 70% as the polymer concentration is increased from 0 to 0.5% w/w. There was about 50% increase in average bubble size when the polymer concentration is

changed from 0.5 to 1.5 %. Increasing polymer concentration above 1.5 % did not seem to have any effect on the size of the bubbles.

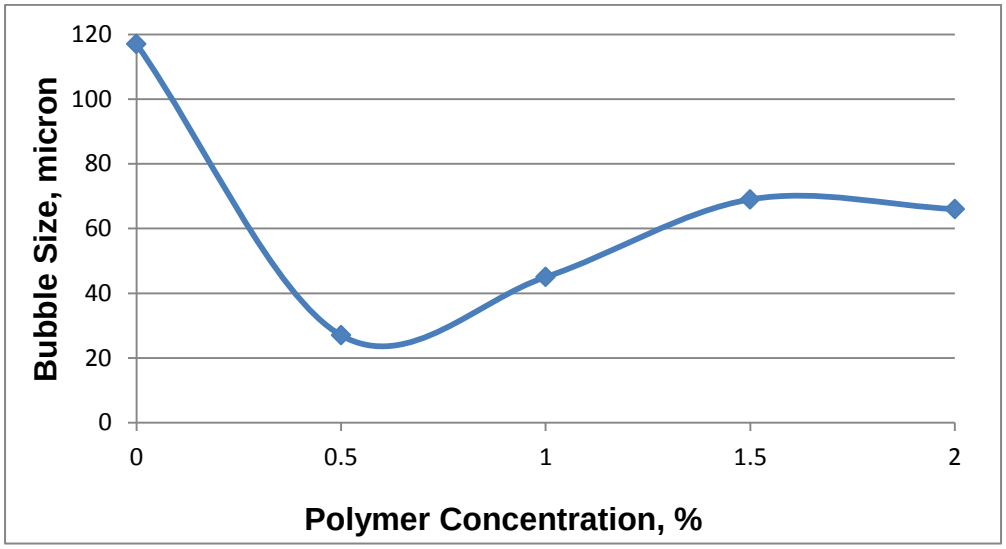

Figure 4-11: Effect of polymer concentration on the average aphron bubble size (D_{50})

4.2.4 **Density**

Density was measured for the aphron fluids over a similar range of surfactant and polymer concentrations. The results are presented in tabular form.

Surfactant effect

The effect of surfactant concentration on the density of the drilling fluid is presented in Table 4-1. The density of the pure mineral oil is 820 kg/m^3. On addition of surfactant the density of the drilling fluid decreases, reaching a minimum of 707 kg/m^3 before increasing again. It was discussed above that the yield is highest for 0.4% surfactant concentration. So, as the volume of air entrained (aphrons) increases, the density of the fluid decreases.

Table 4-1: Change in density with change in surfactant concentration

Surfactant Conc., %	**Density, kg/m^3**
0%	820
0.1%	795
0.2%	737
0.4%	707
0.6%	729
0.8%	747
1%	754

Polymer effect

Varying polymer concentration from 0% to 2% wt/wt did not change the aphron fluid density considerably (

Table 4-2). The slight increase in each step is because of the additional amount of polymer added.

Table 4-2: Change in density with change in polymer concentration

Polymer Conc., %	Density, kg/m^3
0%	707
0.5%	716
1%	714
1.5%	718
2%	716

The aphronized fluid densities reported here are all measured in atmospheric pressure conditions. This may change when the fluid is circulated downhole, where the pressure will be much higher than atmospheric pressure.

4.2.5 **API Filtration**

To have an idea about the effectiveness of the aphron drilling fluid in preventing invasion of the reservoir rock by the drilling fluid, and consequently minimizing formation damage, API filtration loss tests were conducted.

Variation of the filtration loss of aphron base fluid with time is shown in Figure 4-12. The aphron fluid was prepared by using 1.5% polymer and 0.4% surfactant. Initial decrease in the filtration rate (as indicated by declining slope of the filtration volume vs time curve) indicates that external bridging/blocking occurs

due to accumulation of the microbubbles. Rate of filtration then stays constant after the first 10 minutes of filtration.

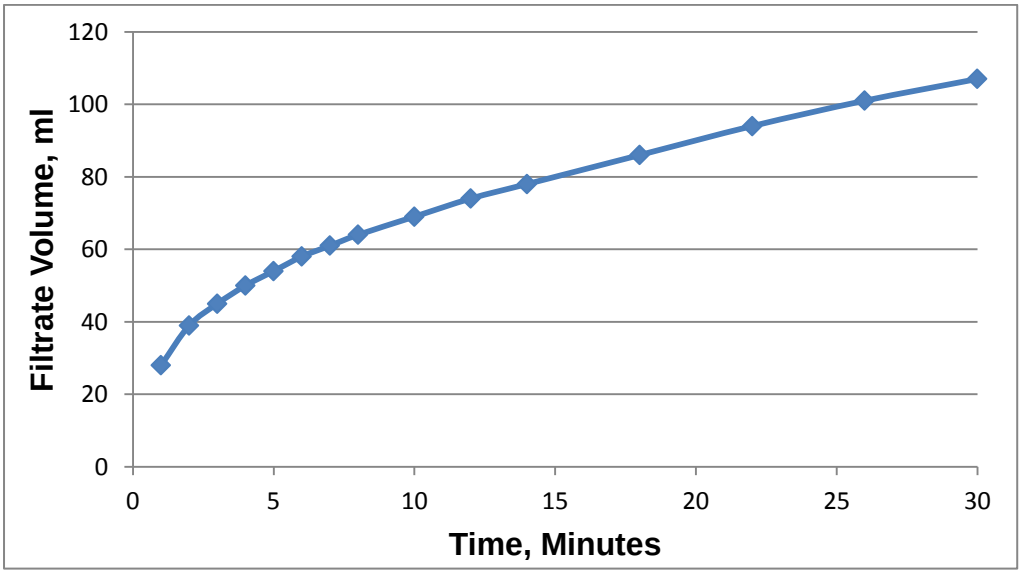

Figure 4-12: Filtration loss of aphron base fluid with time (1.5% Polymer and 0.4% Surfactant)

Effect of Surfactant Concentration

Effect of surfactant concentration on the API filtration loss of aphron fluids is shown in Figure 4-13. Three aphronized fluids were prepared by using 1.5% polymer concentration and 0.2%, 0.4% and 0.6% surfactant concentrations.

Although increased surfactant concentration meant more microbubbles generated, effect of increasing surfactant concentration on the filtration loss of aphron fluids was found to be insignificant. This could be because the test is a static test, not dynamic and a small filter paper area is available for filtration. In a small filtration

area, the number of microbubbles available beyond a certain point does not make a difference.

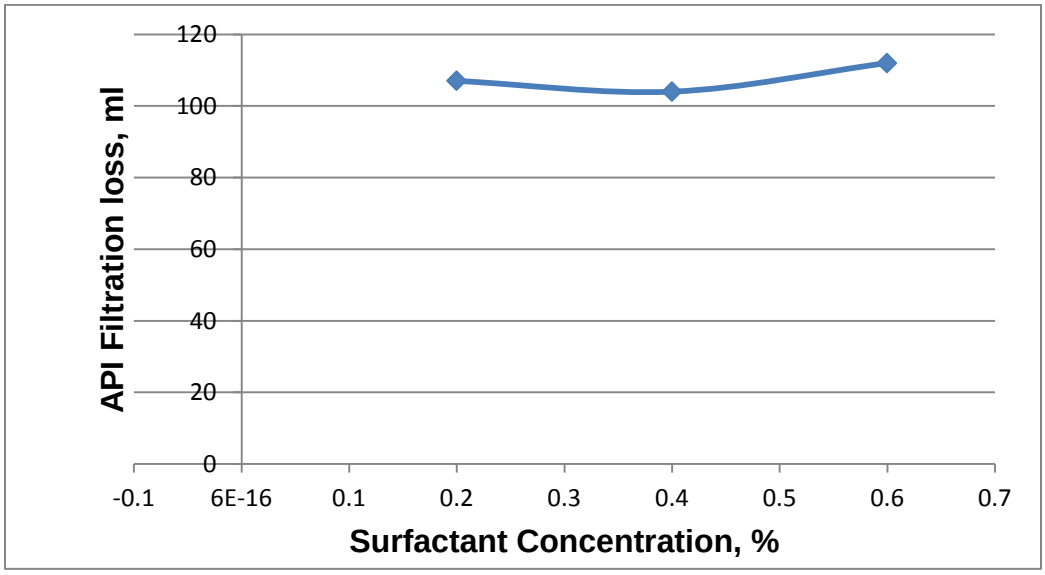

Figure 4-13: Effect of surfactant concentration on the API filtration loss of the aphronized drilling fluid

Effect of Polymer Concentration

Effect of increasing polymer concentration on the API filtration loss of aphron fluids is shown in Figure 4-14. Four aphronized fluids were prepared by using 0.4 % surfactant concentration and 0.5%, 1.0%, 1.5% and 2.0% w/w polymer concentrations. API filtration loss of the aphron fluids were reduced significantly from 229 ml down to 100 ml as the polymer concentration was increased from 0.5% to 1.5%. Increasing polymer concentration above 1.5%, however, did not change the filtration rate significantly.

Decreased filtration rate with increase in polymer concentration is an expected result. This is because higher polymer concentrations lead to higher fluid

viscosities, which in turn increases resistance to flow through the porous filter paper and therefore reduces fluid loss.

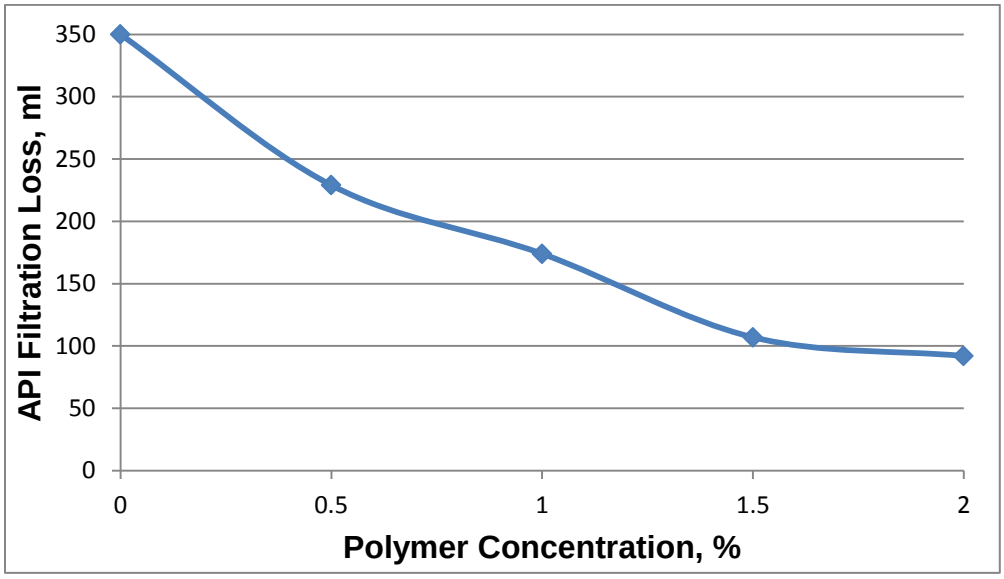

Figure 4-14: Effect of Polymer concentration on the API Filtration loss

Finally, the filtration loss characteristics of an aphronized solution containing 1.5% polymer and 0.4% surfactant was compared to the filtration loss of a mineral oil sample with 1.5% polymer and no surfactant (i.e., no aphrons) and to the filtration loss of pure mineral oil (Figure 4-15). The filtration losses of pure mineral oil and of the solution of mineral oil with 1.5% polymer were much higher than that of the aphronized solution. The results indicate that there is a strong positive effect of aphrons on reducing the amount of fluid loss into formation.

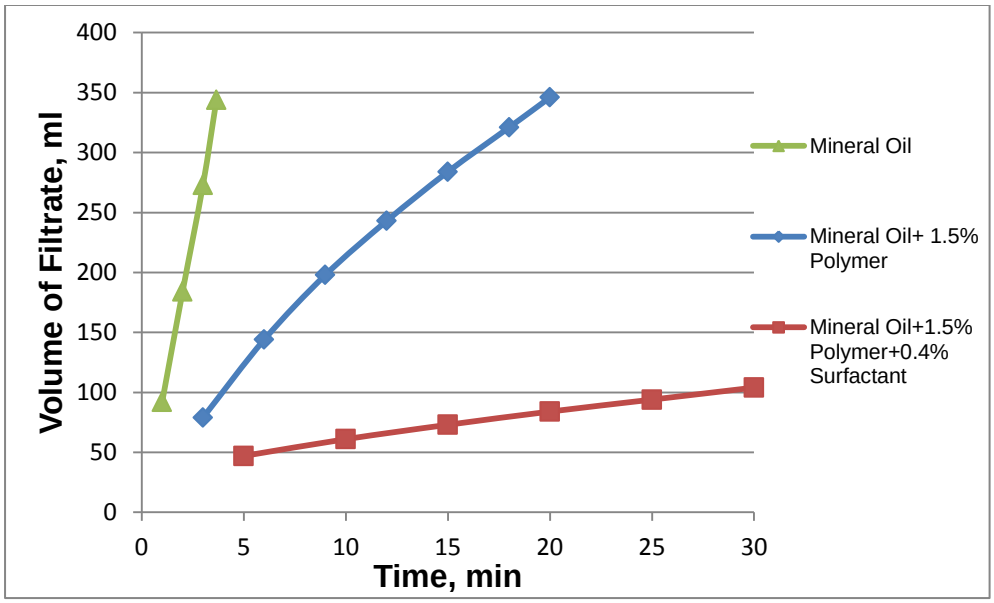

Figure 4-15: Comparison of the filtrate volume and filtration rate of an aphronized fluid (with 1.5% polymer and 0.4% surfactant), a 1.5% polymer + mineral oil mixture with no aphrons and pure mineral oil.

4.2.6 **Rheological Characterization**

The rheological characteristics of the aphron fluid are quantified in two ways:

Surfactant effect on rheology

Effect of surfactant concentration on the rheology of the fluid is shown in Figure 4-16 where the shear stress is plotted against the shear rate. The aphronized drilling fluid behaves like a pseudo plastic type fluid that has shear thinning characteristics. The shear viscosity of the fluid vs. the shear rate is shown in Figure 4-17. Increasing surfactant concentration has made the fluids slightly more shear thinning as compared to pure mineral oil. The highest shear viscosity is observed when surfactant concentration is at 0.4% wt/wt. This is most likely due

to the larger volume of aphrons (i.e., highest yield) generated at 0.4% surfactant concentration.

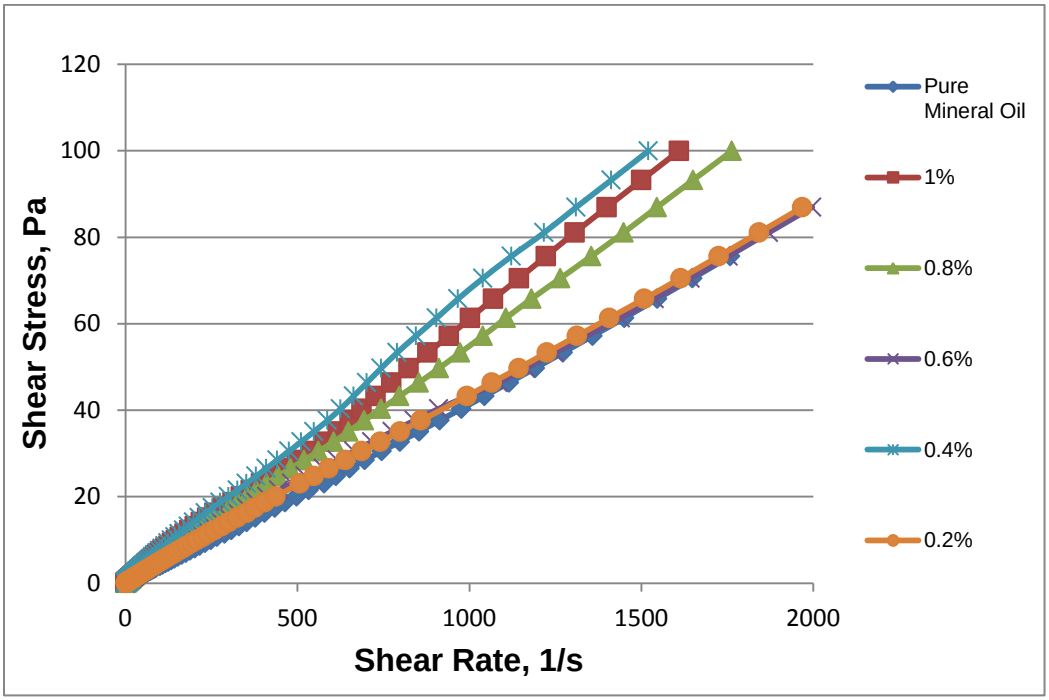

Figure 4-16: Effect of surfactant concentration on the shear stress vs. shear rate profile

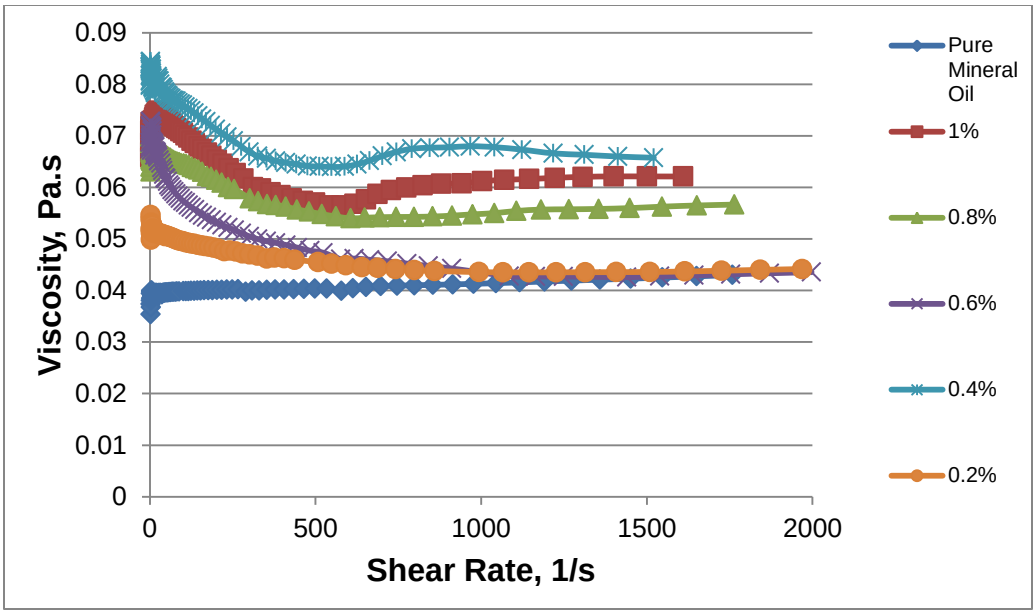

Figure 4-17: Effect of surfactant concentration on the shear viscosity of the aphron fluid

Polymer effect on rheology

Effect of polymer concentrations on the rheology of the fluid is depicted in Figure 4-18. Again, a shear thinning type pseudo plastic characteristic is evident.

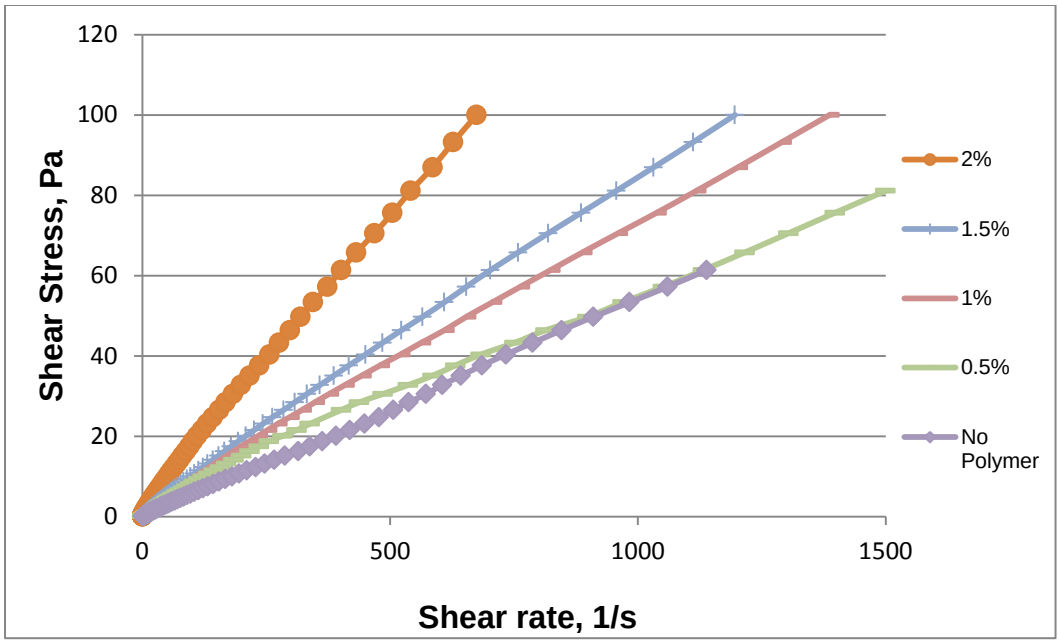

Figure 4-18: Effect of polymer concentration on the shear stress vs shear rate profile of the aphron fluid

The shear viscosity vs. shear rate of the fluid is shown in Figure 4-19. The shear viscosity of the fluid increases significantly as the polymer concentration increases. The increase is particularly large when the polymer amount goes from 1.5% to 2%. This is because as the polymer concentration increases the viscosity of the base fluid increases, thus increasing the overall viscosity of the system.

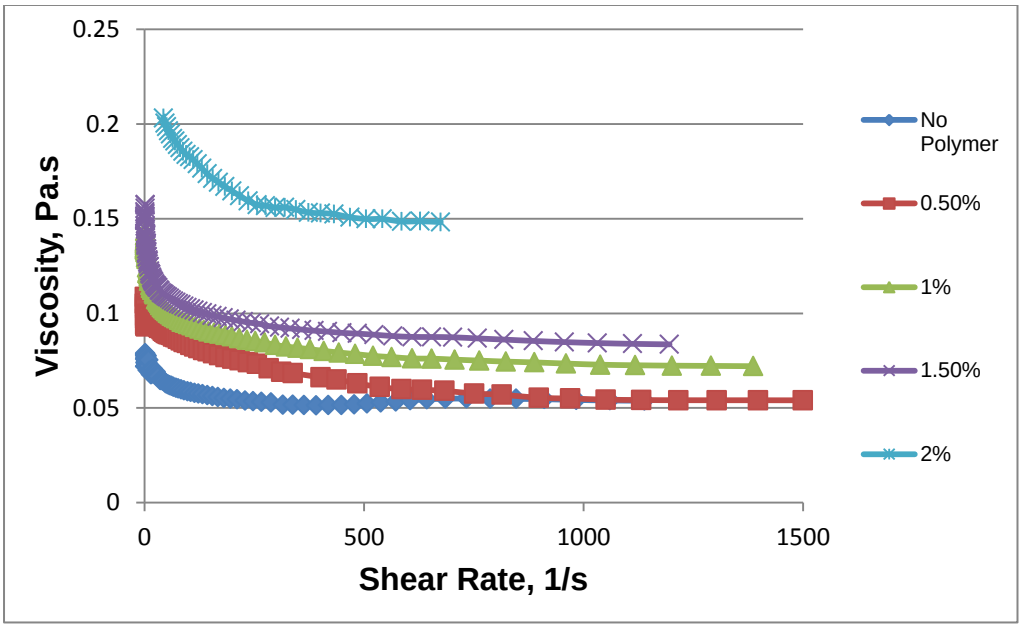

Figure 4-19: Effect of Polymer concentration on the Shear Viscosity of aphron base fluid

Hysteresis in rheological curves

Next, any hysteresis that could be expected in the rheological curves was looked into. For this purpose, the shear viscosity of an aphronized solution was recorded continuously two times- once by increasing the shear rate from 0.1 s^{-1} to 1200 s^{-1} and the other time by decreasing the shear rate from 1200 s^{-1} to 0.1s^{-1}. The viscosity curves thus obtained are plotted in Figure 4-20. The graph shows that the viscosity measured with an increasing shear rate is slightly above the viscosity measured with a decreasing shear rate. A plausible reason for this could be that the fluid is exhibiting some thixotropy. So, when it is sheared highly at the beginning and the shear rate is decreased thereafter, the viscosity is lower than the corresponding increasing shear rate case.

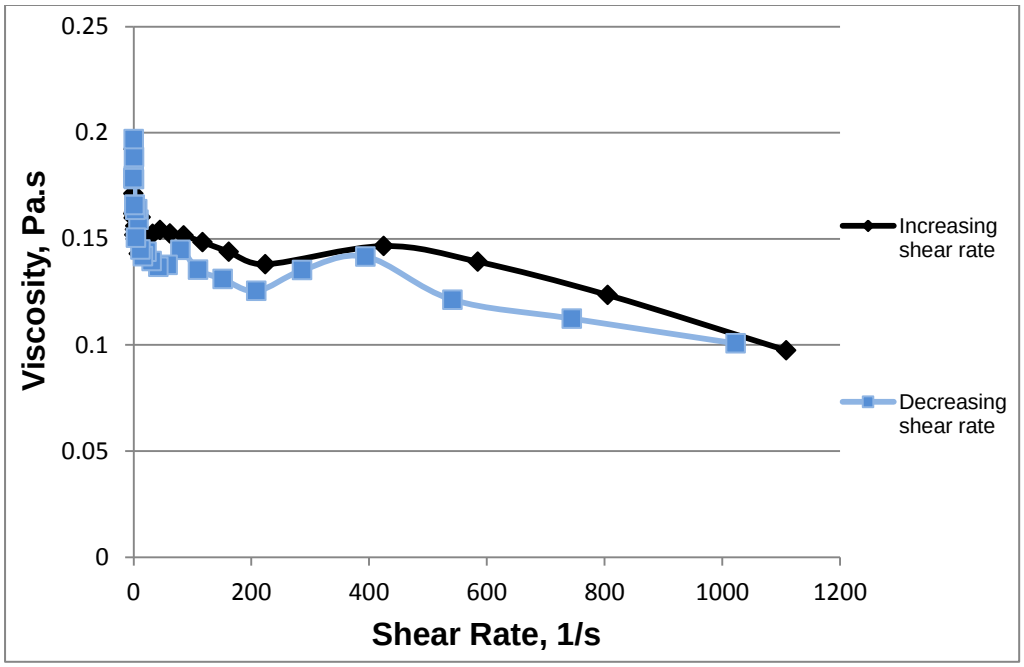

Figure 4-20: Hysteresis in rheological curves

Low Shear Rate Viscosity

The low shear rate viscosity (LSRV) of the aphron fluid was measured (at a shear rate of $0.1s^{-1}$) at different polymer concentrations. A significant jump in the LSRV was observed as the polymer concentration was changed from 1.0% to 1.5% (

Figure 4-21).

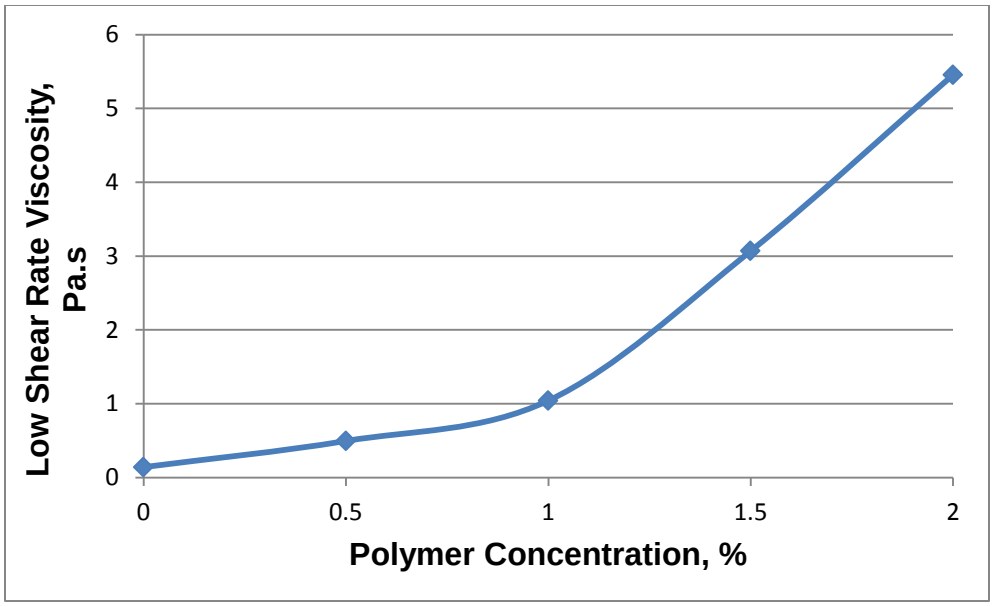

Figure 4-21: Variation of Low Shear rate Viscosity (measured at a shear of $0.1s^{-1}$) with polymer concentration

4.3 Summary

- The yield increased with an increase in surfactant concentration and decreased thereafter. A maximum of yield was recorded for a surfactant quantity of 0.4% w/w. Polymer effect on yield could not be analysed.
- The average aphron diameter (D_{50}) did not change much with diameter. The average diameter was reduced though when polymer was added to the aphron fluid.
- API fluid loss was not affected by changing the surfactant concentration from 0.2% to 0.6%. API fluid loss however came down when the polymer concentration was increased, with a significant drop in the fluid loss when the polymer concentration went from 1% to 1.5%.

- A comparison of filtration characteristics of three different fluids, one with aphrons (i.e. mixture of mineral oil, 0.4% surfactant and 1.5% polymer), one with polymer but no aphrons (i.e., mineral oil +1.5%polymer) and the last one pure mineral oil showed that micro bubbles can effectively block the pores and significantly reduce filtration loss.
- Aphron drilling fluids have become slightly shear thinning upon addition of surfactant. The shear viscosity of the aphronized fluid increased significantly with the addition of polymer. The 2% polymer drilling fluid has a considerably higher shear viscosity. Samples with a polymer content of upto 1.5% have an acceptable viscosity at elevated shear rates that will work. Above that, the shear viscosity is too high for surface pumping and handling operations. The low shear rate viscosity (LSRV) is enhanced significantly when the polymer content goes above 1%. Shear viscosities vs. shear rate rheological curves exhibit some hysteresis which can be attributed to some thixotropy. Overall, the aphron drilling fluid can be termed as pseudo plastic/ shear thinning type fluids.
- The density matches the trend of the yield, with the minimum density observed at 0.4% surfactant amount. Density is not affected much with the variation of polymer amount.
- An optimal formulation with respect to surfactant and polymer concentration for the use of the CGA fluid as an aphron drilling fluid is identified as 1.5% polymer and 0.4% surfactant

5 INVESTIGATION OF THE STABILITY OF NON AQUEOUS CGA FLUID

In this chapter the stability of the CGA fluid has been examined. To determine the effect of time, temperature and pressure on the stability of the CGA fluid, the effect that time, temperature and pressure have on the physico-chemical characteristics of the fluid have been investigated. The CGA fluid used in this section of the study is our optimum formulation CGA fluid. The optimum formulation is 0.4% w/w surfactant and 1.5% w/w polymer. This optimum formulation has been deduced based on the characterization study presented in Chapter 4 wherein the effect of varying the surfactant and polymer concentrations on the physical properties of the fluid has been discussed.

5.1 Experimental Procedure for Investigation of Stability

5.1.1 Yield

Measurement of yield with time

In creaming experiments, the record of how the interface between the creamed layer at the top and the liquid column at the bottom changes with time is a good indication of the stability of aphronized fluid. Yield is expected to decrease as time progresses, because of the growing and breaking of bubbles, which causes the encapsulating fluid to be released. This has been shown schematically in Figure 5-1 where the interface rises while the creamed layer thins out. The total height h_t and the interface height h_i are recorded at continuous time intervals.

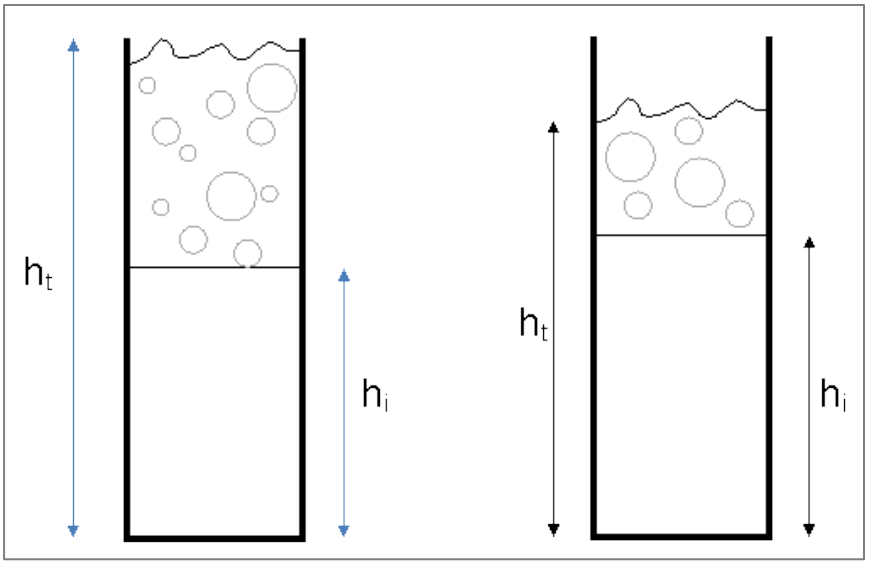

Figure 5-1: Interface rises because of bubble breakup and drainage decreasing yield

In the figure, h_t is the total height of the fluid in the measuring cylinder and h_i is the height of the interface between the creamed layer of bubbles and bulk oil. The total height is seen to have dropped, while the interface height has risen a little. Yield is calculated using equation 4-1.

The stability of CGAs by measuring the drained volume of liquid CGAs with respect to time has been studied earlier. The drainage process of CGAs was written about (Save and Pangarkar (1993), Bjorndalen and Kuru (2006)) to analyze the stability of microbubbles.

The total height and interface height were monitored and recorded for time intervals- 0 hours, 2 hours, 5 hours and 8 hours. Yield was then calculated and plotted against time.

5.1.2 **Measurement of Aphron Bubble Diameter**

Measurement of CGA diameter with different shearing rate

Apart from the effect of polymer and surfactant concentration, the effect of shearing rate during aphronization was also investigated. The fluid to be aphronized was sheared in the high speed homogenizer at shear rates of 5000, 7000 and 9000 rpm. The shearing time for all three cases was the same, 45 seconds. Following this, these fluids were analyzed for average bubble size, D_{50} with the procedure described above using the microscope.

Measurement of CGA diameter over time

For an evaluation of the stability of the fluid with time, CGA bubble diameter was measured with change in time. Four sets of pictures were taken, beginning with the fresh fluid and then after 2 hours, 4 hours and 6 hours. These pictures were then analyzed as described in Figure 4-3 for average bubble size at these intervals.

Measurement of CGA diameter with temperature

Effect of temperature on the bubble size distribution was investigated next. The base fluid (i.e., mineral oil + polymer), was heated to the desired temperature. The heating was done in the stirring hotplate which mixed the fluid uniformly while heating. Surfactant was added to the heated base fluid. The mixture was then aphronized and quickly transferred (to avoid cooling) to a microscopic slide for taking pictures with the microscope. The pictures were then analyzed for bubble size distribution.The process was repeated done at three temperatures of 25°C (room temperature), 50°C and 75°C. The microscopic slide was also heated on the

hotplate to avoid any cooling effects that occur when a little fluid is poured into the slide.

5.1.3 **Filtration**

Filtration at high temperatures

Filtration at high temperature was measured using standard API high pressure high temperature (HPHT) equipment. Filtration rate was measured at an elevated temperature of 70°C. The total 30 min loss and the cumulative filtrate volume vs. time values were recorded.

Filtration at high pressures

Filtration characteristics at elevated pressures were evaluated by using high pressure filtration equipment at a pressure of 300 psi. The 30 minute filtrate volume was reported as the API Filtration loss. Also, the cumulative filtrate volume vs. time was recorded continuously to get an idea about how the filtration rate is changing with time.

The API filtration test was not carried at the standard high pressure value of 500 psi because at 500 psi the fluid flowed out in a very short time.

5.1.4 **Rheology**

High Temperature Rheology

The cone and plate type Bohlin CVO rheometer has a Peltier cell which was used to heat the fluid. CGA fluid was heated to 70°C and the shear viscosity was measured as a function of shear rate at this temperature.

High Pressure Rheology

The rheometer is equipped with a high pressure cell (HPC). In effect, the rotating rheometer shaft and the HPC act like a rotating cylinder viscometer. The shear viscosity is measured at an atmospheric pressure and at a pressure of 500 psi.

Rheology- Effect of adding Suspentone

An organophilic clay was added to the fluid to look at the outcome it has on the viscosity of the fluid. The organic clay is a suspension agent called Suspentone. 1.5% w/w of Suspentone was added to the aphron fluid. The effect of Suspentone on the shear viscosity and LSRV was analysed.

5.1.5 PVT Analysis

The Pressure-Volume-Temperature (PVT) relationship of the fluid was examined using a Schlumberger DBR PVT Cell (100 cc, 15ksi) specifically designed for the measurement of fluid properties and the study of fluid phase behaviour.

The fluid first had to be inserted into the PVT cell by the means of a charging vessel and an accumulator pump. The cell compartment was then sealed. The temperature of the cell can be pre-set to a desired temperature, the fluid was then allowed to heat up in the cell. The pressure inside the cell can then be increased or decreased. This was done by driving a pump which pushes (or pulls back) a piston inside the cell.

An image of the fluid was transmitted to a computer by a camera focused on the cell. The computer had a reference cross marked line. Each time after pressure change, the line was aligned to the top of the fluid. From the level of the fluid top

and some calculations pertaining to the dead volume and scale of the fluid level, the volume of the fluid was calculated.

At a fixed temperature, the pressure of the cell was increased continuously from 0 to 500 psi, at steps of 50 psi. At each pressure level, the rise or drop of fluid level is used to calculate the change in volume with pressure. This was done for four sets of temperatures, 25°C, 50°C, 75°C and 100°C.

After this, the PVT data was used to build an equation of state that will predict the density of the fluid. This equation was developed using a curve fitting technique. The predicted properties given by the equation were then compared to the actual experimental values.

5.2 Results and Discussion (Investigation of Stability)

5.2.1 Yield

How yield changes with time has been used often as an indicator of the stability of the fluid. Measurement of yield with time can be called as measurement of drainage of the CGA fluid. Drainage and the associated half-life time have been used by several authors to look at foam stability. It is expected that yield will decrease as the time progresses because of the growing and breaking of bubbles, which causes the encapsulating fluid to be released.

Yield is expressed in percentage terms; the equation to evaluate yield was presented earlier (Equation 4-1). Yield is then plotted against time in hours in Figure 5-2. Yield decreases very slowly with time, from 14% for the fresh solution to 10% after 8 hours have passed.

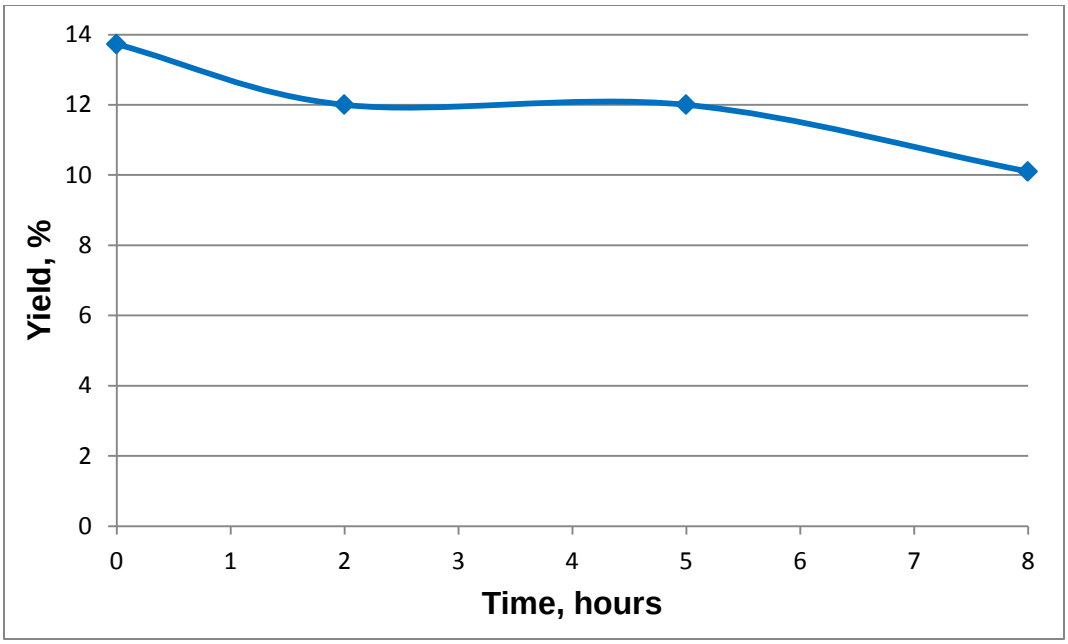

Figure 5-2: Yield of aphrons in the fluid recorded with time

5.2.2 **Aphron Bubble Size**

Aphrons grow in size with time. The size of aphrons at any time is critical- because proper size distribution in accordance with pore size distribution is essential for the ability of the CGA fluid to block rock pores. The longer the microbubbles resist a change in diameter, the more stable the CGA is.

Two pictures of the aphrons were taken on a same scale using the Leica microscope; one of the bubbles in freshly prepared fluid as seen in Figure 5-3 and the other of the bubbles after 6 hours have passed as shown in Figure 5-4. These pictures provide a good illustration of the effect of time on CGA sizes. Evidently, the aphrons grow in size with time accompanied by simultaneous breaking up of bubbles.

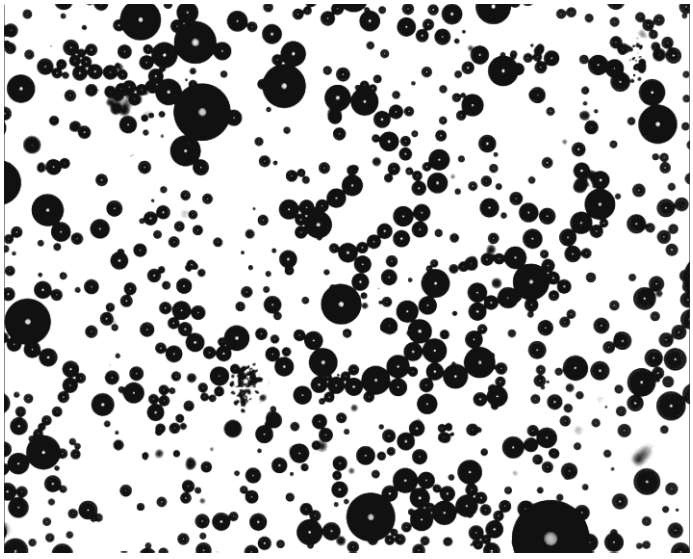

Figure 5-3: A microscopic picture of aphrons freshly prepared

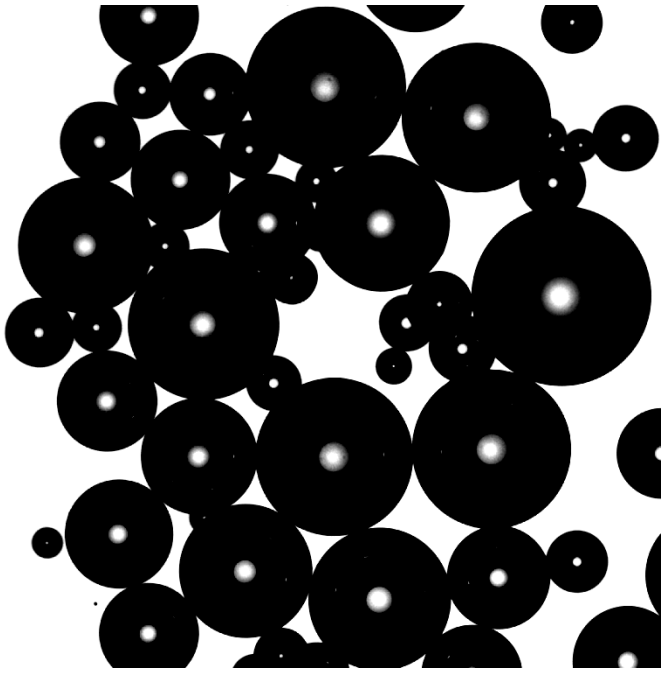

Figure 5-4: Microscopic picture of aphrons after 6 hours

During size distribution analyses, the average bubble diameter was reported as D_{50}. The D_{50} is actually the median diameter, which means 50% of the bubbles have a diameter smaller than the D_{50} and the other 50% have a larger diameter. D_{50} was recorded for four time intervals- fresh bubbles and after 2, 4 and 6 hours have passed.

The D_{50} vs. time curve is shown in Figure 5-5. It can be seen that the average bubble size increases rapidly at the beginning (17µm to 41µm in just 2 hours). After that the growth slows down (41µm to 52µm in the next two hours). The average bubble size then begins to level and stabilize (54µm at 6 hours).

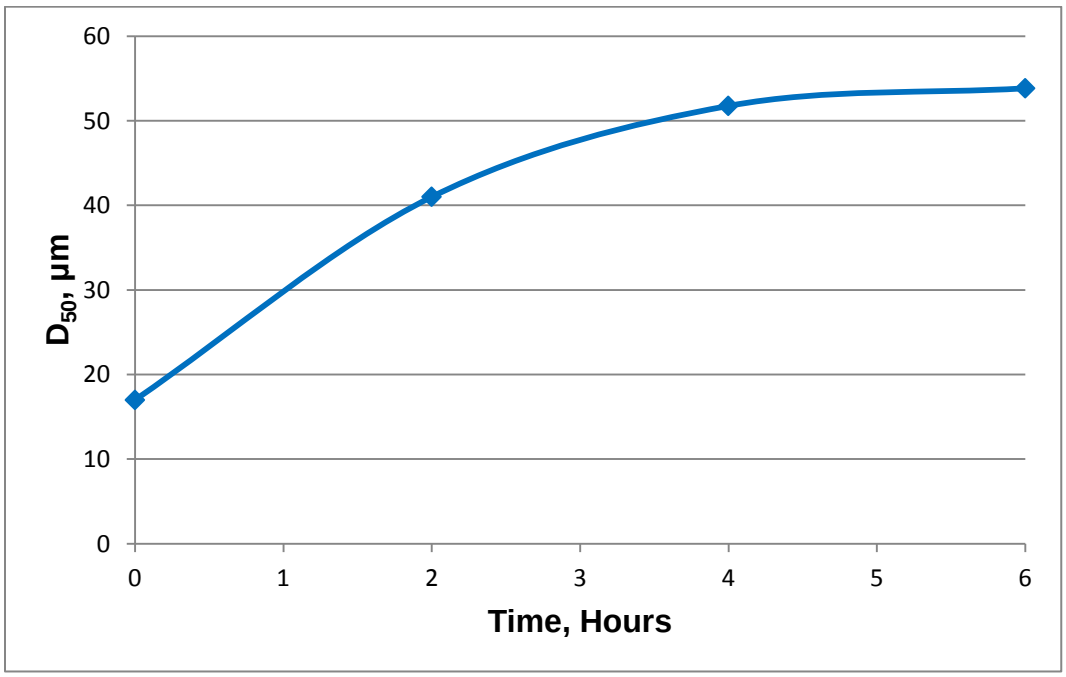

Figure 5-5: Average bubble size (D_{50}) vs. time

The change in bubble size with temperature was looked at to investigate how temperature affects stability of the CGA fluid in terms of average bubble size. As the temperature of the borehole increases, it can have an effect on the CGA size.

The bubble size distribution was examined at three temperatures: 25°C, 50°C and 75°C. The average sizes of the bubbles (D_{50}) at these three temperatures are plotted in Figure 5-6. The D_{50} for all three temperatures is nearly the same (a variation of only 2μm), it is seen that change in temperature has no appreciable effect on the average bubble size.

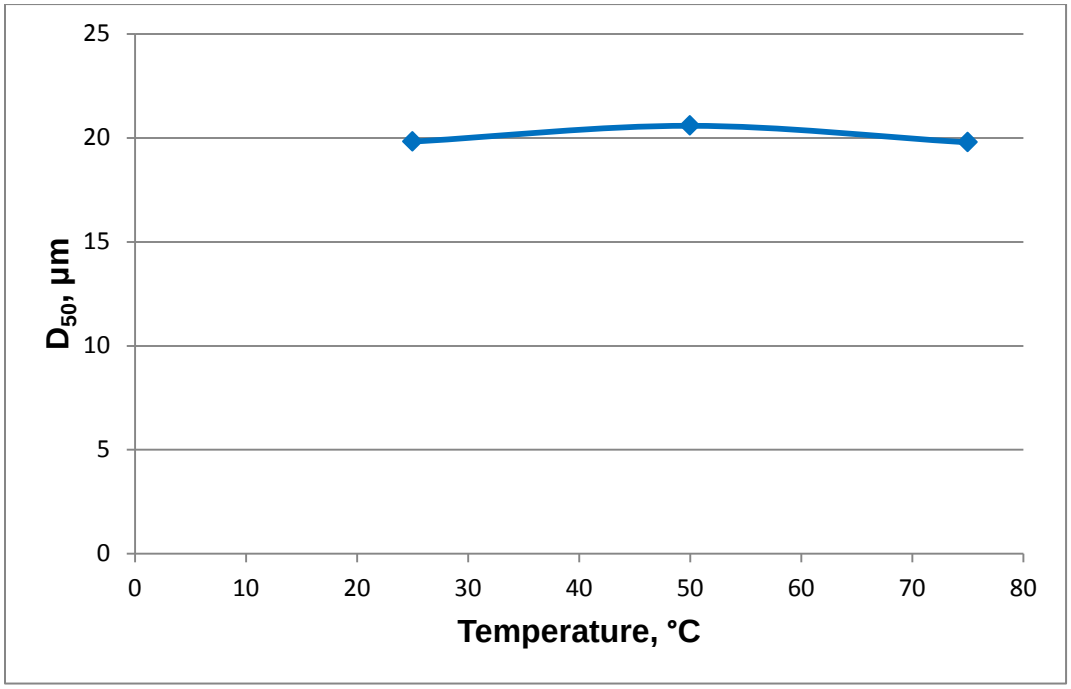

Figure 5-6: Effect of temperature on the average bubble size (D_{50})

It is interesting to see what affect the mixing rate during the process of generation of the fluid will have on the bubble size of the CGA fluid. The average bubble size for the three shear rates of 5000, 7000 and 9000 rpm is presented in Figure

5-7. It can be seen that increasing the shear rate causes a reduction in the average bubble size. From 19.4µm for 5000 rpm, it decreased to 17.4µm for 7000 rpm and 15.1µm for 9000 rpm.

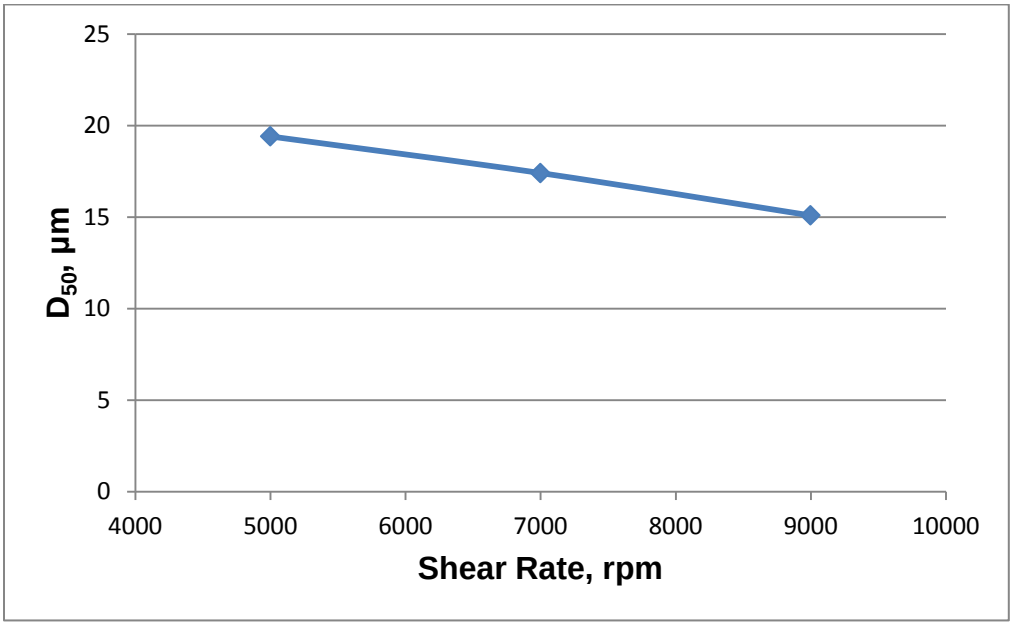

Figure 5-7: How changing the shear rate during generation affects the average bubble size

5.2.3 **Rheology**

Typically a rise in temperature is followed by a decrease in the viscosity of a fluid. Rheology at a high temperature was measured to look how downhole temperature will affect rheology. The cone and plate type rheometer was used to heat the fluid to 70°C and the shear viscosity was measured as a function of shear rate at this temperature. The same measurement over a similar shear rate range was done for the fluid at room temperature.

The curve for shear viscosity vs. shear rate for both temperatures is shown in Figure 5-8. As can be seen, the viscosity decreases with an increase in temperature.

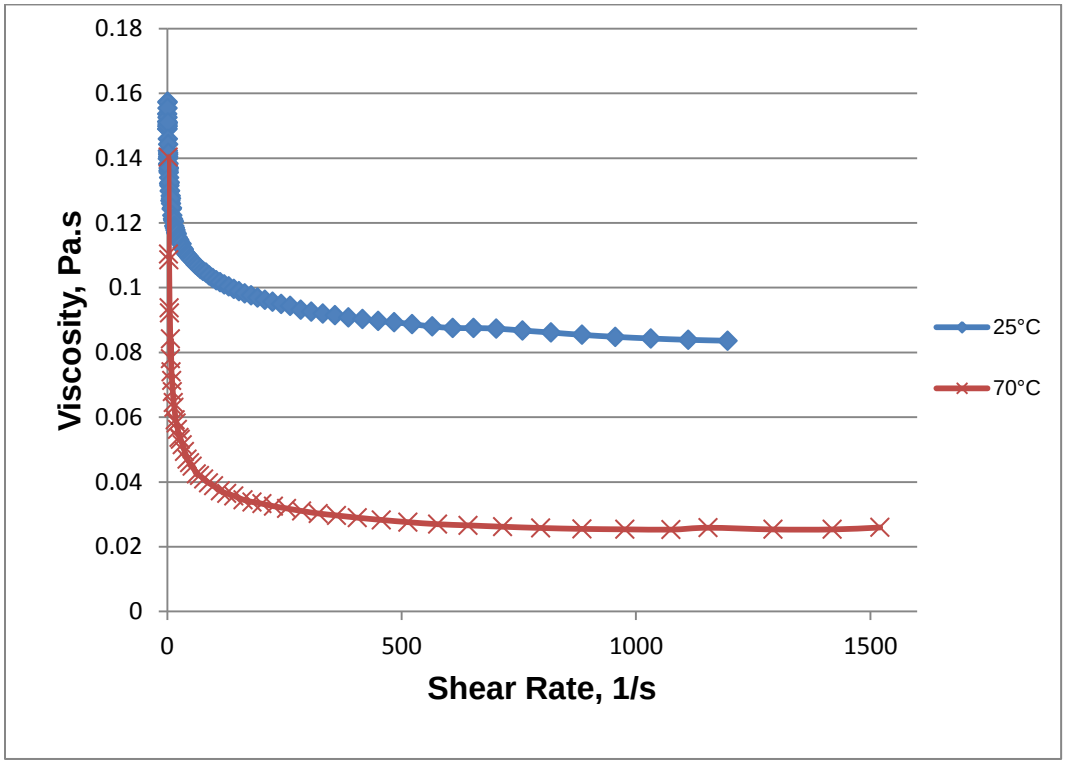

Figure 5-8: Effect of temperature on the shear viscosity of the aphron fluid

Next, the rheology of the fluid was investigated under an elevated pressure. A high pressure cell was used. The rheological characteristics at a high pressure were analyzed by comparing the viscosity vs shear rate curves at atmospheric pressure and at a pressure of 500 psi. Rheology at these two pressures is shown in Figure 5-9. It appears that increasing pressure has little effect on the viscosity, with the viscosity at 500 psi case being slightly higher at high shear rates. This slight increase may be because of the compressibility of the fluid and the foam (aphron layer) phase.

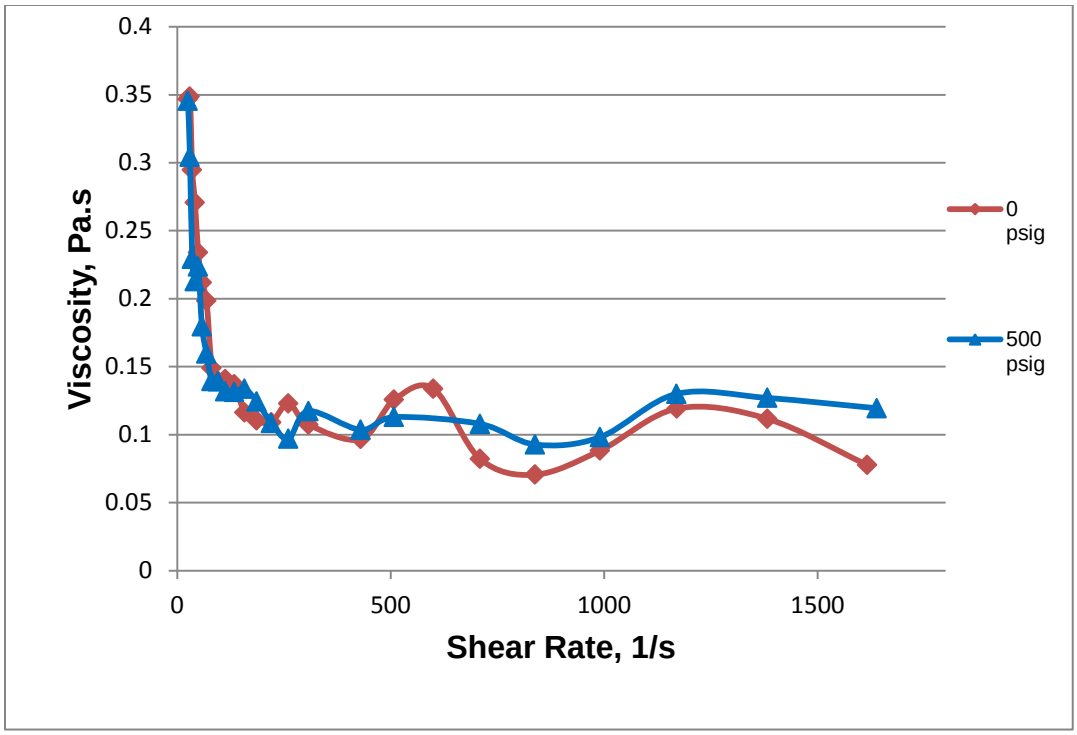

Figure 5-9: Effect of elevated pressure on the viscosity of the fluid

Another topic of interest while analysing the rheology of the CGA fluid is whether the presence of aphrons is having any effect on the viscosity profile of the fluid. To study this aspect we performed a viscosity vs. shear rate test for the base fluid only i.e. mineral oil with 1.5% polymer dissolved into it. The result of this test is then compared to the viscosity vs. shear rate result of an aphronized fluid of our optimum formulation (1.5% polymer + 0.4% surfactant,aphronized). The comparison between both is shown in Figure 5-10.

.

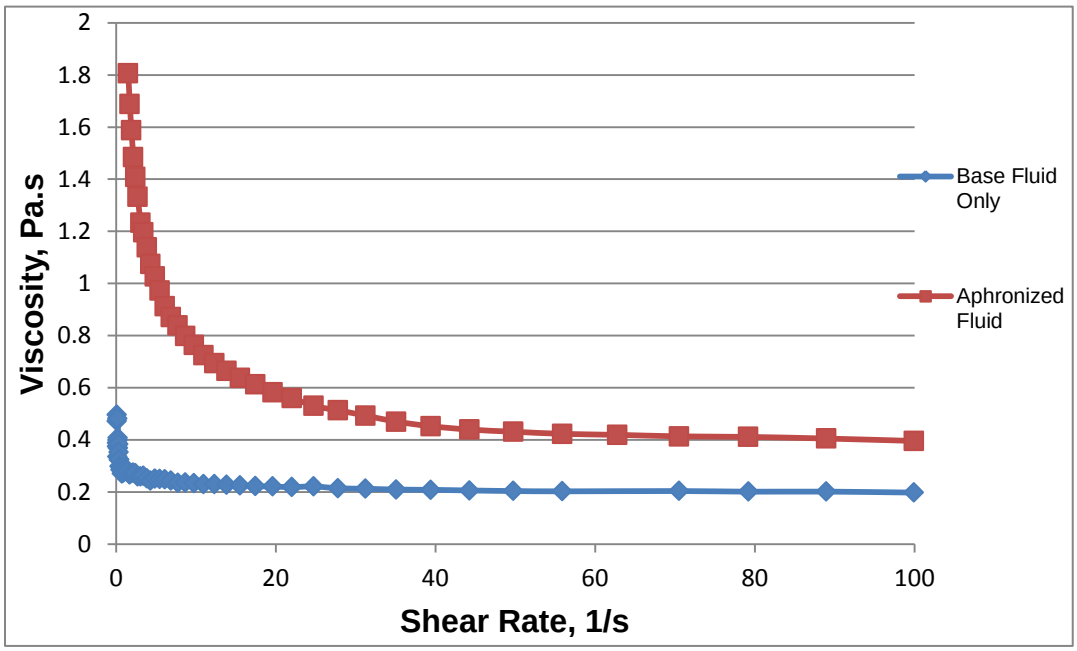

Figure 5-10: Comparison of the viscosity profile for the base fluid and the aphronized fluid

The comparison is done for a smaller shear rate range. It can be seen that the presence of microbubbles has a very significant effect on the shear viscosity of the aphron fluid. There is a marked difference in the shear viscosity at high shear rates while the difference in the viscosity at lower shear rates is a lot more.

5.2.4 **Effect of adding organophilic clay on rheology**

Organophilic clays are commonly used to improve the solids suspension ability of oil-based drilling fluids. To enhance the solids suspension characteristics of the oil-based aphron drilling fluid, an organophilic clay called Suspentone was used. Physical properties of suspentone have been described in Section 3.1.4.

An examination of the action of Suspentone on the rheological characteristics of the aphron drilling fluid was done in the same way by comparing the shear viscosity vs. shear rate. The first fluid is the aphronized optimum formulation fluid (1.5% polymer + 0.4% surfactant) and the second fluid is the same with an addition of 1.5% Suspentone (1.5% polymer + 0.4% surfactant + 1.5% suspentone). The two curves are shown in Figure 5-11.

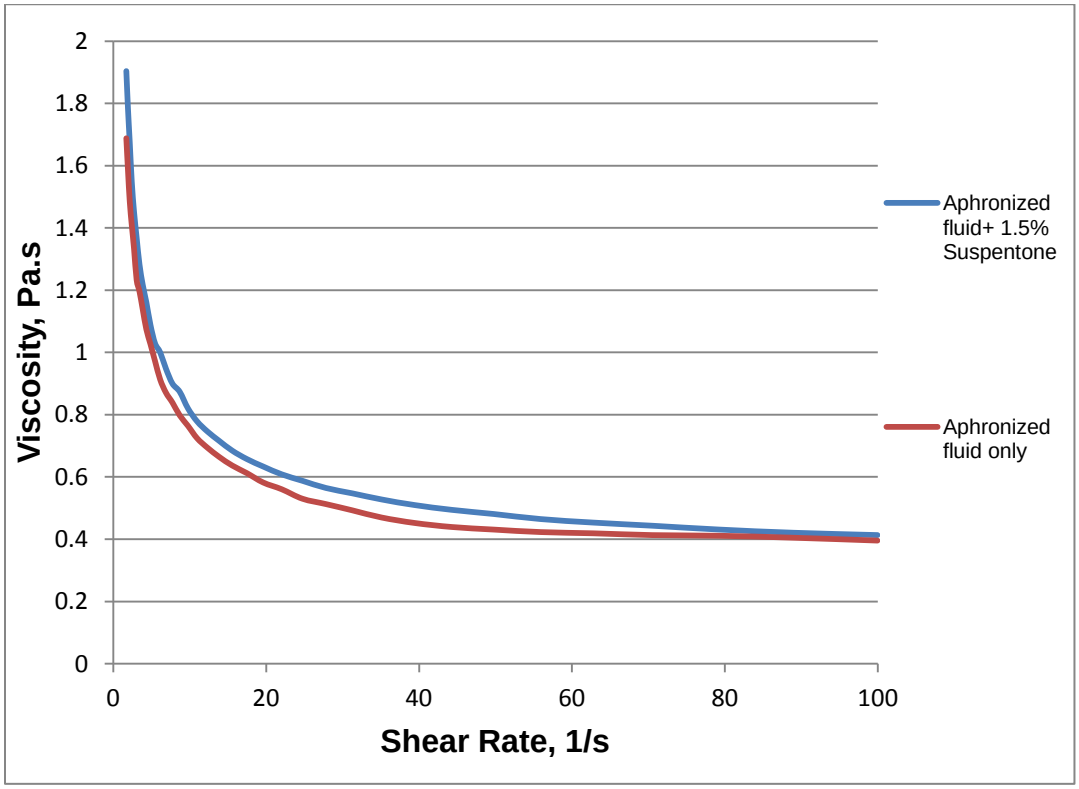

Figure 5-11: Result in viscosity profile after adding Suspentone (at a concentration of 1.5%) to the aphron drilling fluid

The comparison is done for a smaller shear rate range. There is not a lot of difference between the two curves; the Suspentone curve is slightly above the

curve for aphronized fluid only. So, the presence of the organic clay has little effect on the viscosity of the aphron fluid.

It was believed that the Low shear rate viscosity of the aphron fluid will be influenced considerably by the addition of Suspentone. To analyze the ability of Suspentone to enhance LSRV the viscosity at a low shear rate value of $0.1s^{-1}$ was measured for two fluids: the optimum formulation fluid and the optimum formulation fluid strengthened with 1.5% w/w of Suspentone. The comparison between the LSRV's of the two fluids is presented in Figure 5-12.

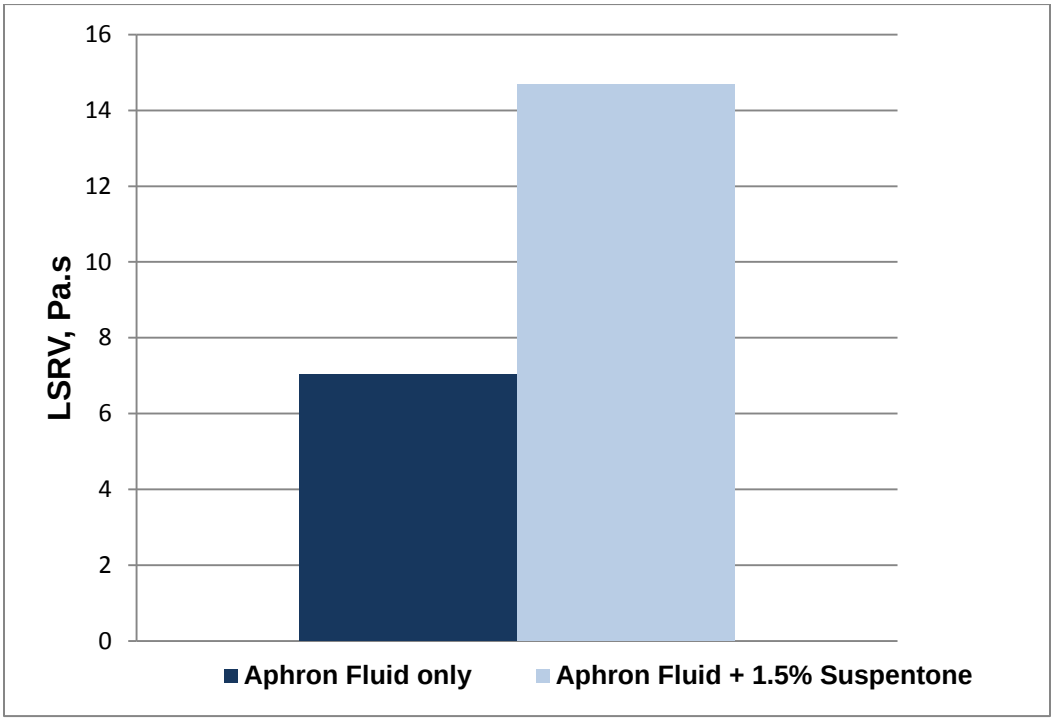

Figure 5-12: Change in the LSRV upon addition of Suspentone (1.5%) to the aphron drilling fluid

There is an influence of the organic clay in increasing the LSRV by about 2 times. However, given the high concentration of Suspentone added (1.5%), the increase in LSRV is not as much as expected.

5.2.5 **Filtration Loss**

High pressure and high temperature filtration results are presented to understand how much fluid loss increases in elevated temperature and pressure conditions. The change in filtration loss when the temperature is raised from 25°C to 70°C at a pressure of 100 psi is shown in Figure 5-13. The total 30 min loss has increased from 107 ml at 25°C to 350 ml at 70°C. Besides the total loss, the filtrate volume was recorded continuously as a function of time, plotted in Figure 5-13. It is visible that the slope of the 70°C curve is much higher than the slope of the 25°C curve. This implies that the filtration occurs at a faster rate when the temperature is increased.

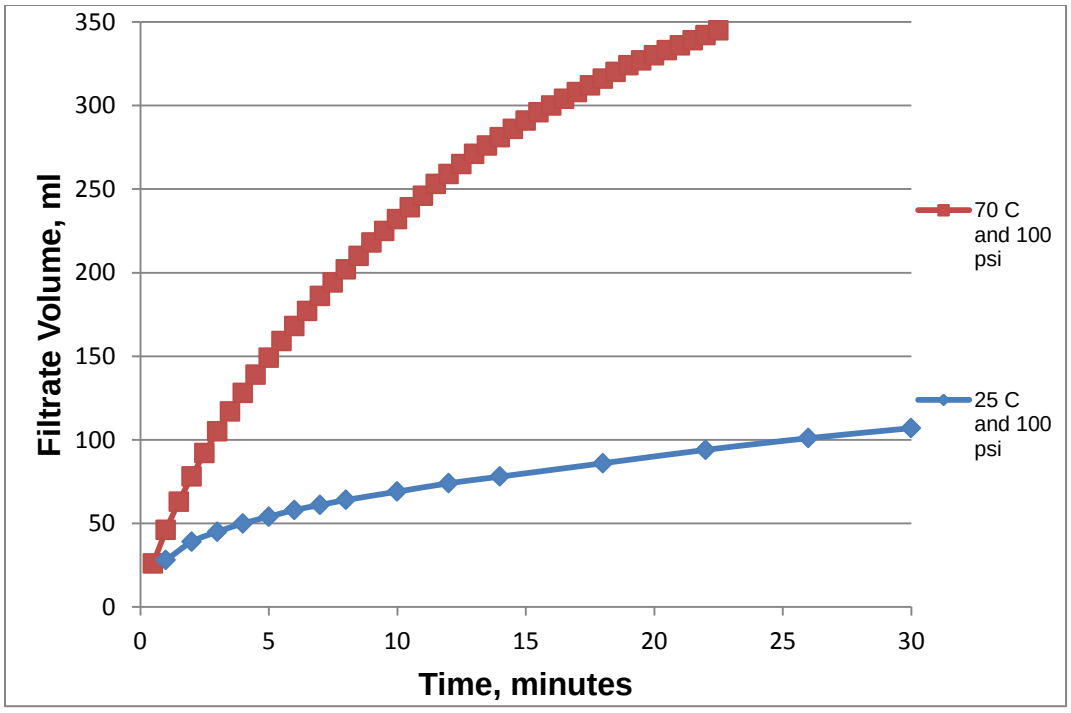

Figure 5-13: How filtration rate is affected by increasing the temperature

The effect of pressure on the filtration characteristics of the fluid was examined in the same way, by comparing the filtration rate and fluid loss volume at a pressure of 100 psi and 300 psi, both at room temperatures. The filtrate volumes vs. time curves are shown in Figure 5-14. Increasing the pressure from 100 psi to 300 psi caused the total 30 minute loss to increase from 107 ml to 160 ml. Again, the slope of the 300 psi curve is higher than the slope of the 100 psi curve, which concludes that the rate of filtration is higher at high pressure.

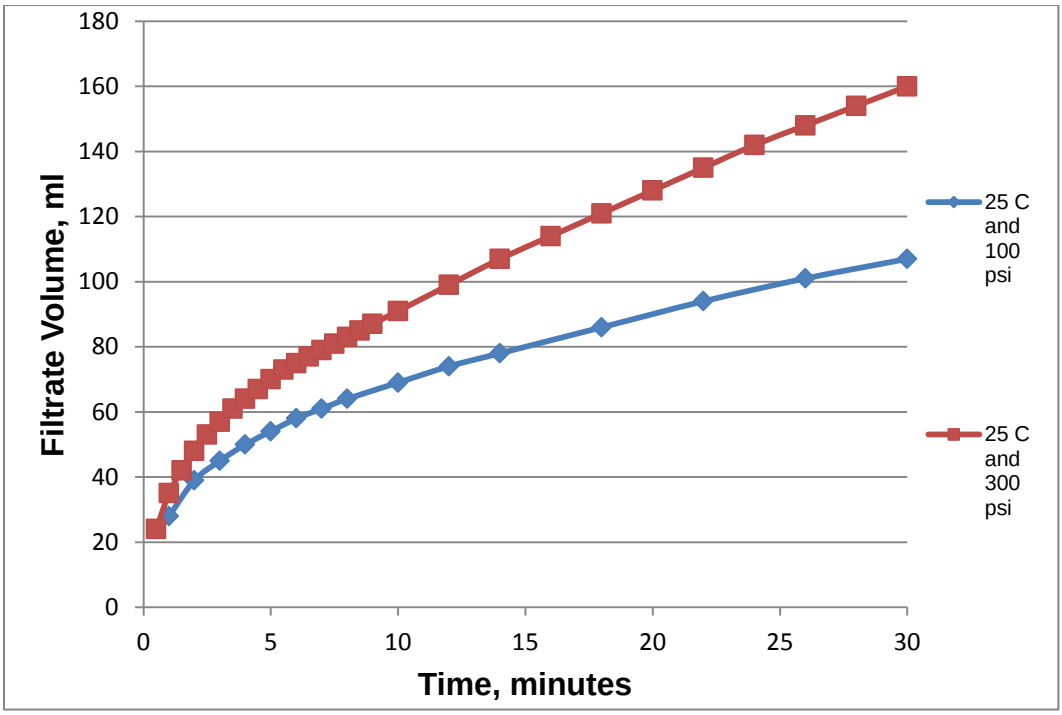

Figure 5-14: How filtration rate is affected by increasing the pressure

The HPHT API filtration test was not carried at the standard high pressure value of 500 psi because at 500 psi the fluid flowed out in a very short time.

5.2.6 **PVT Analysis**

The Pressure-Volume-Temperature relationship was analyzed in the PVT cell. The pressure was increased from 0 to 500 psi in steps of 50 psi at four different temperatures; 25°C, 50°C, 75°C and 100°C. The results of the PVT tests are shown in Figure 5-15. Here, the density of the fluid has been plotted against the pressure.

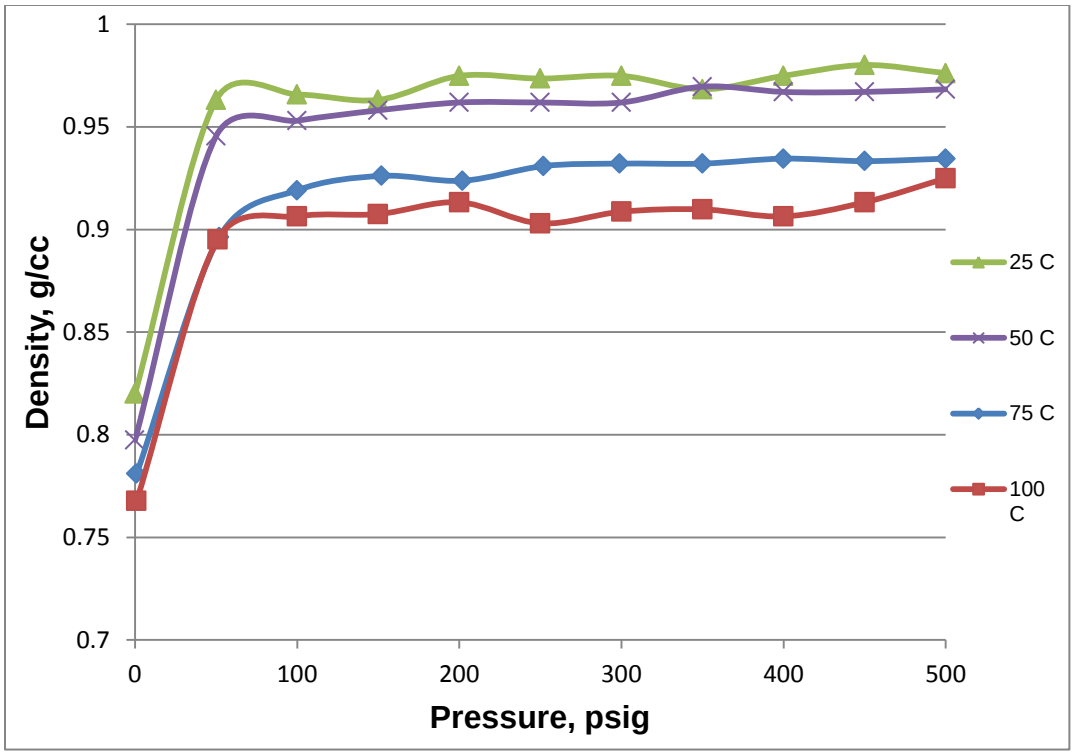

Figure 5-15: PVT analysis to determine change in density with temperature and pressure

Evidently, the density increases with increase in pressure. The density climbs up rapidly in the beginning, and increases slowly after a pressure of 50 psi has been applied.

The density decreases with increase of temperature. This is seen in Figure 5-15 where for any given pressure value, the density value comes down when the temperature increases.

The results of the PVT tests were then used to build an equation of state that describes the relation between the PVT properties of the fluid. The equation 5-1 was developed using a curve fitting technique:

$$\rho = (0.02686 - 2.87*10^{-5}T)\ln(P) - 0.000778T + 0.853384 \qquad \text{(Equation 5-1)}$$

where ρ is the density of the fluid in g/cc, T is the temperature of the fluid in °C and P is the pressure of the system in psi.

Measured and predicted density values match well as shown in Figure 5-16. For the sake of simplicity, measured and predicted density values for only two temperatures 50°C and 100°C are shown.

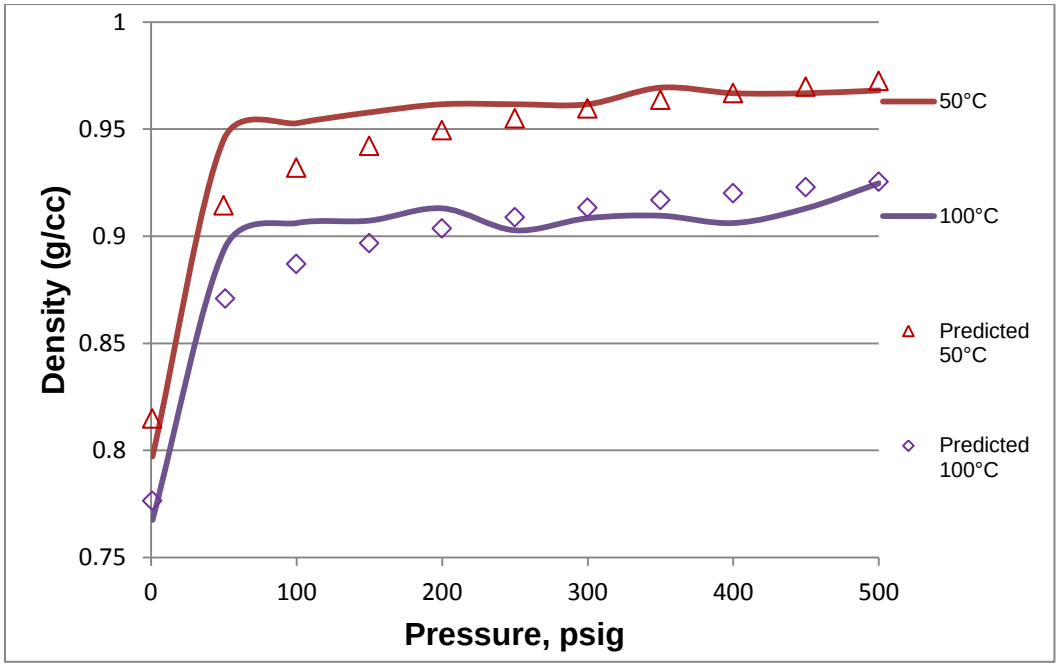

Figure 5-16: Comparison of the measured and predicted CGA fluid density values

5.3 Summary

- Yield of the fluid decreased slowly with increase in time. A change of yield value from an initial value of about 14% to about 10% was observed in 8 hrs.
- By observing the change in aphron size over a period of 6 hours, it was seen that the average aphron size D_{50} increased significantly initially, after which it was more or less stable. Change in temperature did not affect the average bubble size, D_{50}, significantly.
- The presence of CGAs has a very significant effect of increasing the viscosity of the aphron fluid as compared to the base fluid only. There is a marked difference in the shear viscosity at high shear rates while the difference in the viscosity at lower shear rates increases a lot more.
- Shear viscosity is reduced significantly (almost 3 times) by increasing temperature from 25°C to 70°C. However, increasing pressure had no major impact for the shear viscosity of the CGA fluid.
- The addition of organic clay Suspentone (1.5%) does not raise the shear viscosity by a significant amount. The LSRV is doubled on addition of Suspentone at 1.5%.
- Increasing the temperature from 25°C to 70°C caused the API filtration loss value to increase more than 3 times. When the differential pressure changed from atmospheric pressure to 300 psi, the API filtration loss increased by 1.6 times.

- The density of the fluid decreases when temperature is increases; it increases with an increase in pressure.
- The equation of state predicted for non-aqueous CGA fluids is

$$\rho = (0.02686 - 2.87*10^{-5}T)\ln(P) - 0.000778T + 0.853384$$

  The proposed equation of state gave reasonably good prediction of CGA fluid density when compared to the experimental results.

- Increasing the shear rate during aphronization led to a reduction in the average bubble size, D_{50}.

6 INVESTIGATION OF THE FLOW OF OIL BASED CGA DRILLING FLUID THROUGH POROUS MEDIA

The CGA drilling fluid is expected to have a blocking ability by virtue of the aphrons which will form a bridge like structure across the rock pores. The core flow tests are done here by flooding a radial sand packed core with the CGA fluid. This will determine the maximum pressure drop caused by the CGA across the porous media. The maximum pressure drop attained by the CGA fluid is indicative of the extent of bridging and blocking of pores.

The return permeability is evaluated too. The amount of change in the return permeability with respect to the original permeability will be indicative of the extent of formation damage caused by the CGA fluid.

The effect of changing the injection rate of CGA drilling fluid, the packing-saturating fluid and the wettability of the porous media on the pressure drop and return permeability have been investigated.

6.1 Experimental Procedure for Core Flooding Experiments

6.1.1 Core Flooding Setup

The core flooding experiments were conducted by injecting the aphron drilling fluid through porous media packed within a radial cell. The experimental setup is shown in Figure 6-1

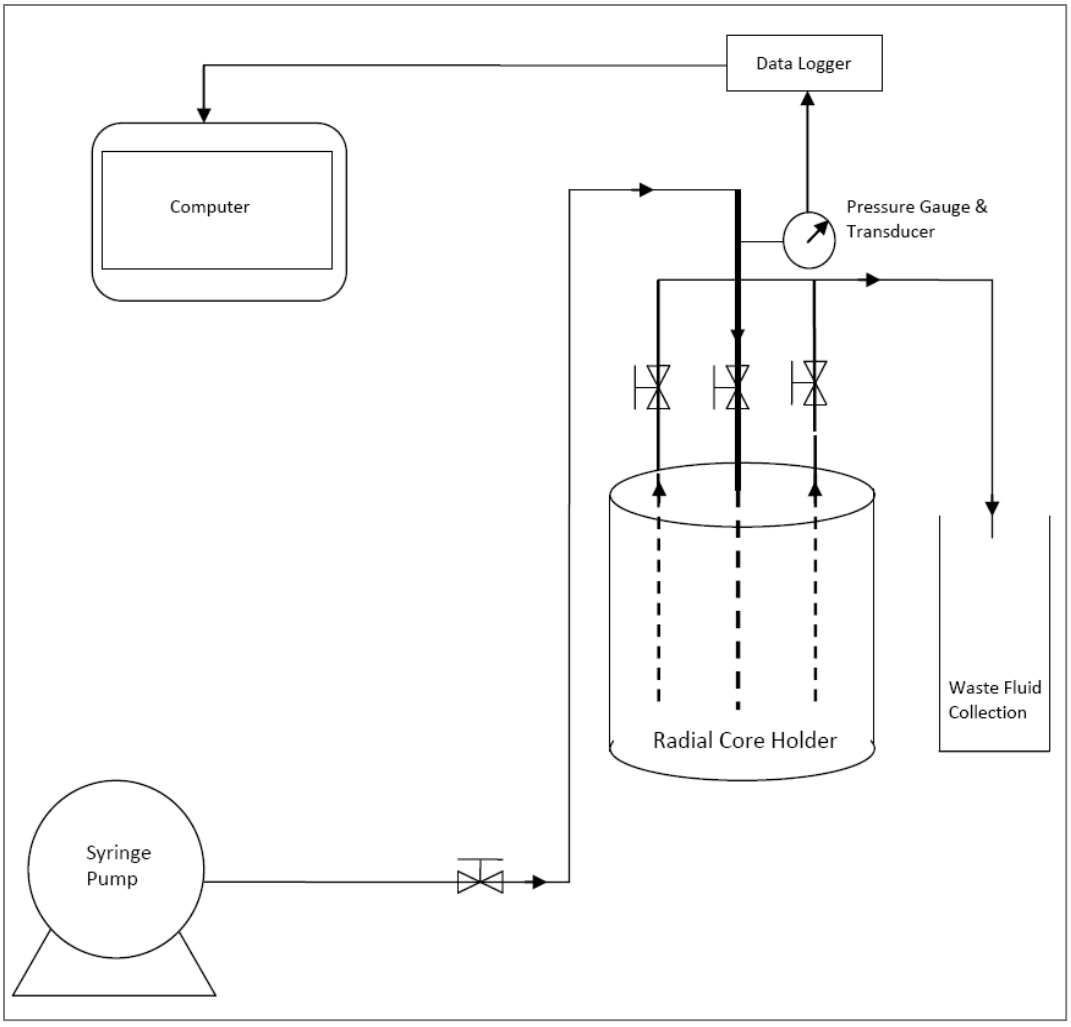

Figure 6-1: Schematic diagram of the experimental setup for the core flooding experiments

The syringe pump is used for saturating the radial core holder with the fluid. The pressure transducer reads the total injection pressure and feeds it to a data acquisition system. The data acquisition system transfers the data to the computer where it is recorded.

6.1.2 **Packing**

The core holder was cleaned and packed with the dry spherical glass beads. Packing was done through the sand packing port at the bottom of the core holder. The core holder was continuously mechanically agitated while beads were poured into it regularly. A mechanical vibrator operated by air pressure and a hammer were used. The hammer was used to knock the radial cell and the mechanical vibrator was pressed against the cell wall while dry glass beads were poured into the core holder. This vibration and knocking with the hammer continued until the entire granular material dispersed evenly and packed closely in the core holder. When no more glass beads could be loaded, the loading was stopped and the core holder was sealed by closing the sand packing port and tightening the sealing rings.

6.1.3 **Saturation**

An ISCO syringe pump was filled with the saturation fluid (i.e, either water or mineral oil depending on the type of experiments). After the core holder was packed with dry glass beads, it was saturated with the saturation fluid. The saturation was done at a very low flow rate, typically 0.5-1 ml/min. Saturation was carried out so as to fully fill all the void spaces in the packing. Techniques like pressurization and depressurization were used to achieve the highest possible level of saturation.

6.1.4 **Baseline Pressure Drop**

Following overnight saturation, the saturation fluid baseline pressure drop was determined. Saturation fluid baseline pressure drop means the pressure drop measured while the saturation fluid is being pumped through the core when the core is 100% saturated with the same fluid. The flow rate is the same as the flow rate that will be used for the CGA fluid that will be pumped through the core.

6.1.5 **CGA Fluid Injection**

After saturation and recording of baseline pressure drop readings, the core flooding experiments were begun. The Isco syringe pump was refilled, this time with the aphron drilling fluid. At the desired flow rate, the pump was turned on. At the same time, the transducer and data acquisition system was switched on, so that pressure at the injection well is recorded continuously. The pressure at the production wells was atmospheric. So the pressure difference between injection and production was essentially the pressure measured at the injection well. Pressure was monitored throughout the experiments. All pressure readings were reported in pressure drop per metre travelled through the porous media. Pressure readings were plotted against the pore volumes of fluid injected. The inference drawn from here was how the pressure build up on the core occurs. The effluent fluid collected from the two producing wells of the radial core was discarded. After every 500 ml of injection (the pump capacity), the pump was stopped and all the valves were closed. More CGA fluid was prepared again and the pump was refilled. After re-filling, the pump was started again and pressure build-up began from the dropped point.

The CGA fluid was injected into the packed bed until a close to maximum pressure was obtained. This occurs after an extended period of injection time when the pressure build-up does not go up significantly.

6.1.6 **Saturation Fluid Re-injection**

Once the approximate maximum injection pressure was reached, the CGA fluid injection was stopped. The pump was now filled with the reservoir saturation fluid. The saturation fluid was injected into the radial core holder. This was done until a continuous close to minimum pressure is obtained. Minimum pressure is the point when there is no significant pressure decrease for an extended period of time. The saturation fluid was injected at the same rate as the CGA fluid. The purpose of saturation fluid re-injection was to get an idea of how easily the CGA fluid could be removed from the system and also to get an indication of the return permeability.

6.1.7 **Return Permeability Calculation**

An objective of the core flooding tests has been to look at how much the absolute permeability is affected by the invasion of the aphron drilling fluid. For radial steady state flow, absolute permeability is given by Darcy's law. Darcy's law for radial flow is written below:

$$Q = \frac{2\pi k h(P_e\text{-}P_w)}{\mu \ln(r_e/r_w)} \qquad \text{(Equation 6-1)}$$

where:

k is the absolute permeability of the porous medium

h is the height of the core

μ is the dynamic viscosity of water, which equals 0.00089 Pa.s at 25˚C

r_e is the radius at the external boundary

P_e is the pressure at the external boundary

r_w is the radius of the wellbore

P_w is the pressure at the wellbore.

From (Equation 6-1); we can see that for the same radial core setup (i.e. for the same geometry) and injection fluid, if the flow rate is kept same and the pressure monitored for two separate cases, the ratio of the pressure drops will give ratio of the absolute permeabilities.

So at the end of the core flooding experiments, all the pressure readings from the pressure transducer i.e., baseline pressure drop, CGA fluid injection pressure drop and saturation fluid re-injection pressure drop are plotted on the same graph. The ratio of the baseline pressure drop and the saturation fluid re-injection pressure drop is used to determine how much the return permeability has been affected. The permeability has undergone some alteration from its original value because of the formation damage that has been caused by the aphron fluid. The percentage change in return permeability is given by:

$$\text{Altered Permeability, \%} = \frac{\text{Baseline pressure drop}}{\text{Saturation fluid reinjection pressure drop}} \times 100$$

(Equation 6-2)

6.1.8 **Core Flooding for Different Flow Rates**

The radial core holder was packed with glass beads and saturated with mineral oil. The maximum flow rate that the Isco syringe pump can provide is 400 ml/hour (6.67 ml/min). So we did experiments with three flowrates- 4, 5 and 6 ml/min. Base line pressure drop was measured while injecting mineral oil through the packed radial core holder (already saturated with mineral oil) at the rate of 4 ml/min. The CGA fluid was then injected through the packed core at 4 ml/min. saturated with mineral oil. Pressure drop across the core sample was measured. Following the CGA fluid injection, the core was flushed with mineral oil until the pressure drop reaches to a new stabilized level. Formation damage potential of the CGA drilling fluid was evaluated by comparing the pressure drop observed for CGA fluid flow to the base-line pressure drop. The same procedure was repeated for injection rates of 5 and 6 ml/min.

6.1.9 **Core Flooding with Different Saturation Fluids**

Effect of the type of reservoir saturating fluid was investigated next. The radial core holder was packed with glass beads. Injection rate was 5 ml/min for all the

experiments conducted under this category. Water and mineral oil were the two fluids used to saturate the core samples. In each case, the pressure drop was measured as the base line pressure drop initially by flowing only water or only mineral oil. Aphron drilling fluid was then injected until pressure drop reaches a stable maximum value. After finishing the CGA fluid injection, core samples were again flushed with saturating fluids and corresponding final pressure drops were measured. Final pressure drop values were compared to baseline pressure drop values to estimate formation damage potential of the CGA fluid in each case.

6.1.10 **Core Flooding with Changed Wettability of Packing Beads**

The glass beads we have are normally water wet. The wettability of the water wet beads was chemically altered to oil-wet to study the effect of wettability. For this, Surfasil siliconizing fluid was used. SurfaSil fluid directly reacts with polar groups on the object's surface and results in a hydrophobic surface.

The Surfasil siliconizing fluid can be applied by wipe-on or immersion methods. We used immersion technique which is described here. The Surfasil fluid is diluted in a nonpolar organic solvent such as acetone, toluene, carbon tetrachloride, methylene chloride, chloroform, xylene or hexane. Typical working concentrations are 1-10% mass to volume were suggested. We used 10% concentration of Surfasil in acetone (the organic solvent). The glass beads were completely immersed in the diluted SurfaSil Solution. The solution was agitated to ensure a uniform coat. A thin film coats the surface of the glass beads. Following this, the glass beads were rinsed with the same solvent in which the reagent was diluted, i.e., acetone. After rinsing with acetone, the glass beads were

rinsed with methanol. Rinsing with methanol was required to prevent interaction of the SurfaSil Coating with water and thus, reversal of siliconization. Finally, the glass beads were air dried for 24 hours.

The dried glass beads were then packed into the radial pressure vessel using the procedure described earlier. This core was saturated with a saturating fluid (mineral oil or water). The CGA injection was then done at 5ml/min. The pressure buildup was monitored and the return permeability was evaluated.

6.1.11 **Porosity Measurement**

For measurement of porosity, the volume of the core holder was calculated first. The pore volume of the porous medium (beads packing) would be then the volume of the glass beads subtracted from the volume of the core holder. For the volume of the beads, the weight of the glass beads loaded into the core holder was recorded and the volume of the material was determined by dividing the weight of the beads by their density. A specific gravity of 2.5 as specified by the glass beads manufacturer was used in density calculations.

6.2 Results and Discussion (Core flooding Investigation)

Core flooding tests were conducted at different flow rates, saturation fluid and wettability conditions.

6.2.1 **Porosity Measurement**

The volume of the core holder was measured to be 1395 ml. In each experiment while doing the packing, the weight of glass beads packed into the core holder

was 1950 g. Since the specific gravity of the glass beads is 2.5 g/cc, the volume of glass beads packed into the core holder is 780 ml. The difference between this beads volume and the total volume gives us the total pore volume to be 615 ml. Hence, the porosity is 44%.

6.2.2 **Effect of Flow Rate**

Figure 6-2 shows the pressure drop across the core sample plotted against the pore volumes of fluid injected. This figure is given for a CGA fluid pumped at a rate of 4 cc /min. The dark line at the bottom is the baseline which represents the injection of the saturating fluid (mineral oil) at 4 ml/min rate into the packed core saturated with mineral oil. After injection of the aphronized fluid for about 3.2 pore volumes, the core sample was flushed with saturation fluid (mineral oil) again. The CGA injection and saturation fluid re-injection curves are separated by a vertical line.

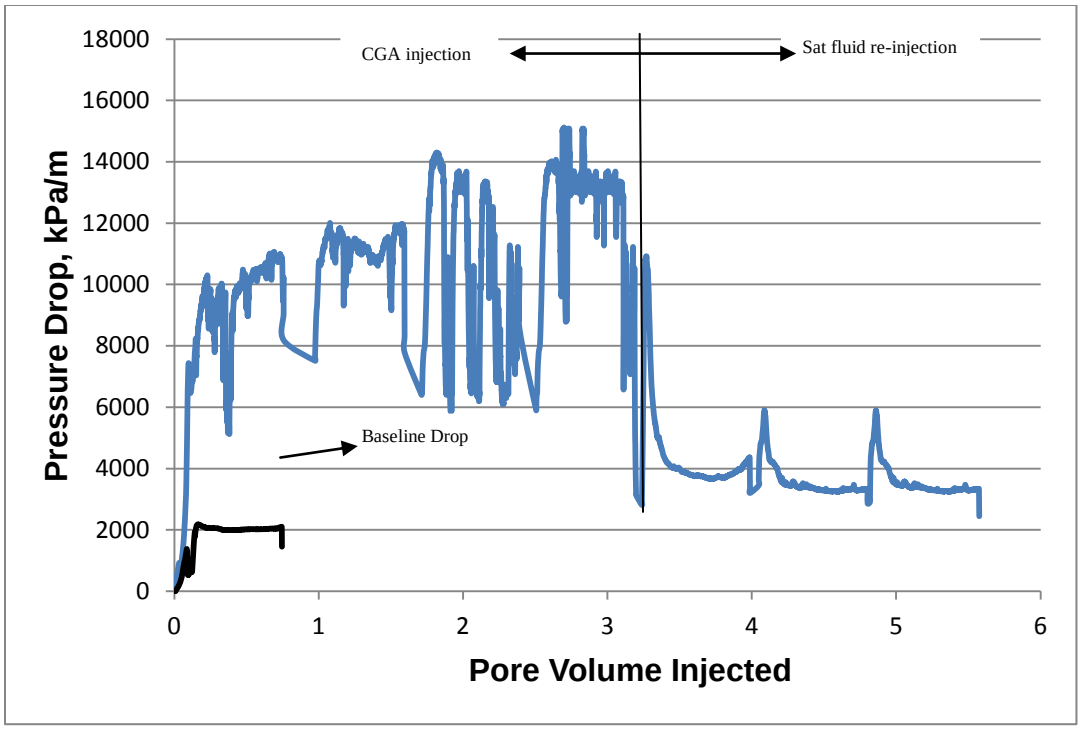

Figure 6-2: Injection of CGA fluid at 4cc/min into a core saturated with mineral oil

Figure 6-3 shows variation of the pressure drop across the core sample as a function of the pore volumes of fluid injected, this time for a CGA fluid pumping rate of 5 ml/min. The dark line at the bottom is the baseline which represents the injection of the saturating fluid (mineral oil) at the rate of 5 ml/min into the packed core saturated with mineral oil. Following the CGA fluid injection of 3.4 pore volumes, the core sample was flushed by saturation fluid (mineral oil) again.

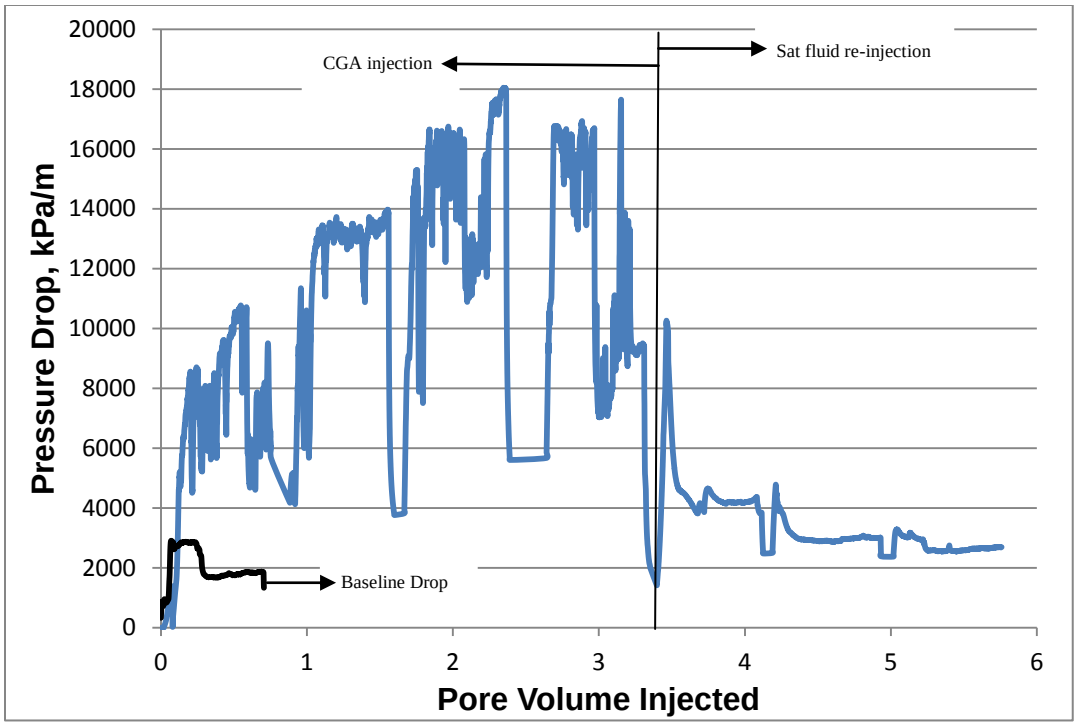

Figure 6-3: Injection of CGA fluid at 5cc/min into a core saturated with mineral oil

Similarly, results of the experiments conducted using 6 ml/min injection rate were plotted in Figure 6-4. Again the dark line at the bottom is the baseline which represents the injection of the saturating fluid (mineral oil) at the rate of 6 ml/min into the packed core saturated with water. After injection of 4.4 pore volumes of aphronized fluid, the core sample was again flushed with saturating fluid (mineral oil). The vertical divider line separates the CGA injection and saturation fluid re-injection data.

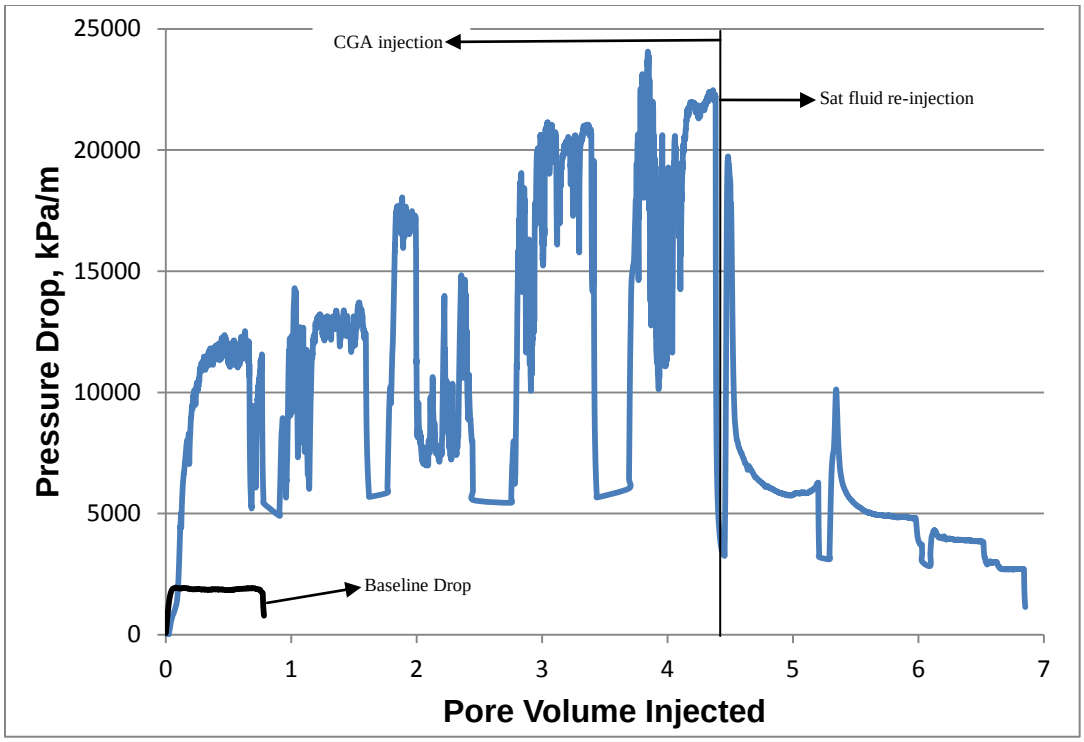

Figure 6-4: Injection of CGA fluid at 6cc/min into a core saturated with mineral oil

Next, a comparison of the values of the pressure drop across the radial core measured at the three different flow rates was made. The results are shown in Figure 6-5. The maximum pressure drop values of 15,000 kPa/m, 18,000 kPa/m and 24,000 kPa/m were observed at the flow rates of 4 ml/min, 5 ml/min and 6 ml/min respectively.

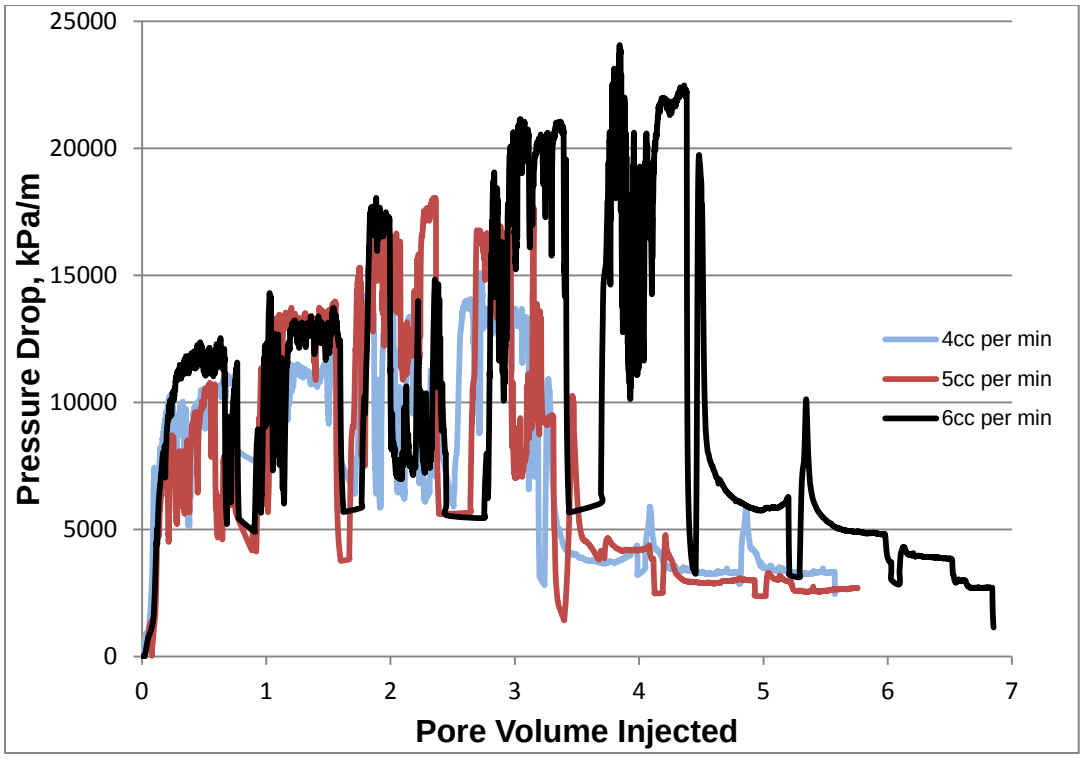

Figure 6-5: Comparison of injection of CGA fluid at different flowrates into a core saturated with mineral oil

A comparison of the formation damage that has occurred as a consequence of CGA fluid invasion was made next. The extent of the formation damage was measured from the percentage change that permeability has undergone from the original permeability (before CGA injection began) to the final permeability (after completing CGA fluid injection). Equation 4-2 is used to evaluate the percentage change in the permeability. The altered permeability results are summarized in Table 6-1.

Table 6-1: Effect of changing the flow rate on the return permeability

Flowrate	Baseline pressure drop, kPa/m	Saturation fluid re-injection drop, kPa/m	Return Permeability, %
4 cc/min	2000	3200	62.5%
5cc/min	1850	2700	68.5%
6cc/min	1900	2900	65.5%

The inference that can be drawn from comparison of the permeability alteration for the three flow rates is that the formation damage caused is similar, more or less within the same range.

6.2.3 **Effect of Saturating Fluid**

Injection of the CGA drilling fluid was done for the core saturated with two saturating fluids. First, the packed core was saturated with mineral oil. Second, the core was packed with the same amount of glass beads and saturated with water. Injection of the optimum formulation CGA drilling fluid was done next. The flow rates in both cases were at 5ml/min level.

Figure 6-6 shows the results of the pressure drop measurements obtained when injecting the CGA fluid into a water saturated core. The injection rate was 5ml/min. Again, the dark line at the bottom is the baseline which represents the

pressure drop recorded during the injection of the saturating fluid (water in this case) at 5ml/min into the packed core saturated with water prior to CGA fluid injection. After injection of the aphronized fluid for about 3.3 pore volumes the saturation fluid (water) re-injection was begun (data points seen after the vertical separating line), both at 5 ml/min.

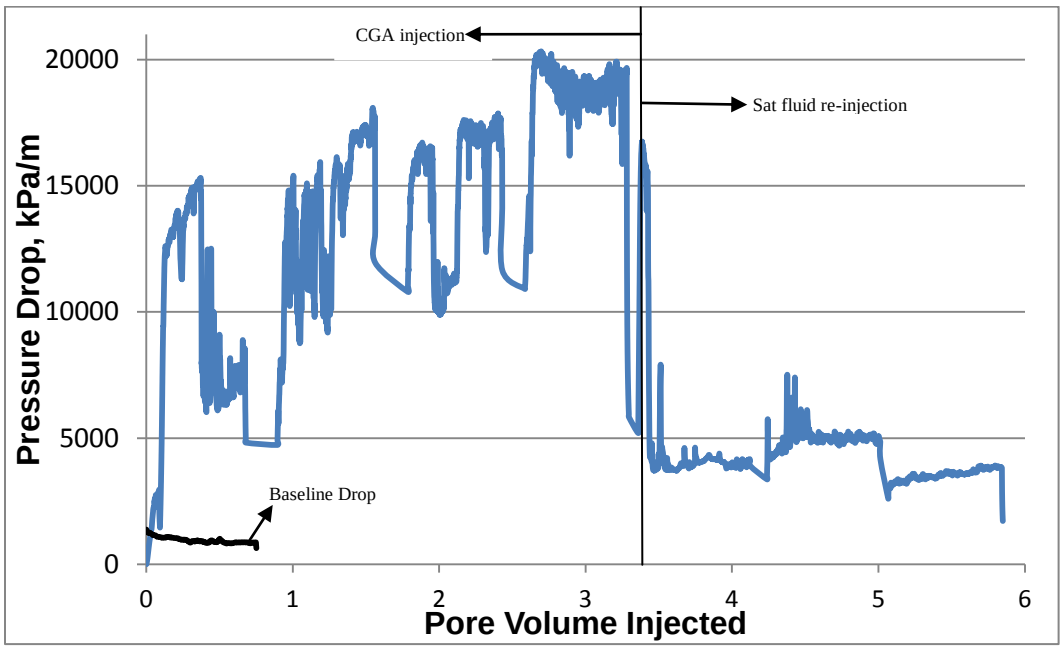

Figure 6-6: CGA fluid injection at 5cc/min into a water saturated core

A comparison of the pressure drop values measured during the flow of CGA fluids through cores saturated with water and mineral oil are shown in Figure 6-7. Apart from the beginning period, the pressure profiles for both saturating fluids are quite similar with several coinciding high points. The maximum pressure drop achieved for the oil saturated core was around 18,000 kPa/m. The maximum pressure drop achieved for the water saturated core was around 20,500 kPa/m.

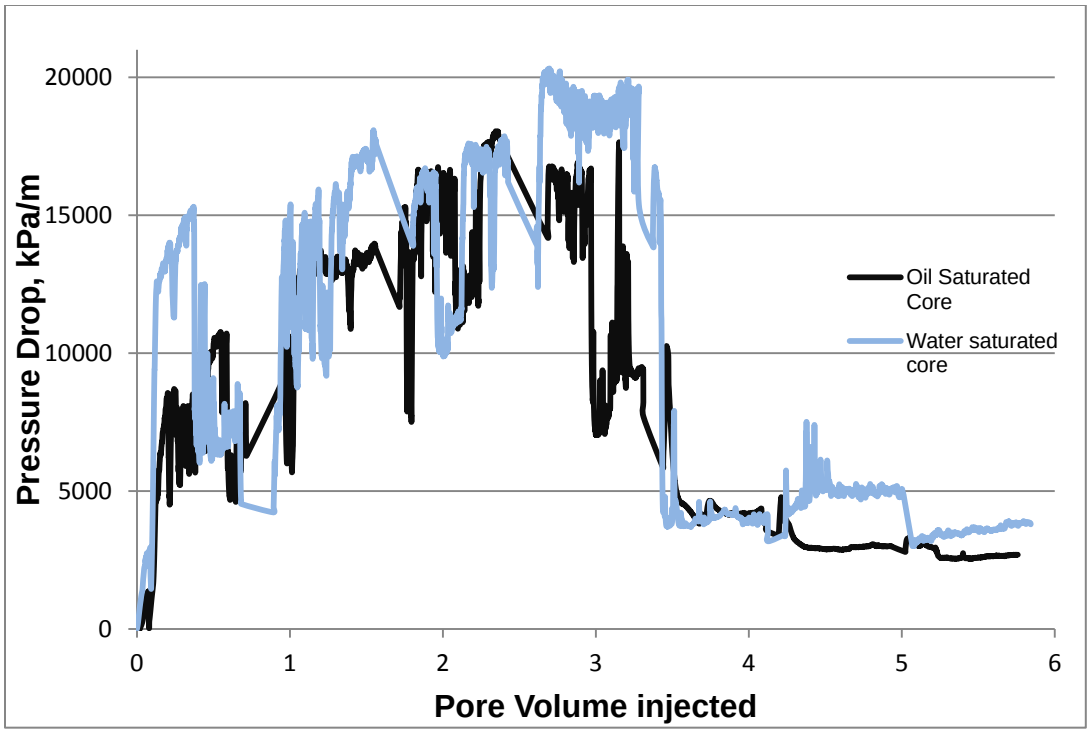

Figure 6-7: Comparison of CGA injection at 5cc/min into an oil saturated and water saturated core

Of particular interest in this case is how the pressure develops in the injection well in the initial phase of aphron drilling fluid pumping. To analyze this initial pressure buildup more finely, the pressure drop was plotted against the pore volumes up to a point where about 1 pore volume was injected. This graph is plotted for both- a water saturated core and a mineral oil saturated core. The graph is shown in Figure 6-8.

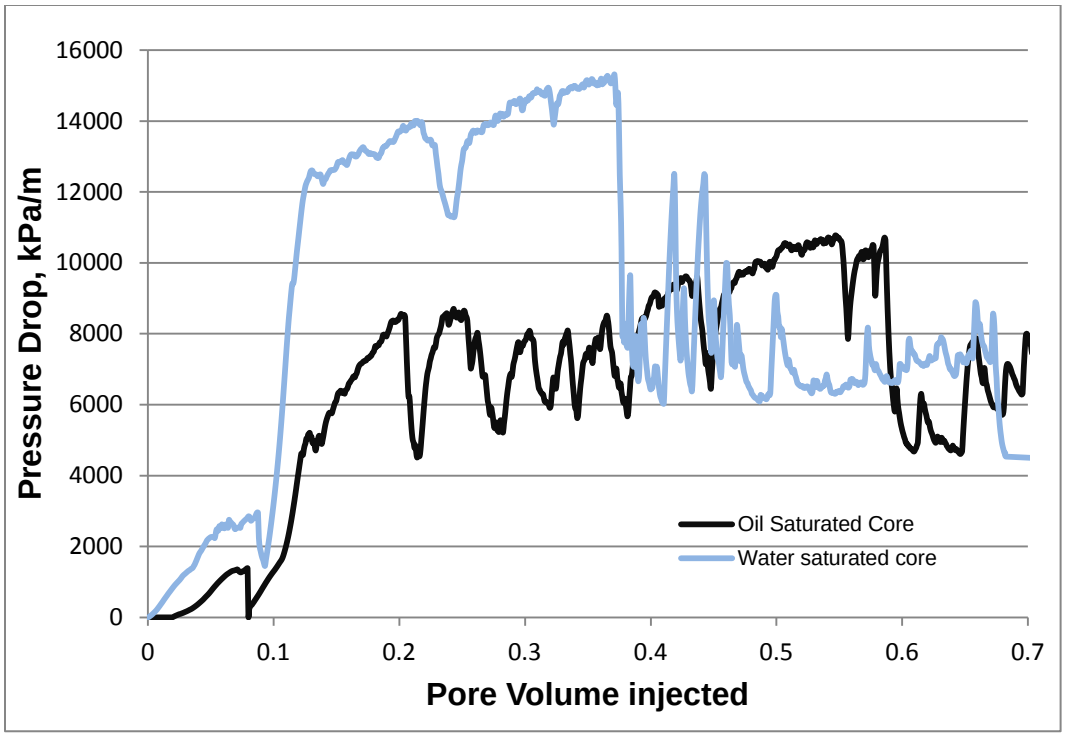

Figure 6-8: Comparison of initial pressure buildup when CGA fluid at 5cc/min is injected into oil saturated and water saturated core

Evidently, the pressure build up in the beginning is sharper when the core is saturated with water than in the case when the core is saturated with mineral oil. This observation gives strength to the suggestion that pushing CGA fluid into water saturated formation is more difficult than that of into oil saturated formation. Later on, after 0.4 pore volumes of pumping is over, both pressure profiles have a similar range.

A comparison of the formation damage that has occurred as a consequence of CGA fluid invasion in the two cases of saturating fluids was made next. The formation damage extent is given by the return permeability. It is the percentage change that permeability has undergone from the original permeability (before

CGA injection began) to the final permeability (after completing CGA fluid injection). Equation 6-2 is used to evaluate the percentage change in the permeability. The altered permeability results are given in Table 6-2.

Table 6-2: Effect of changing the saturation fluid on the permeability alteration

Saturating Fluid	Baseline pressure drop, kPa/m	Sat fluid re-injection pressure drop, kPa/m	Return permeability, %
Mineral oil	1850	2700	68.5%
Water	1300	3200	40.6%

An assessment of the return permeabilities tells us that the amount of alteration in the permeability from original to final has changed with change in the saturation fluid. The permeability alteration when the core is water saturated is more pronounced (the return permeability is only 41%) as compared to when the core is saturated with mineral oil (return permeability 68.5%).

6.2.4 **Effect of Changed Wettability**

The effect of wettability of porous media on the pressure drop across the core due to CGA fluid flow was investigated next. The glass beads used for packing the core are normally water wet. The wettability of these water-wet glass beads was

reversed by application of the Surfasil Siliconizing fluid. The procedure was described step by step in section 6.1.10.

After the wettability of the glass beads had been reversed to make them oil wet, the radial core packed with these oil wet beads was saturated- once with mineral oil and once with water. The CGA drilling fluid was then injected through the radial core. Results of the pressure drop measurement conducted during the flow of CGA fluid through the oil wet porous media saturated with mineral oil are shown in Figure 6-9. CGA drilling fluid was injected at the rate of 5 ml/min. The saturation fluid re-injection, done at 5cc/min too, is shown on the other side of the vertical dividing line.

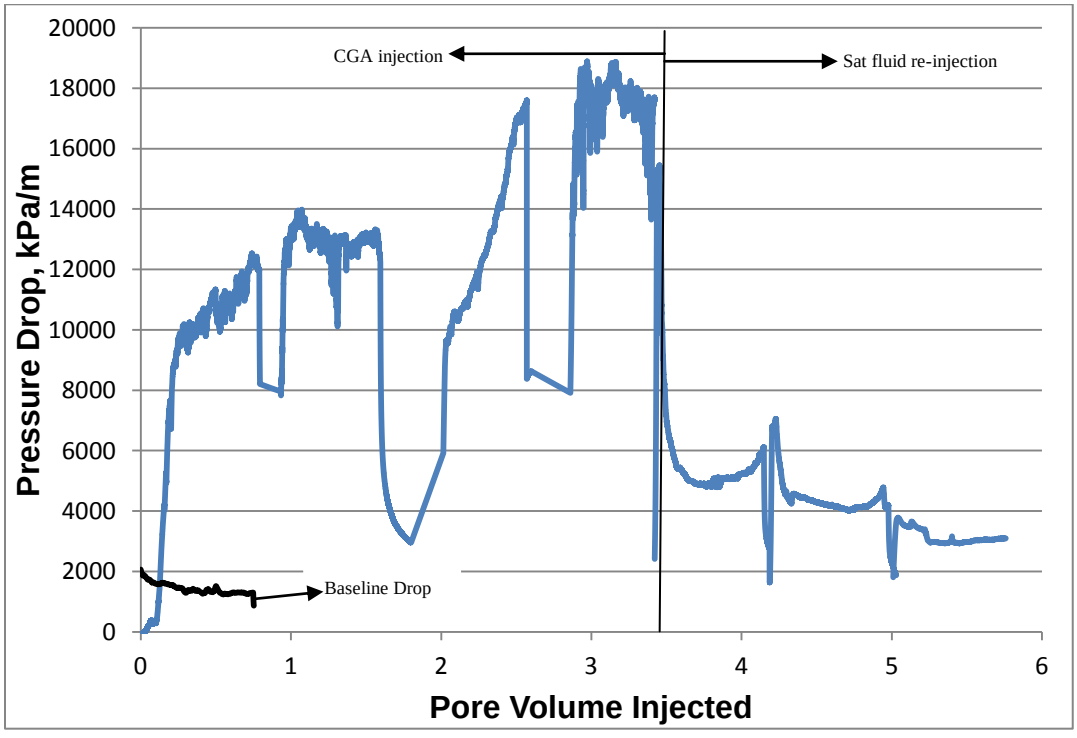

Figure 6-9: CGA fluid injection at 5cc/min into an oil saturated core packed with oil-wet beads

The dark line at the bottom corresponds to injection of the saturating fluid mineral oil (baseline) at 5cc per min into the oil wet beads saturated with mineral oil. After determining the mineral oil baseline, pumping of the CGA fluid into the core was begun. After flushing the core with the aphronized fluid for about 3.4 pore volumes, the saturation fluid (mineral oil) was re-injected again.

Subsequently, the oil wet beads were packed again into the core. This time saturation was done with water. Injection of the CGA drilling fluid was then done for the radial core at 5cc per minute. In Figure 6-10, the pressure drop between the injection and production wells is shown for the reversed wettability glass beads saturated with water.

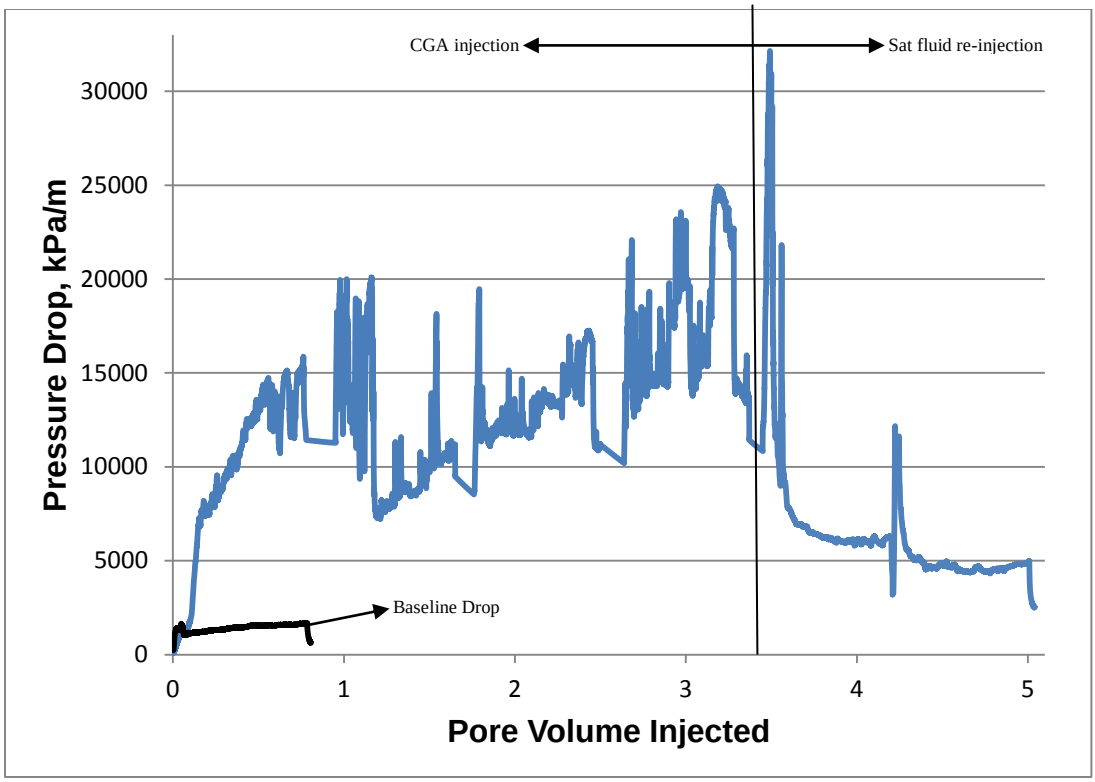

Figure 6-10: CGA fluid injection at 5cc/min into a water saturated core packed with oil-wet beads

Again, baseline pressure drop obtained for the injection of saturation fluid (water in this case) at the rate of 5 ml/min into the oil wet beads is represented by the dark line at the bottom. After determining the baseline pressure drop due to water flow, pumping of the CGA fluid into the core was begun. Following the observation of a close to maximum pressure during CGA fluid injection (at 3.5 pore volumes), the saturation fluid (water) re-injection was carried out.

Following this, a comparison was made of the pressure drop profile across the mineral oil saturated radial core for two cases: water-wet beads saturated with mineral oil and oil-wet beads saturated with mineral oil. This will show us the

effect that reversing of wettability of the glass beads has on the pressure profile. Injection of CGA fluid is done at 5ml / min. The results are shown in Figure 6-11.

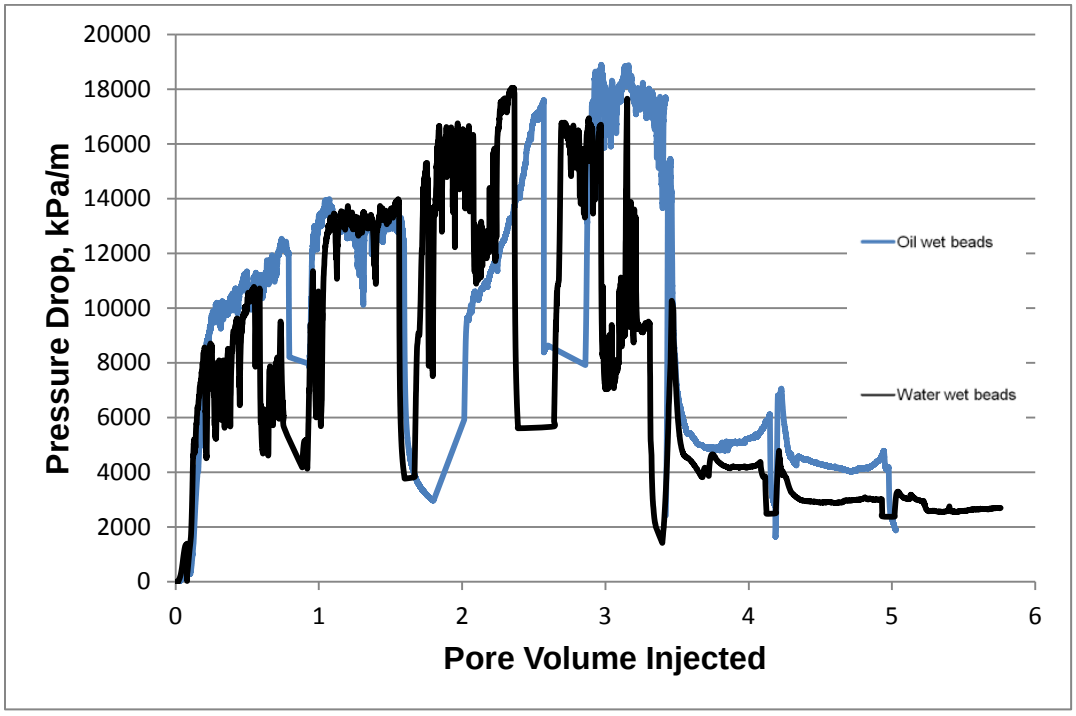

Figure 6-11: Effect of reversing the wettability of glass beads on the pressure drop profile when CGA fluid is injected at 5cc/min into a mineral oil saturated core

The difference between the two pressure profiles for the opposite wettabilities is not noticeable. The maximum pressure drop peaks are within a close range for both cases.

Like the analysis above, a comparison was made for pumping through water-wet and oil-wet beads. This time the saturation fluid used was water. So, the pressure drop profile was recorded across the packed radial core for two cases: water-wet

beads saturated with water and oil-wet beads saturated with water. Injection of CGA fluid is done at 5ml/min. The graph is Figure 6-12.

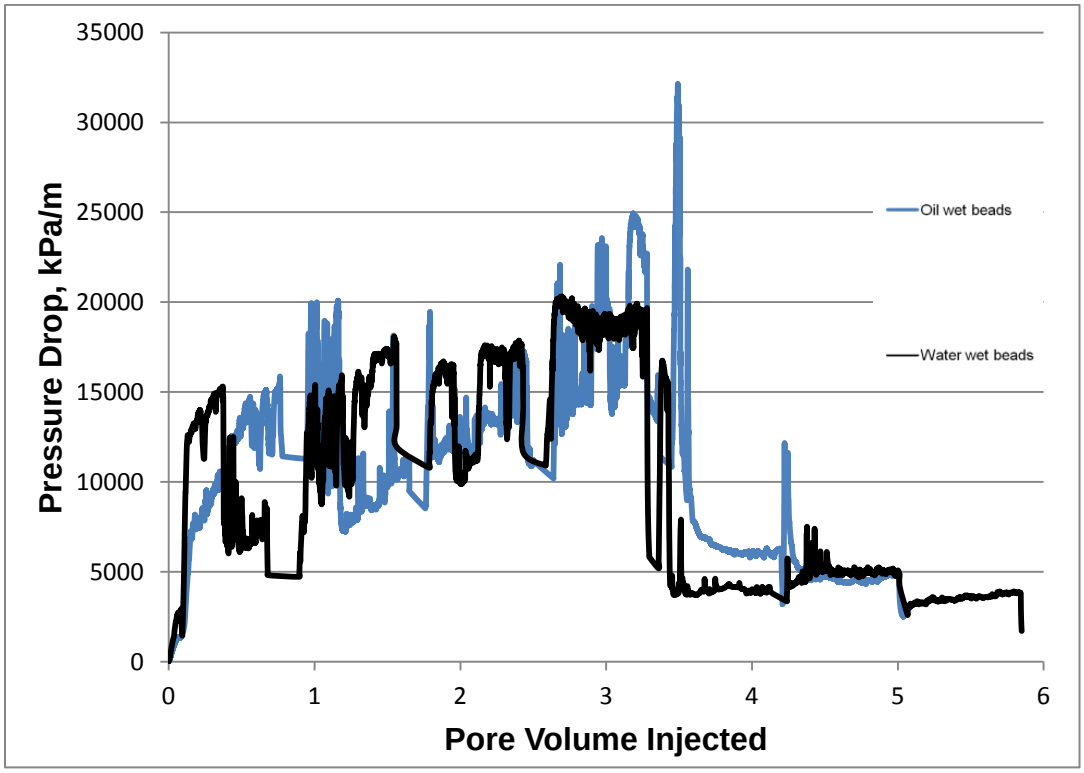

Figure 6-12: Effect of reversing the wettability of glass beads on the pressure drop profile when CGA fluid is injected at 5cc/min into a water saturated core

In this case a difference in the pressure profiles can be seen. The pressure peaks in the water saturated core that is packed with oil-wet beads are higher than the corresponding peaks in the water saturated water-wet beads. This difference can be attributed to the opposite wettabilities in the two cases, all the other experimental parameters being the same. The variation is more significant when the pore volumes injected are higher.

An assessment of the formation damage that has occurred as a consequence of CGA fluid invasion in the two cases of different packing beads was made now. The cases considered are mineral oil saturated oil-wet beads and mineral oil saturated water-wet beads. The CGA fluid injection rate is 5cc per minute. The formation damage extent is given by the return permeability. It is the percentage change that permeability has undergone from the original permeability (before CGA injection began) to the final permeability (after completing CGA fluid injection). Equation 6-2 is used to evaluate the percentage change in the permeability. The altered permeability table is given in Table 6-3.

Table 6-3: Effect of reversing the wettability of glass beads on the return permeability

Wettability of packing beads	Baseline pressure drop, kPa/m	Saturating fluid re-injection drop, kPa/m	Return permeability, %
Water-wet	1850	2700	68.5%
Oil-wet	1700	2900	58.6%

An assessment of the return permeabilities tells us that the amount of alteration in the permeability from original to final has changed with change in the wettability of beads. There is a small difference in the permeability alteration when the core

is packed with water wet beads (return permeability is 68%) than when the core is packed with beads of reversed permeability (return permeability is 59%).

6.3 Summary

- As the pore volumes of CGA fluid injected increase, the peaks of pressure drop across the porous media also increase.
- When the flowrate of CGA fluid being injected was increased, the maximum pressure required for pushing the CGA fluid across the porous media also increased. The return permeability was not affected greatly by the change in flow rate.
- Initially, the pressure drop across the porous media was higher when the saturation fluid was changed from mineral oil to water. After more than one pore volumes of the CGA fluid had been injected, the pressure buildup was similar for both saturating fluid cases. The return permeability is lesser for the water saturated core than the oil saturated core (about 28% difference)
- Reversing the permeability of the glass beads from water-wet to oil-wet has no effect on the pressure drop profile when the saturating fluid is oil. However, when the saturating fluid is water, reversing the permeability from water-wet to oil-wet has increased the pressure required to inject CGA fluid across the porous media significantly. The return permeability is slightly lower when the glass beads are oil-wet than when they are water-wet (a difference of about 10%).

7 CONCLUSIONS AND RECOMMENDATIONS

In this chapter, a summary of the results is given. Some suggestions for further research are also provided at the end.

7.1 Conclusions

Most of the objectives stated in the first chapter have been completed. On the basis of the experimental study, the following conclusions can be given:

1. Generation of CGAs in mineral oil

- A literature review and theoretical study about the classes of surfactants suitable in mineral oil and their potential to create stable Colloidal Gas Aphrons (CGAs) was done. A non-ionic Sorbitan fatty acid ester (SMAZ 20 M1) and a Styrene-Butadiene block copolymer (Kraton G17302H) proved successful in generating aphrons.
- CGAs can be generated with a high speed homogenizer. A constant mixing rate of 7000 rpm for 45 seconds was employed.

2. Characterization of the CGA fluid

- A surfactant concentration of 0.4% w/w was suitable for giving the maximum yield of aphrons.
- A polymer concentration of 1.5% w/w gave good results in the API filtration test. The shear viscosity was too high for fluids with a polymer concentration higher than 1.5%.

- Consequently, the optimum formulation for the use of the CGA fluid as an aphron drilling fluid was identified as mineral oil with 0.4% surfactant and 1.5% polymer.

3. Investigation of the stability of the fluid

- Yield of the fluid decreased slowly with time. The average CGA bubble size increased rapidly in the beginning but it stabilized later on.
- Elevated temperatures have reduced the shear viscosity and increased the API fluid loss considerably.
- Elevated pressures have increased the API fluid loss while no effect is seen on the rheology
- The presence of CGAs has a very significant effect of increasing both the shear viscosity and the LSRV of the aphron fluid as compared to the base fluid only.
- The addition of organic clay Suspentone (1.5%) does not raise the shear viscosity by a significant amount. The LSRV is doubled on addition of Suspentone at 1.5%.
- The equation of state predicted for non-aqueous CGA fluids is

$$\rho = (0.02686 - 2.87*10^{-5}T)\ln(P) - 0.000778T + 0.853384$$

  The proposed equation of state gave reasonably good prediction of CGA fluid density when compared to the experimental results.

- Increasing the shear rate during aphronization led to a reduction in the average bubble size, D_{50}.

4. Performance of the fluid in core flow experiments

- As the pore volumes of CGA fluid injected increase, the peaks of pressure drop across the porous media also increase.
- An increasing resistance to flow of CGA drilling fluids through the glass bead packed radial core holder was observed. This shows that the microbubble buildup across the pore structure of the packed cell can establish an effective seal for controlling fluid invasion into the formation.
- The return permeability was not affected greatly by the change in flow rate. Change in the saturation fluid from mineral oil to water and reversal of the wettability of the packing beads from water-wet to oil-wet reduced the return permeability of the system.

7.2 Recommendations

The following recommendations are suggested for future research work:

- Aphrons were generated in Mineral Oil in this study. The possibility of generating aphrons in another organic medium should be explored. For example, Canola oil for its environment friendly nature should be tested.
- The rheological nature of the fluid was not so satisfactory; the low shear rate viscosity for drilling fluids is expected to be much higher. So a different polymer or a polymer blend should be added for enhanced viscosifying properties.
- Addition of water to create an emulsion based aphron fluid can be the subject of future work.
- If polyaphrons (oil-core aphrons with water as the continuous phase) can be generated, they can be particularly useful as aphron drilling fluids.
- The effect of pressure on the average bubble size and the yield of aphrons could not be studied. The effect of temperature on the yield could not be studied too. These effects should be determined for better understanding of high temperature and pressure implications.
- The filtration tests results presented here are those of a static filtration test. If a dynamic filtration test could be performed, the results would be more indicative of the leak-off nature of the aphron drilling fluid.
- Temperature affects the rheology and filtration loss considerably. A temperature stabilizer additive should be added.

- No visualization study has been done here. If a visualization study consisting of injecting the CGAs into a micromodel is done, the mechanism of aphron bridging could be better understood.
- In the coreflow study, injection rates higher than 6cc per minute (as would be expected with drilling fluid operations) should be studied.
- The effect of using other saturating fluids like crude oil or brine should be looked at.
- Different types of packing beads can be tried, to look at what effect the change of permeability has.
- Injection of the CGA fluid into a porous media which is at an elevated temperature will give an indication of the ability of aphrons to do bridging under downhole conditions.
- Subsequent theoretical studies can be done to come up with models for prediction of CGA diameter, drainage rate and the effect of temperature and pressure on these parameters.

8 REFERENCES

Abrams, A. (1977) Mud Design to Minimize Rock Impairment due to Particle Invasion. Journal of Petroleum Technology, May, 586-592.

Amiri, M.C. and Woodburn, E.T. (1990) A Method for the Characterization of Colloidal Gas Aphron Dispersions. Trans IChemE, 68, Part A, 154-160, March.

ANSI/API Recommended Practice 13B-1 (2009) Recommended Practice for Field Testing of Water-based Drilling Fluids.

API Recommended Practice 13B-2 (2005) Recommended Practice for Field Testing of Oil-based Drilling Fluids.

Basu, S. and Malpani, P.R. (2001) Removal of Methyl Orange and Methylene Blue Dye from Water Using Colloidal Gas Aphron – Effect of Process Parameters. Separation Science and Technology, 36, 13, 2997–3013.

BASF® Technical Bulletin for Surfactant S-MAZ 20 M1.

Bjorndalen, N., Jossy, E., Alvarez, J.M. and Kuru, E. (2008) Reducing Formation Damage with Microbubble Based Drilling Fluids: Understanding the Bridging Ability. Journal of Canadian Petroleum Technology, 47(11):63-69.

Bjorndalen, N., E. Jossy, Alvarez, J.M. and Kuru, E. (2009) A Study of the Effects of Colloidal Gas Aphron Composition on Pore Blocking, SPE 121417, 2009 SPE International Symposium on Oilfield Chemistry, April 20-22, The Woodlands, TX. Accepted to SPE Drilling and Completion, Manuscript DC-1109-0018.

Bjorndalen, N., Jossy, E., Alvarez, J.M. and Kuru, E. (2010) A Laboratory Investigation of the Factors Controlling Filtration Loss when Drilling with Colloidal Gas Aphrons (CGA) Fluids. SPE International Symposium and Exhibition on Formation Damage Control, Lafayette, LA, February 10-12, 2010.

Bjorndalen, N. and Kuru, E. (2008a) Physico-Chemical Characterization of Aphron Based Drilling Fluids. Journal of Canadian Petroleum Technology, 47(11): 15-21

Bjorndalen, N. and Kuru, E. (2008b) Stability and Downhole Characterization of Colloidal Gas Aphron (CGA) Drilling Fluid. Journal of Canadian Petroleum Technology, 47(6):40-47

Brookey, T. (1998) "Micro-Bubbles": New Aphron Drill-In Fluid Technique Reduces Formation Damage in Horizontal Wells. SPE 39589, presented at the SPE International Symposium on Formation Damage Control, February 18 – 19.

Chaphalkar, P.G., Valsaraj, K.T. and Roy, D. (1993) A Study of the Size Distribution and Stability of Colloidal Gas Aphrons Using a Particle Size Analyzer. Separation Science and Technology, 26, 6, 1287 – 1302.

Dai, Y. and Deng, T. (2003) Stabilization and Characterization of Colloidal Gas Aphron Dispersion. Journal of Colloidal and Interface Science, 260, 360-365.

Edwards, S., Matsutsuyu, B., and Willson, S. (2003) Imaging Unstable Wellbores While Drilling. SPE/IADC 79846, presented at the SPE/IADC Drilling Conference, Amsterdam, The Netherlands, February 19-21.

Feng, W., Singhal, N. and Swift, S. (2009). Drainage Mechanism of Microbubble Dispersion and Factors Influencing its Stability. Journal of Colloid and Interface Science 337 (2009) 548–554.

Gardescu, I.I. (1930) Behavior of Gas Bubbles in Capillary Spaces. AIME Technology Publication, 306.

Growcock, F.B., Ivan, C.D. and Friedheim, J.E. (2002) Chemical and Physical Characterization of Aphron-Based Drilling Fluids. SPE 77445 presented at the SPE Annual Technical Conference and Exhibition held in San Antonio, Texas, September 29-October 2.

Growcock, F.B., Khan, A.M., and Simon, G.A. (2003) Application of Water-Based and Oil-Based Aphrons in Drilling Fluid. SPE 80208, presented at the SPE International Symposium on Oilfield Chemistry, Houston, TX, February 5-7.

Growcock, F.B., Simon, G.A., Rea A.B., Leonard, R.S., Noello, E. And Castellan, R. (2004) Alternative Aphron-Based Drilling Fluid. IADC/SPE 87134 presented at the IADC/SPE Drilling Conference held in Dallas, Texas, March 2-4.

Growcock, F. (2005) Enhanced wellbore Stabilization and Reservoir Productivity with Aphron Drilling Fluid Technology. Final Report, DPE Award Number DE-FC26-03NT42000, October.

Growcock, F.B., Belkin, A., Irving, M., O'Connor, R., Fosdick, M. And Hoff, T. (2005) How Aphron Drilling Fluids Work. SPE 96145, presented at the SPE Annual Technical Conference and Exhibition held in Dallas, Texas, October 9-12.

Growcock, F.B., Belkin, A., Fosdick, M., Irving, M., O'Connor, B. and Brookey, T. (2006) Recent Advances in Aphron Drilling Fluid. IADC/SPE Drilling Conference, Miami, FL, February 21-23.

Hashim. M.A., Kumar, S.V. and Gupta B.S. (2000) Particle Bubble Attachment in Yeast Floatation by Coloidal Gas Aphrons. Bioprocess Engineering 22 (2000) 333±336 Ó Springer-Verlag 2000.

Hashim, M.A., Dey, A. Hasan, S. and Gupta, B.S. (1999) Mass transfer Correlation in Floatation of Palm Oil by Colloidal Gas Aphrons. Bioprocess Engineering 21 (1999) 401±404 Ó Springer-Verlag 1999.

Hashim, M.A., SenGupta, B. and Subramaniam, B. (1995) Investigations on the Flotation of Yeast Cells by Colloidal Gas Aphrons (CGA) Dispersion. Biosepatartion, 5, 167-173.

Hayatdavoudi, A. (2006) Removing Oil and Grease from Produced Water Using Micro-Bubble Floatation Technique: From Theory to Field Practice. OTC 17751, presented at the Offshore Technology Conference held in Houston, Texas, May 1-4.

Ivan, C.D., Growcock, F.B. and Friedheim, J.E. (2002) Chemical and Physical Characterization of Aphron-Based Drilling Fluids. SPE 77445, presented at the SPE Annual Technical Conference and Exhibition, San Antonio, TX, September 29 - October 2.

Ivan, C.D., Montilva, J., Friedheim, J. And Bayter, R., (2002) Aphron Drilling Fluid: Field Lessons From Successful Application in Drilling Depleted Reservoirs in Lake Maracaibo. OTC 14278, presented at the Offshore Technology Conference held in Houston, Texas, May 6-9.

Ivan, C.D., Quintana, J.L. and Blake, L.D. (2001) Aphron-Base Drilling Fluid: Evolving Technologies for Lost Circulation Control. SPE 71377, presented at the SPE Annual Technical Conference and Exhibition, New Orleans, LA, September 30 – October 3.

Jauregi, P. and Varley J. (1996) Lysozyme Separation by Colloidal Gas Aphrons. Progr Colloid Polym Sci (1996) 100:362-367.

Jauregi, P., Gilmour, S. and Varley, J. (1997) Characterization of Colloidal Gas Aphrons for Subsequent use for Protein Recovery. The Chemical Engineering Journal, 65, 1 – 11.

Jauregi, P., Mitchell, G.R. and Varley, J. (2000) Colloidal Gas Aphrons (CGA): Dispersion and Structural Features. AIChE Journal, 46, 1, 24-36.

Kraton Technical Bulletin for Kraton G17302H.

Labour, J.Y. (2009) Rheological Characterization of Oil based Aphron (Microbubble) Drilling Fluids. Graduate Research Project Report, University of Alberta.

Leica Microsystems, Leica DM 6000 User Manuals

Longe, T.A. (1989) Colloidal Gas Aphrons: Generation, Flow Characterization and Application in Soil and Groundwater Decontamination. PhD Thesis, Virginia Polytechnic Institute and State University.

Malvern Instruments, User Manual Bohlin CVOR.

MacPhail, W.F., Cooper, R.C., Brookey, T. and Paradis, J. (2008) Adopting Aphron Fluid Technology for Completion and Workover Applications. SPE 112439, presented at the SPE International Symposium and Exhibition on Formation Damage Control held in Lafayette, Louisiana, February 13-15.

Medimurec, N.G. and Pasic, B. (2009) Aphron Based Drilling Fluids: Solution for Low Pressure Reservoirs. Rud.-geol.-naft. zb., Vol. 21, 2009

Oliveira, R.C.G., Oliveira J.F. and Moudgil, B.M. (2004) Optimizing Micro-foam Rheology for Soil Remediation. Progr Colloid Polym Sci (2004) 128: 298–302.

Oyatomari, C., Orellan, S., Alvarez, R. and Rojani, R. (2002) Application of Drilling Fluid System Based on Air Microbubbles as an Alternative to Underbalanced Drilling Technique in Reservoir B-6-X.100 Tia Juana, Lake Maracaibo. International Association of Drilling Contractors 'Global Leadership for the Drilling Industry Conference', Madrid, June 5-6.

Pan, G. (2008) Formulation of Oil Based Aphron Drilling Fluid. Master of Engineering Project Report, University of Alberta.

Parthasarathy, R., Jameson, G.J., and Ahmed, N. (1991) Bubble Break Up in Stirred Vessels, Predicting the Sauter Mean Diameter. Transaction of the Institute of Chemical Engineers, 69, 295.

Polytron User Manual for PT 6100

Quintero, L. and Jones, T.A. (2003) An Alternative Drill-in Fluid System for Low-Pressure Reservoirs. SPE 82280, presented at the SPE European Formation Damage Conference held in The Hague, Netherlands, May 13-14.

Ramirez, F., Greaves, R and, Montilva, J. (2002) Experience Using Microbubbles - Aphron Drilling Fluid in Mature Reservoirs of Lake Maracaibo. SPE 73710, presented at the SPE International Symposium and Exhibition on Formation Damage Control, Lafayette, Louisiana, February 20-21.

Rea, A.B., Alvis, E.C., Paiuk, B.P., Climaco, J.M., Vallerjo, M., Leon, E., Inojosa, J. (2003) Application of Aphrons Technology in Drilling Depleted Mature Fields. SPE 81082, presented at the SPE Latin American and Caribbean

Petroleum Engineering Conference, Port-of-Spain, Trinidad, West Indies, April 27-30.

Reid, P. and Santos, H. (2003) Novel Drilling, Completion and Workover Fluids for Depleted Zones: Avoiding Losses, Formation Damage and Stuck Pipe. SPE 85326, presented at the SPE/IADC Middle East Drilling Technology Conference and Exhibition, Abu Dhabi, UAE, October 20 – 22.

Roy, D., Valsaraj, K.T. and Kottai, S.A. (1992a) Separation of Organic Dyes from Wastewater by Using Colloidal Gas Aphrons. Separation Science and Technology, 27, 5, 573 -588.

Roy, D., Valsaraj, K.T. and Tamayo, A. (1992b) Comparison of Soil Washing using Conventional Surfactant Solution and Colloidal Gas Aphron Suspensions. Separation Science and Technology, 27, 12, 1555-1568.

Roy, D., Valsaraj, K.T., Constant, W.D. and Darji, M. (1994) Removal of Hazardous Oily Waste form a Soil Matrix using Surfactants and Colloidal Gas Aphron Suspensions under Different Flow Conditions. Journal of Hazardous Materials, 38, 127-144.

Roy, D., Kommalapati, R.R., Valsaraj, K.T. and Constant, W.D. (1995a) Soil Flushing of Residual Transmission Fluid: Application of Colloidal Gas Aphrons Suspensions and Conventional Surfactant Solution. Water Research, 29, 2, 589 – 595.

Roy D., Kongara, S. and Valsaraj, K.T. (1995b) Application of Surfactant Solutions and Colloidal Gas Aphron Suspension in Flushing Naphalene from Contaminated Soil Matrix. Journal of Hazardous Materials, 42, 247-263.

Save S.V. and Pangarkar, V.G. (1993) Characterisation of Colloidal Gas Aphrons. Chemical Engineering Communications, 127, 35-54.

Sebba, F. (1985) An Improved Generator for Micron-Sized Bubbles. Chem. Ind. 3, pp. 91-92.

Sebba, F. (1987) Foams and Biliquid Foams-Aphrons, John Wiley and Sons, Toronto. 236p.

Shivhare, S. And Kuru, E. (2010) Physico-Chemical Characterization of Non-Aqueous Colloidal Gas Aphron Based Drilling Fluids. SPE 133274, presented at the Canadian Unconventional Resources & International Petroleum Conference held in Calgary, Alberta, Canada, October 19–21.

Shivhare, S. and Kuru, E. (2011) Rheology and Stability of Non-Aqueous Microbubble Based Drilling Fluids. SPE 141166, presented at the SPE International Symposium on Oilfield Chemistry held in The Woodlands, Texas, USA, April 11–13.

Spinelli, L.S., Neto, G.R., Freire, L.F.A., Monteiro, V., Lomba, R., Michel, R. and Lucas, E. (2010) Synthetic Based Aphrons: Correlation between Properties and Filtrate Reduction Performance. Colloids and Surfaces A: Physicochem. Eng. Aspects 353 (2010) 57–63.

Wang, J, Luo, X, and Luo, P. (1992) Temporary Plugging Technology in Mid-low permeability Rock, Drilling Fluid and Completion Fluid, 9(3):15-17.

White, C.C., Chesters, A.P., Ivan, C.D., Maikranz, S. and Nouris, R. (2003) Aphron-based Drilling Fluid: Novel Technology for Drilling Depleted Formations in the North Sea. SPE/IADC 79840, presented at the SPE/IADC Drilling Conference, Amsterdam, The Netherlands, February 19-21.

Xu, Q., Nakajima, M., Ichikawa, S., Nakamura, N., Roy, P., Okadome, H. and Shiina, T. (2009). Journal of Colloid and Interface Science 332 (2009) 208‑214.

Zhao, J., Pillai, S. and Pilon, L. (2009) Rheology of Colloidal Gas Aphrons (Microfoams) made from Different Surfactants. Colloids and Surfaces A: Physicochem. Eng. Aspects 348 (2009) 93–99.